

**UCLA ENG 96-160**

**September 1996**

**Physico-Chemical Treatment of Water Contaminated with RDX and HMX  
Using Activated Carbon Adsorption and Alkaline Hydrolysis**

**Harro M. Heilmann, Graduate Student  
Michael K. Stenstrom, Chair**

**Civil & Environmental Engineering Department  
Civil & Environmental Engineering Department**

**PHYSICO-CHEMICAL TREATMENT OF  
WATER CONTAMINATED WITH RDX AND HMX USING  
ACTIVATED CARBON ADSORPTION AND ALKALINE HYDROLYSIS**

by

**Harro M. Heilmann**

and

**Michael K. Stenstrom**

**Civil and Environmental Engineering Department  
University of California, Los Angeles**

1996

**School of Engineering and Applied Science  
Report UCLA-ENG-96-160**

# TABLE OF CONTENTS

LIST OF FIGURES	iv
LIST OF TABLES	vi
PREFACE	viii
ABSTRACT	ix
<b>1. INTRODUCTION</b>	<b>1</b>
<b>2. HIGH EXPLOSIVES</b>	<b>5</b>
2.1 Production of High Explosives	5
2.1.1 RDX and HMX	5
2.2 Current Demilitarization Situation	9
2.3 Available Treatment Technologies	11
2.3.1 Open Burning/Open Detonation	11
2.3.2 Incineration	13
2.4 Third Generation Technologies	13
2.4.1 Molten Oxidation	14
2.4.2 Bioremediation/Composting	14
2.4.3 Alkaline Hydrolysis	15
<b>3. HIGH EXPLOSIVES CONTAMINATED WATER</b>	<b>21</b>
3.1 Contaminated Water Sources	21
3.2 Possible Future Technologies	23
3.2.1 Oxidative Treatment	23
3.2.2 Surfactant Technology	25
3.2.3 Biological Treatment	26
3.3 Adsorption	27
3.3.1 Activated Carbon	28
3.3.2 Resins	30
3.4 Adsorbent Regeneration	31
3.4.1 Thermal Adsorbent Regeneration	31
3.4.2 Biological Adsorbent Regeneration	32
3.4.3 Chemical Adsorbent Regeneration	33
3.4.4 Alkaline Hydrolysis Regeneration	35
<b>4. OBJECTIVES OF THIS STUDY</b>	<b>37</b>
<b>5. MATERIALS AND METHODS</b>	<b>41</b>
5.1 Materials	41

## TABLE OF CONTENTS (Cont'd)

5.1.1	High Explosives	41
5.1.2	Activated Carbon	41
5.2	Analytical Methods	42
5.2.1	High Performance Liquid Chromatography (HPLC)	42
5.2.2	Ion Chromatography (IC)	45
5.2.3	Gas Chromatography/Mass Spectrometry (GC/MS)	46
5.2.4	BET-Surface Area Measurements	47
5.2.5	Gas Analysis	47
5.2.6	Miscellaneous Analytical Methods	48
5.3	Batch Experiments	49
5.3.1	Chemical Kinetics Studies	49
5.3.2	Ammonia Experiments	50
5.3.3	Activated Carbon Isotherms	50
5.4	Fixed Bed Adsorber Experiments	51
<b>6.</b>	<b>RESULTS AND DISCUSSION</b>	<b>54</b>
6.1	Aqueous Homogeneous Alkaline Hydrolysis	54
6.1.1	Objectives	54
6.1.2	Chemical Kinetics	54
6.1.3	Temperature Dependency of Rate Constants	64
6.1.4	Intermediates and Endproducts	67
6.1.5	Conclusions	76
6.2	Adsorption	84
6.2.1	Objectives	84
6.2.2	Isotherms of Virgin Activated Carbon	85
6.2.3	Adsorption Kinetics	89
6.2.4	Conclusions	101
6.3	Batch Regeneration of Activated Carbon	102
6.3.1	Objectives	102
6.3.2	Regeneration Kinetics	103
6.3.3	Readsorption Products	106
6.3.4	Regeneration Cycles	107
6.3.5	Acid Post Treatment	111
6.3.6	BET-Surface Area Measurements	113
6.3.7	Residual Adsorbates after Regeneration	116
6.3.8	Conclusions	118
6.4	Fixed Bed Studies	119
6.4.1	Objectives	119
6.4.2	Column Adsorption	120

## TABLE OF CONTENTS (Cont'd)

6.4.3	Column Regeneration	123
6.4.4	Repeated Adsorption and Regeneration	127
6.4.5	Conclusions	128
7.	<b>SUMMARY</b>	129
	<b>REFERENCES</b>	133
	Appendix A Notation	141
	Appendix B Derivation of the Equations Describing the Homogeneous Surface Diffusion Model (HSDM)	143

## LIST OF FIGURES

Figure 1	Chemical formulas of RDX (Hexahydro-1,3,5-trinitro-1,3,5-triazine) and HMX (Octahydro-1,3,5,7-tetranitro-1,3,5,7-tetrazocine)	6
Figure 2	Reaction pathway of the alkaline hydrolysis of RDX	18
Figure 3	Proposed process scheme for the treatment of high explosives contaminated water using activated carbon adsorption and regeneration of laden activated carbon by alkaline hydrolysis	40
Figure 4	UV-spectra of RDX and HMX from HPLC-diode array detection	44
Figure 5	Fixed bed adsorber set-up	53
Figure 6	The aqueous homogeneous alkaline hydrolysis of RDX at pH 10.7 and 11	58
Figure 7	The aqueous homogeneous alkaline hydrolysis of RDX at pH 11.5 and 12	59
Figure 8	The aqueous homogeneous alkaline hydrolysis of HMX at pH 10 and 11	60
Figure 9	The aqueous homogeneous alkaline hydrolysis of RDX at pH 12	61
Figure 10	Pseudo first-order rate constants as a function of the OH <sup>-</sup> -concentration	63
Figure 11	Temperature dependence of the 2nd-order rate constants ( $k_2$ ) of the aqueous homogeneous alkaline hydrolysis of RDX and HMX ( <i>Arrhenius</i> -plot)	66
Figure 12	Product formation kinetics of the alkaline hydrolysis of RDX at 50°C; $c_0 = 0.16$ mmol RDX/L	68
Figure 13	Product formation kinetics of the alkaline hydrolysis of RDX at 80°C; $c_0 = 0.16$ mmol RDX/L	69
Figure 14	Chromatograms (GC/MS) of the alkaline hydrolysates of RDX and HMX	77

## LIST OF FIGURES (Cont'd)

Figure 15	Mass-spectra of some compounds identified in the alkaline hydrolysates of RDX by GC/MS-analysis	79
Figure 16	Mass-spectra of some compounds identified in the alkaline hydrolysates of HMX by GC/MS-analysis	81
Figure 17	Proposed new reaction pathway of the alkaline hydrolysis of RDX	84
Figure 18	Virgin isotherms of RDX and HMX on activated carbon	88
Figure 19	Homogeneous Surface Diffusion Model (after Hand et al., 1983)	92
Figure 20	Adsorption of RDX on activated carbon Filtrasorb-400	97
Figure 21	Influence of agitation on HSDM batch rate data	100
Figure 22	Product formation kinetics during the alkaline hydrolysis of RDX in a aqueous homogeneous system and on activated carbon for pH 12; $c_0 = 0.16$ mmol RDX/L	105
Figure 23	Isotherms of repeatedly regenerated activated carbon	109
Figure 24	Isotherms of regenerated and acid post-treated activated carbon Filtrasorb-400	114
Figure 25	Adsorption of RDX on Filtrasorb-400 in continuous flow fixed-bed adsorbers	122
Figure 26	Regeneration of RDX-laden activated carbon at 80°C and pH 12	125
Figure 27	Regeneration of RDX-laden activated carbon from pH 11 to 12	126
Figure 28	Breakthrough curves of virgin and repeatedly regenerated activated carbon F-400 in fixed-bed adsorbers	127

## LIST OF TABLES

Table 1	Properties of RDX and HMX	7
Table 2	Surplus of explosives expected to result from nuclear weapon dismantlement in the USA	10
Table 3	Second-order rate constants of the alkaline hydrolysis of RDX (literature results)	15
Table 4	Second-order rate constants of the alkaline hydrolysis of HMX (literature results)	16
Table 5	Results of the experimental activation energy for the alkaline hydrolysis of RDX and HMX (literature results)	16
Table 6	Results for the Freundlich-isotherm of RDX and activated carbon in the literature	30
Table 7	Manufacturer specifications for activated carbons Filtrasorb-400 and Alamo Brand Granular ABG-30	42
Table 8	Pseudo first-order rate constants and correlation coefficients for the aqueous homogeneous alkaline hydrolysis of HMX	61
Table 9	Pseudo first-order rate constants and correlation coefficients for the aqueous homogeneous alkaline hydrolysis of RDX	62
Table 10	Calculated 2nd-order rate constants for the aqueous homogeneous alkaline hydrolysis of RDX and HMX and correlation coefficients	62
Table 11	Temperature dependence of the 2nd-order rate constants for the aqueous homogeneous alkaline hydrolysis of RDX and HMX ( <i>Arrhenius</i> -parameters)	65
Table 12	Normalized molar yields for the products of the alkaline hydrolysis of RDX	71
Table 13	Normalized molar yields for the products of the alkaline hydrolysis of RDX	71

## LIST OF TABLES (Cont'd)

Table 14	Carbon and nitrogen balance for the alkaline hydrolysis of RDX	76
Table 15	<i>Freundlich</i> -constants and correlation coefficients for virgin activated carbon	88
Table 16	Polynomial coefficients (from Hand et al., 1983)	96
Table 17	Evaluation of the best-fit surface diffusion coefficient $D_s$	98
Table 18	Adsorption kinetics of RDX on activated carbon Filtrasorb-400 at different stir speeds	100
Table 19	<i>Freundlich</i> -isotherm constants for regenerated activated carbon	112
Table 20	Results of the BET-surface area measurements of activated carbon	116

## PREFACE

This report is adapted from the Doctor of Engineering dissertation of Harro M. Heilmann from the Technical University of Berlin, Germany. The experimental research was performed primarily at UCLA in the Civil and Environmental Engineering Department Laboratories. Dr. Heilmann was a doctoral candidate at the Technical University, and Professor Udo Wiesmann was his research supervisor and was responsible for supervising the writing of the dissertation. Duplicate sections written in German in the dissertation are not included in this report.

This research was supported in part by the Department of Energy through contracts from the Lawrence Livermore National Laboratory and the Pantex Plant, operated by Silas Mason and Hanger. The authors are grateful for the assistance of Phil Goodfellow of the Pantex Plant, Jeff Daniels and John Knezovich from Lawrence Livermore, and Stan Caulder from the Naval Surface Warfare Center. The BET surface area experiments were performed in Dr. Caulder's laboratory. Important experiments to quantify gas production during hydrolysis were performed at the Pantex Plant.

## ABSTRACT

The heterocyclic nitroorganic compounds RDX (Hexahydro-1,3,5-trinitro-1,3,5-triazine) and HMX (Octahydro-1,3,5,7-Tetranitro-1,3,5,7-Tetrazocine) are the most widely used high performance explosives. These compounds are major components of nuclear and conventional weapons. Destruction of these compounds has been traditionally performed by open burning or open detonation, processes that are undesirable because they result in incomplete combustion and the production of unwanted byproducts. This report investigates the use of an alternative destruction technology using hydrolysis at high pH and elevated temperatures.

Alkaline hydrolysis is shown to be effective in transforming HMX and RDX into non-energetic and less hazardous by products. Experiments were performed over temperatures ranging from 50 to 80°C and pH ranging from 10 to 12. Kinetics, including the Arrhenius equation, are reported. They are approximately 20 to 30% greater at the elevated temperatures and pH than rates extrapolated from previous research performed at lower temperatures and pH. Mass balances on carbon and nitrogen recovered are 94% and 90% respectively. The major by-products of hydrolysis are nitrite, formate, acetate, formaldehyde, ammonia, nitrous oxide and nitrogen gas. Consistent molar ratios of the products were measured. No trace by products were observed using gas chromatography/mass spectrophotometry analysis.

Alkaline hydrolysis of RDX and HMX-laden activated carbon was successful and produced the same by-products in the same molar ratios. Experiments were performed in complete mixing reactors and packed columns. Carbon regenerated with alkaline hydrolysis was free of measurable RDX and HMX. Regenerated carbon capacity to adsorb RDX and HMX was similar to virgin carbon.

The research presented in this report, along with other research performed in this laboratory, suggest that waters contaminated with RDX and HMX can be treated using activated carbon, which can be regenerated with alkaline hydrolysis. The regenerated carbon is free of energetic materials and may be reused. No energetic hazardous wastes are produced, and the wastes that are produced can be treated in biological treatment plants.

## 1. INTRODUCTION

The interest in military waste has recently increased due to growing environmental concerns and political changes after the end of the cold war. The environmental fate and health impacts of high explosives waste and their appropriate treatment technologies are yet to be identified. In addition to bulk high explosives, contaminated ground- and process waters from closed military bases, former production plants, contaminated soil and weapon dismantling facilities will need to be treated. Problems related to contaminated sites and demilitarization activities particularly exist in the USA, in Europe and on the territory of the former Soviet Union, with some of the sites dating back to World Wars I and II.

The heterocyclic nitroorganic compounds RDX (Hexahydro-1,3,5-trinitro-1,3,5-triazine) and HMX (Octahydro-1,3,5,7-tetranitro-1,3,5,7-tetrazocine) are the most widely used high performance explosives today, and are major components in nuclear and conventional weapons. The classic high explosive TNT (2,4,6-Trinitrotoluene) was partly replaced by RDX after World War II and later also by HMX, where ultra-high performance is needed. This occurred not only for nuclear weapons applications but also for high performance conventional weapons. Therefore, HMX, the most energetic production explosive in the world, is a potential disposal problem at US Department of Energy (DOE) sites. The DOE is responsible for the nuclear weapons development, construction and disassembly in the USA. This study was conducted in close coordination with the DOE's Lawrence Livermore Laboratory and DOE's Pantex Plant, near Amarillo Texas. Assistance

was also received from DOE's Los Alamos National Laboratory, and the Naval Surface Warfare Center.

Due to the large US demilitarization inventory, the disposal of weapons may be as important as the cleanup of contaminated sites. In Germany the demilitarization inventory is smaller, and contaminated sites are the main focus of scientific and technological research today. Therefore, the technical approach for demilitarization and remediation may be different between both countries. In both countries, tighter environmental regulations regarding the disposal and treatment of high explosives and high explosives contaminated water are expected in the near future.

High explosives contaminated waters, particularly water contaminated with RDX and HMX, contain only small concentrations of the respective compounds. This is due to the low water solubility of the heterocyclic compounds [solubility limits at 25°C: approximately 5 mg HMX/L (Rosenblatt et al., 1991) and approximately 50 mg RDX/L (Gibbs and Popolato, 1980)]. Therefore, treatment technologies for bulk high explosives may not be appropriate for contaminated water treatment. However, processes for bulk high explosives may be combined with other technologies such as adsorption to preconcentrate the high explosives for contaminated water treatment.

The instability of heterocyclic nitroorganic explosives at high pH has long been known and alkaline hydrolysis has been used to destroy RDX and HMX in the past. The fact that the process transforms energetic materials into non-energetic materials and therefore makes them unusable for further military applications was the main reason for its use. The safety aspect was emphasized and the possible production of hazardous by-products was not

yet a concern. Interest in the by-products of the alkaline hydrolysis of RDX and HMX and their environmental impact has only recently become important.

More recent studies at the Los Alamos National Laboratory (Spontarelli et al., 1993) and present work focus on alkaline hydrolysis as an environmental treatment technology. Therefore, the product formation and composition were more extensively studied. Nevertheless, direct treatment of contaminated water with alkaline hydrolysis is still not economical.

The objective of this study was to combine alkaline hydrolysis with activated carbon treatment for contaminated water treatment. This combination allows large volumes of dilute contaminated water to be conveniently treated by alkaline hydrolysis by concentrating the high explosives on the activated carbon. The results of this study have implications on both the treatment of bulk high explosives with alkaline hydrolysis and the application of the process for contaminated water treatment/activated carbon regeneration.

The alternative treatment process investigated used activated carbon adsorption of HMX and RDX onto granular activated carbon (GAC) and subsequent offline-regeneration of spent GAC through alkaline hydrolysis. In this process (Figure 3) the contaminated water is first treated through HMX- and RDX-adsorption onto GAC, which concentrates the contaminants (approximately 2000:1) on the carbon and reduces the volume of material to be treated with alkaline hydrolysis. The spent carbon is regenerated with alkaline hydrolysis and can be reused to treat another charge of contaminated water. The end-products are low molecular weight compounds which can easily be degraded in regular wastewater treatment plants with nitrification/denitrification stages.

In this dissertation, an overview of the current demilitarization problem is first presented. A literature review of the demilitarization inventory and current treatment technologies, as well as regulatory and environmental impacts, is next introduced. The situation in the USA, where this study was conducted and where much of the data are available, is presented. The information will also be applicable to the worldwide demilitarization problem. The implications for Germany, where this work is submitted, have also been addressed.

New results of the investigation of the alkaline hydrolysis of RDX and HMX as a regeneration process for spent activated carbon are presented in four sections:

1. Mechanism and chemical kinetics of the alkaline hydrolysis of RDX and HMX at elevated temperature and pH;
2. Batch studies of adsorption of RDX and HMX on activated carbon;
3. Batch studies of regeneration of RDX- and HMX-laden activated carbon with alkaline hydrolysis;
4. Continuous flow adsorption and regeneration of RDX and HMX in fixed-bed adsorbers.

The present work shows a potential new technology to economically treat high explosives contaminated water using activated carbon adsorption and regeneration with alkaline hydrolysis.

## **2. HIGH EXPLOSIVES**

### **2.1 Production of High Explosives**

High explosives as opposed to low explosives are characterized by high velocity detonation accompanied by very high rates of reaction and high pressure. RDX (Royal Demolition Explosive, Rapid Detonation Explosive or Research Department Explosive) and HMX (Her Majesty's Explosives or High Melting Explosive) are now the most important production high explosives in the USA (Borman, 1994).

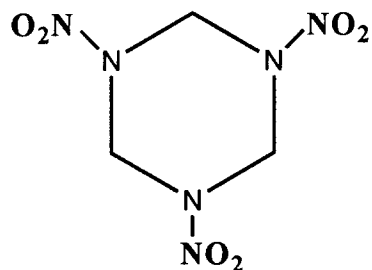
The classic high explosive TNT is better known to the public but has not been produced in the USA for several years (Rosenblatt, 1991). Due to its historic importance, TNT is a major contamination problem and it constitutes the largest share of high explosives to be treated in the USA and worldwide from demilitarization activities. RDX, which became very important during and after World War II, is now being replaced by its homologue HMX in new high performance explosive devices (Gibbs and Popolato, 1980). Although new high explosives are being developed for special applications (Borman, 1994), RDX and HMX will maintain their importance as the most important high explosives in the USA. Their production will continue and contaminated water treatment will still be required.

#### **2.1.1 RDX and HMX**

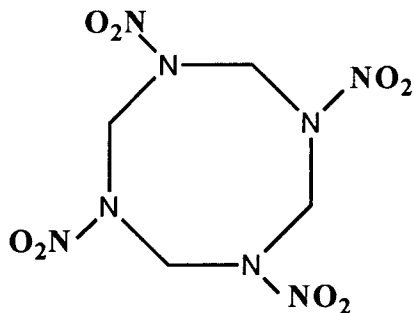
##### *i. Chemistry*

RDX and HMX, shown in Figure 1, are major components in nuclear and conventional weapons (Dobratz, 1981). Today, they are widely used as part of high-

performance explosive compositions in the USA, such as plastic bonded explosives (Table 2). In older high performance compositions TNT was mixed with RDX (composition B-3 and cyclotol; see Table 2). Evidently, HMX, the most energetic production explosive available in the world (Pruneda et al., 1993), has replaced its homologue RDX in importance in the USA. It is more often used in recently manufactured explosive devices, particularly DOE-formulations. This is due in part to HMX's greater energetic yield as well as its resistance to unwanted detonation.



RDX (Hexahydro-1,3,5-Trinitro-1,3,5-triazine; C<sub>3</sub>H<sub>6</sub>N<sub>6</sub>O<sub>6</sub>)



HMX (Octahydro-1,3,5,7-Tetranitro-1,3,5,7-Tetrazocine; C<sub>4</sub>H<sub>8</sub>N<sub>8</sub>O<sub>8</sub>)

Figure 1 Chemical formulas of RDX (Hexahydro-1,3,5-trinitro-1,3,5-triazine) and HMX (Octahydro-1,3,5,7-Tetranitro-1,3,5,7-Tetrazocine).

HMX and RDX (Figure 1) are sparingly soluble in water [solubility limits at 25°C: approximately 5 mg HMX/L (Rosenblatt et al., 1991) and approximately 50 mg RDX/L (Gibbs and Popolato, 1980)]. Due to their low vapor pressures (see Table 1), volatilization can be neglected. Commercial grade RDX usually contains 8 to 10% HMX by weight. HMX is unintentionally produced in synthesizing RDX. HMX is more pure; it seldom contains more than 1% RDX.

Table 1 Properties of RDX and HMX.

	RDX	HMX
Chemical formula	$C_3H_6N_6O_6$	$C_4H_8N_8O_8$
Chemical name	Hexahydro-1,3,5-trinitro-1,3,5-triazine	Octahydro-1,3,5,7-Tetranitro-1,3,5,7-Tetrazocine
Molecular Weight	222.1 g/mol	296.2 g/mol
Solubility in water (25°C)	50 mg/L	5 mg/L
Density	1.806 g/cm <sup>3</sup>	1.905 g/cm <sup>3</sup>
Vapor pressure (25°C)	$5.37 \cdot 10^{-9}$ mbar	$4.44 \cdot 10^{-14}$ mbar
Melting point	204°C	275°C
Heat of Explosion	5757 kJ/kg	6197 kJ/kg

is 35 µg/L RDX or HMX. For the protection of aquatic life 300 µg/L RDX or HMX is allowable. For comparison, the concentrations for TNT are 49 µg/L and 60 µg/L, respectively. Sullivan et al. (1979) also recommended 24-hour average concentrations of no more than 300 µg RDX/L for the protection of aquatic life. These limits do not reflect potential for carcinogenesis.

The current lifetime health advisory for drinking water in the USA defined by the EPA (Environmental Protection Agency, Office of Drinking Water) is 2 µg RDX/L and 350 µg HMX/L (McLellan et al., 1988a and b; Rosenblatt et al., 1991). The equivalent concentration for TNT is 20 µg/L (Rosenblatt et al., 1991). These concentrations are still advisory, and no maximum contaminant standards yet exist.

RDX and HMX adsorb only weakly onto sand and other soil particles (Tsai et al., 1980). In lysimeter-studies its migration rate was only limited by its low solubility (Hale et al., 1979). It is therefore poorly immobilized in soil (Spanggord, 1980). Spalding and Fulton (1988) found RDX to migrate in an aquifer with almost no retention.

## **2.2 Current Demilitarization Situation**

The destruction of both surplus conventional and nuclear weapons produces high explosives wastes that require treatment. Both conventional and nuclear weapons have a limited storage life, which requires that they be periodically replaced. Therefore, RDX- and HMX-contaminated wastes can be anticipated, even after the world-wide surplus amount is destroyed (Layton et al., 1987).

ii. *Environmental and Health Impact*

RDX has important health and toxicity effects. In numerous studies RDX was shown to be toxic to humans (Yinon, 1990). It was also used as a rat poison (Merck & Co., 1989). RDX was found to be toxic to the fathead minnow (*Pimephales promelas*) and other aquatic species (Bentley et al., 1977). In a recent study Burton et al. (1994) found RDX to be acutely and chronically toxic to the fathead minnow (*Pimephales promelas*).

RDX has also been classified as a class C possible human carcinogen in the USA and it has adverse effects on the central nervous system in mammals (McLellan, 1988a). Furthermore it produces convulsions and/or unconsciousness on exposure by inhalation and ingestion. The evidence for carcinogenicity of RDX from mammalian studies is limited.

It was also reported that RDX can be reduced biologically to its nitroso-derivative hexahydro-1,3,5-trinitroso-1,3,5-triazin (TNX), which is an experimental carcinogen in animal tests (Urban and Danz, 1976). It is possible that TNX is produced during digestion by humans, which presents an indirect carcinogenic risk.

HMX also has important health and toxicity effects: It affects the central nervous system, but only at higher concentrations than RDX (McLellan et al., 1988b). Generally, less is known about HMX and further carcinogenicity and toxicity studies are needed.

Bentley et al. (1977) found concentrations of 3.6 to 6.4 mg RDX/L to have an acute toxic effect on all freshwater fish species. The results of the same study for HMX were not conclusive enough to define a toxic concentration range. Interim discharge criteria were defined by the US Army Medical Bioengineering Research and Development Command, Fort Detrick, Maryland (Burrows et al., 1984). For drinking water protection the maximum

Byrd and Humphreys (1993) report a US demilitarization inventory at the end of fiscal year 1992 from Department of Defense- (DOD) activities of 313,000 metric tons of high explosives (e.g. RDX, HMX and TNT). They also expect another 50,000 kg/year of excess high explosives generated through the year 2000 from the current nuclear weapons dismantling efforts by the US Department of Energy (DOE). Pruneda et al. (1993) identified the amount of excess high explosives from nuclear weapons dismantlement in the USA with more detail (Table 2). For DOE sites HMX is the compound of the greatest interest.

Table 2 Surplus of explosives expected to result from nuclear weapon dismantlement in the USA (Pruneda et al., 1993).

Explosive	Amount (kg)	Composition (mass-%)
Composition B-3	110	60% RDX, 40% TNT
Cyclotol 75/25	1,030	75% RDX, 25% TNT
LX-04-01	45,095	85% HMX, 15% Viton A
LX-07-02	753	90% HMX, 10% Viton A
LX-10-02	14,305	94.7% HMX, 5.3% Viton A
LX-11	23	80% HMX, 20% Viton A
LX-17	642	92.5% TATB, 7.5% Kel-F 800
PBX-9011	9,504	90% HMX, 10% Estane
PBX-9404	75,465	94% HMX, 3% NC, 3% CEF
PBX-9501	4,917	95% HMX, 2.5% Estane, 2.5% BDNPA-F
PBX-9502	18,365	95% TATB, 5% Kel-F 800
<b>Total</b>	<b>170,209</b>	

explosives: RDX (Hexahydro-1,3,5-trinitro-1,3,5-triazine), HMX (Octahydro-1,3,5,7-Tetranitro-1,3,5,7-Tetrazocine), TATB (1,3,5-Triamino-2,4,6-trinitrobenzene), TNT (2,4,6-Trinitro-toluene); energetic binder: NC (Nitrocellulose); plastic binders: Viton A (Dupont), Kel-F 800 (3M), Estane (BF Goodrich), CEF, BDNPA-F

The abbreviations LX- and PBX- accompanied with the respective number are the code names for plastic bonded explosives developed by the Lawrence Livermore National Laboratory (LX) and by the Los Alamos National Laboratory (PBX).

In Germany detailed numbers of the demilitarization inventory have not yet been defined, but contaminated sites are now being characterized. The major compounds that make up site contaminations with explosives and the German demilitarization inventory are TNT and RDX. HMX is expected to be found in smaller concentrations since it is produced along with RDX. Haas et al. (1990) report six sites of possible RDX- and HMX-contaminations. Former production sites at Bobingen, Hanau-Wolfgang and Rottweil, as well as the load, assemble and pack (LAP) facilities at Hessisch-Lichtenau, Clausthal-Zellerfeld and Stadtallendorf, where RDX was mixed with TNT, were identified. They also expect contamination at incineration sites.

## **2.3 Available Treatment Technologies**

### **2.3.1 Open Burning/Open Detonation**

Currently high explosives are being destroyed by open burning/open detonation (Ansell, 1993; Byrd and Humphreys, 1993). At the DOE's Pantex Plant approximately 45,000 kg of high explosives from nuclear weapons disassembly are treated this way annually (Patterson and Phelan, 1993). In fiscal year 1992 80% of the US. Department of Defense's annual demilitarization tonnage of 56,000 metric tons was destroyed using open

burning/open detonation technologies; however, due to environmental and legal concerns, this technology may soon be prohibited (Byrd and Humphreys, 1993).

Combustion of high explosives can lead to various unwanted toxic by-products and emissions. Patterson and Phelan (1993) report emissions of hydrogen fluoride that were close to the maximum allowable amount of  $4.9 \mu\text{g}/\text{m}^3$  during open burning. The fluoride has its origin in plastic binders that usually make up less than five percent of the explosive composition. Holl and Schneider (1992 and 1993) investigated the combustion of RDX and other nitrate-esters. They detected large amounts of NO, which was produced from the nitrate-esters  $\text{NO}_2$ -groups under the influence of heat and oxygen deficiency. The varying NO-concentrations from the open burning process would not meet the legal requirements in Germany, regulated by the 17. BImSchV (Federal Regulation of Emissions, 17th ed., Germany). They also documented a pyrolytic reaction under critical conditions (delayed ignition; low ignition heat; accidental smolder fire) that leads to the formation of large amounts of hydrocyanic acid (HCN) during RDX combustion.

Furthermore, the open burning of explosives and propellants leads to soil contamination at the demilitarization sites (Holl and Schneider, 1992 and 1993). Typically, one can find Cu-, Pb-, Zn-, Ba-, Al-, and Mg-molecules, as well as Hg, S and P from primers, stabilizers and other weapons components, as well as the explosives TNT, RDX and HMX in the vicinity of open-burning sites.

### **2.3.2 Incineration**

Incineration is a second-generation technology and anticipated to succeed first-generation open burning/open detonation, which means the technology is now available in the USA and Europe; nevertheless, commercial or industrial facilities have not yet been constructed, or are not yet in operation. In the USA current legislation will increase the regulatory requirements for incinerator permits, and hence this technology may also be not available in the long term (Byrd and Humphreys, 1993). The German situation has not progressed as far as in the USA and reliable regulations will depend on further basic research. Holl and Schneider (1992) report a trend of constantly decreasing threshold values for emissions in Germany, which they believe will lead to more preemptive measures. Therefore, so-called third-generation technologies such as biological treatment and treatment with alkaline hydrolysis are now being investigated. More basic research is necessary before these technologies will find application in industrial or commercial facilities.

## **2.4 Third Generation Technologies**

The US Departments of Energy and Defense (DOE and DOD) are now combining their efforts to identify possible future processes for demilitarization in the USA. The following third-generation technologies were identified as alternatives to first- and second-generation treatment processes.

#### **2.4.1 Molten Salt Oxidation**

Molten Salt Oxidation or molten salt destruction is effective in neutralizing high explosives. RDX and HMX are both subject to molten salt oxidation (Pruneda et al., 1993). In this process the energetic materials are introduced into a reactor containing molten salt at 400 - 900°C. The molten salt is a mixture of alkali- or alkaline-earth carbonates such as sodium carbonate, potassium carbonate, calcium carbonate and lithium carbonate. Acid gases are neutralized and the molten salt catalyzes the oxidation of organic materials. At the Lawrence Livermore Laboratory RDX and HMX were successfully neutralized at 500 - 700°C (Pruneda et al., 1993). The off-gases of the process which were analyzed using mass spectroscopy were primarily composed of carbon dioxide, nitrogen and water. No residual explosives were found in the molten salt. The process requires high process temperatures. The required energy makes the process expensive and more research is needed.

#### **2.4.2 Bioremediation/Composting**

Direct bioremediation of bulk high explosives has not been investigated. However, composting of high explosives contaminated soil suggests that biological treatment is possible. The biological treatment of contaminated water is discussed later (see Section 3.2).

Garg et al. (1991) composted RDX, HMX and TNT under mesophilic (35 - 40°C) and thermophilic (55 - 60°C) conditions. The half-lives in an aerated static pile were 31 hr (mesophilic) and 17 hr (thermophilic) for RDX and 43 hr (mesophilic) and 25 hr (thermophilic) for HMX. The total explosives concentration in the piles of 16,460 mg/kg and 17,870 mg/kg were reduced to 326 mg/kg (98% reduction) and 74 mg/kg (99.6% reduction),

respectively. High explosives decay was only investigated. No end-product characterization was performed in this study. Further research is needed before industrial facilities can be constructed.

### 2.4.3 Alkaline Hydrolysis

Alkaline hydrolysis has been known as a disposal method for various explosives since World War II. Clear and Rinkenbach (1945) report methods to decompose RDX and explosive compositions that contain RDX in alkaline solutions. For the disposal of 45 kg RDX they used approximately 1100 L of an aqueous solution that contained 5% NaOH. The mixture was heated at the boiling point for 30 minutes. They also reported NaOH to be effective for the disposal of Dinitrotoluene (DNT), Nitrocellulose, composition A and composition C-3. The alkaline hydrolysis of bulk Nitrocellulose combined with biological treatment was recently also investigated by Dahn (1993).

Table 3 Second-order rate constants of the alkaline hydrolysis of RDX (literature results).

Study	Temperature (°C)	Second-order rate constant (L/mol·min)
Epstein and Winkler, 1951 (pH 11 - 12)	0	5.1
	15.5	21.8
Hoffsommer, 1977a (pH 11 - 14)	25	0.23
	35	0.84
	45	2.9
Croce and Okamoto, 1979 (pH not stated)	25	0.24

**Table 4** Second-order rate constants of the alkaline hydrolysis of HMX (literature results).

Study	Temperature (°C)	Second-order rate constant (L/mol·min)
Epstein and Winkler, 1951 (pH 12 - 13)	0	0.0078
	15.5	0.064
	27	0.47
Croce and Okamoto, 1979 (pH not stated)	25	0.018

Several researchers have investigated the alkaline hydrolysis of RDX. In early investigations, Epstein and Winkler (1951) measured rates of the alkaline hydrolysis of RDX and HMX in aqueous acetone systems to determine the amount of HMX impurity in RDX. They found the reaction to be second-order. The activation energies obtained in this study from data for 0°C, 15.5°C and 27°C vary significantly for RDX and HMX (Table 5 ).

**Table 5** Results of the experimental activation energy for the alkaline hydrolysis of RDX and HMX (literature results).

Study	Energy of Activation $E_{A,RDX}$ (kJ/mol)	Energy of Activation $E_{A,HMX}$ (kJ/mol)
Epstein and Winkler, 1951	59	105
Jones, 1953	92	-
Hoffsommer, 1977a	94	-
Croce and Okamoto, 1979	-	102

Jones (1953) presented results regarding the mechanism and stoichiometry of the alkaline hydrolysis of RDX. In this study a classic E2-elimination mechanism was first proposed but was not proven (see next paragraph). No organic intermediates could be detected in this work and therefore intermediates of the mechanism were only proposed. The result for the experimental activation energy (Table 5) varies from the earlier study of Epstein and Winkler (1951). The results are only partially comparable, because different solvents and bases were used. Furthermore, Epstein and Winkler (1951) only briefly described their experimental procedure, making a thorough interpretation of their results difficult.

Hoffsommer et al. (1977a) identified intermediates and end-products of the aqueous homogeneous alkaline hydrolysis of RDX. They showed a kinetic isotope effect in their experiments with deuterium-labeled RDX and concluded that a classic E2-elimination mechanism is the initial and rate-determining step of the alkaline hydrolysis of RDX. The E2-elimination is the most important elimination mechanism in organic chemistry and follows a second-order rate law ( $dc/dt = k_2 \cdot c_{substrate} \cdot c_{base}$ ). If the base also shows nucleophilic character it is accompanied by a nucleophilic substitution (Sykes, 1981); here at the electron-poor C-atom of RDX's heterocyclic ring system.

Identified end- and by-products are  $\text{NO}_2^-$ ,  $\text{N}_2$ ,  $\text{NH}_3$ ,  $\text{N}_2\text{O}$ ,  $\text{HCOO}^-$ ,  $\text{CH}_2\text{O}$  and  $\text{H}_2$ . The formaldehyde is subject to a *Canizarro*-reaction at the elevated pH and produces additional formate (Sykes, 1981). They also experimentally confirmed the hydrolysis to be a second-order reaction. Second-order rate constants were calculated from pseudo first-order

rate data (for excess  $\text{OH}^-$ ). The experimental activation energy (Table 5) is in close accordance to the value Jones (1953) found in his experiments.

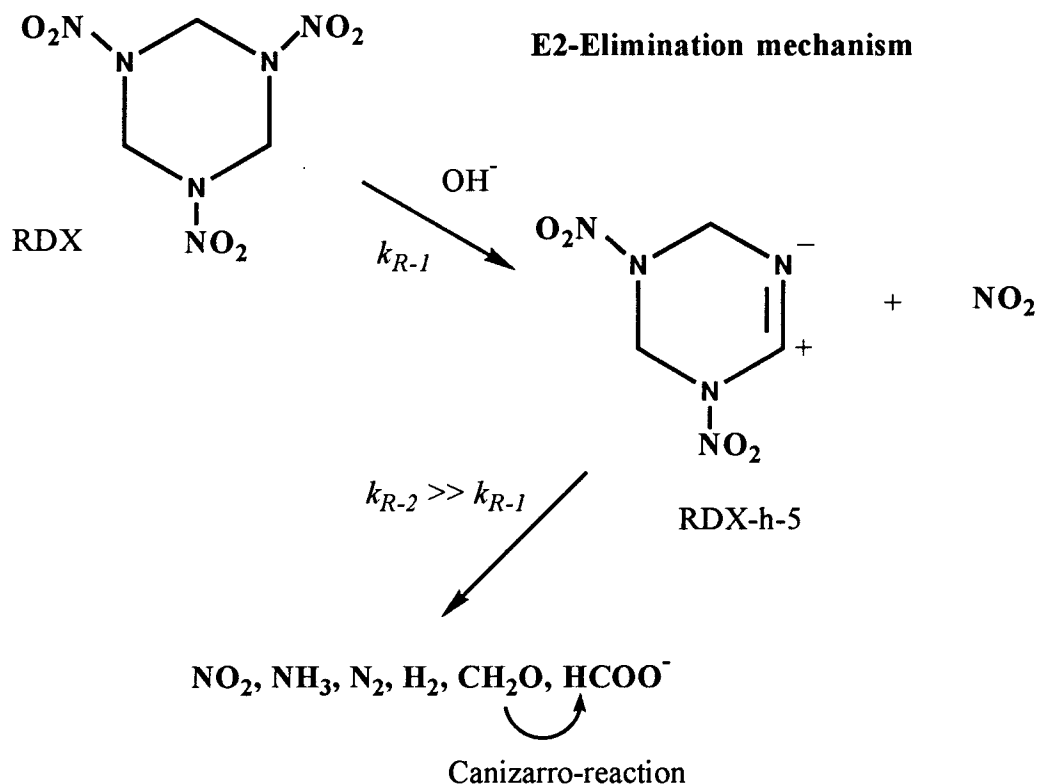


Figure 2 Reaction pathway of the alkaline hydrolysis of RDX (Hoffsommer et al., 1977a).

Rate enhancement effects for the alkaline hydrolysis of RDX and HMX in the presence of a cationic surfactant system were investigated by Croce and Okamoto (1979). Maximum rate enhancements of 100-fold for the alkaline hydrolysis of RDX and 27-fold for the alkaline hydrolysis of HMX were observed. This effect was later applied by Freeman and Colitti (1982) and Freeman (1985) for the treatment of pink water. The results for the

second-order rate constant for the alkaline hydrolysis of RDX at 25°C is in close accordance to the study published by Hoffsommer et al. (1977a). The rate for HMX varies significantly from the results of Epstein and Winkler (1951), which confirms the need for special interpretation of this study. The experimental activation energies obtained for the alkaline hydrolysis of HMX confirm Epstein and Winkler's (1951) earlier study (Table 5). Unfortunately, no new results of the activation energy of the alkaline hydrolysis of RDX were presented in Croce and Okamoto's (1979) study.

Overall, less research has been performed on the alkaline hydrolysis of HMX; however, some similarities to the alkaline hydrolysis of RDX can be anticipated. Epstein et al. (1951) concluded that the alkaline hydrolysis of HMX is second-order. Croce and Okamoto (1979) proposed that the alkaline hydrolysis of HMX follows the same basic mechanism as RDX, with regard to the almost similar activation parameters for HMX and RDX in Hoffsommer et al.'s (1977) and their rate studies. Nevertheless, Croce et al. (1979) also report aqueous standard solutions containing 6, 9 and 12 mg HMX/L, which are above the solubility limit of 5 mg HMX/L. Possible heterogeneous effects in this study may need special interpretation.

Current research is also underway at the Los Alamos National Laboratory. The emphasis in these investigations is on the heterogeneous alkaline hydrolysis of solid RDX, HMX and other bulk high explosives and their accompanying binders in explosive compositions. Spontarelli et al. (1993) demonstrated that many propellants, explosives and pyrotechnics can be base hydrolyzed at temperatures ranging from 60 to 150°C. Much of the research was conducted with the explosive composition PBX-9404 which contains

Nitrocellulose as an energetic binder (see Table 2). As expected, Nitrocellulose also hydrolyzed completely. The alkaline hydrolysis of Nitrocellulose was also applied in other studies on the disposal of nitrocellulose-based propellants (Dahn, 1993). Many of the plastic binders were decomposed as well by alkaline hydrolysis, which will have important implications for future commercial and industrial use of the process. The plastic binders have trace compounds which may create trace hazardous compounds in the hydrolysate.

Mass transport was found to limit the rates of the alkaline hydrolysis of bulk high explosives. Significant rate enhancements were achieved through particle size reduction of the bulk high explosives. Evidently, this can be achieved by appropriate agitation. Ultrasonic agitation was suggested as an alternative to stirring. For the post-treatment of hydrolysis products, biological treatment and treatment by supercritical water oxidation was suggested (Spontarelli et al., 1993).

Alkaline hydrolysis is very slow at neutral pH and ambient temperature. Therefore directly treating large quantities of wastewaters will not be economical due to the energy and base requirements. This has important implications for contaminated water treatment which will be discussed in the next section on the treatment of high explosives contaminated water.

### **3. HIGH EXPLOSIVES CONTAMINATED WATER**

#### **3.1 Contaminated Water Sources**

High explosives contaminated waters exist at former and existing production and loading sites. They are also produced during the production and demilitarization of weapons. Although high explosives contaminated water was discharged without treatment directly into surface waters or into wastewater lagoons and evaporation ponds in the past, current regulations require more appropriate treatment prior to discharge. Wastewaters containing RDX, TNT and small amounts of HMX are created at load, assemble and pack facilities (LAP) and are called pink water. Soil and water contamination usually accompany each other at contaminated sites.

Patterson et al. (1976a, b) report a case of an ammunition plant that discharged about 500 kg of RDX into a nearby river. This wastewater consisted of cooling water, pump seal water, condensate and washdown. By-products of the production process (e.g. HMX) were discharged along with the RDX. Stillwell et al. (1977) reported an average daily discharge of 20 kg of HMX in wastewater at a facility that produced 2.6 tons HMX per day, which is almost 1% of the yield. At full mobilization Kitchens et al. (1978) estimated the discharge of the Holston Army Ammunition plant to be 61 kg of HMX per day. Up to 2000 m<sup>3</sup>/day of contaminated washwater can be produced from one production line due to safety technology requirements (Kooke et al., 1981).

The average yearly effluent concentrations at the only US-facility currently manufacturing RDX and HMX, the Holston Army Ammunition Plant, varied between 2 and

6 mg/L. These wastewaters have been discharged directly in the past and dilution in the receiving surface water reduced the concentrations below the detection limit a few kilometers downstream (Rosenblatt, 1991). Burrows et al. (1984) also report an effluent concentration at the Holston Army Ammunition Plant of 2.8 mg RDX/L and 1.7 mg HMX/L. At six LAP-facilities the wastewater concentrations varied between 0 and 180 mg RDX/L and 0 and 16 mg HMX/L (Patterson et al., 1976a). Only one of these facilities used activated carbon treatment; all others discharged into catch basins or evaporation ponds.

Historically, the US-Army used lagoons for the disposal of wastewater and bulk explosives waste. These lagoons were usually unlined (Garg et al., 1991). Soil contamination at existing and former production and demilitarization sites can lead to significant contamination of groundwater. The primary compounds at these sites are RDX, HMX and TNT. The usual concentrations vary between 70 - 80 mg/kg for RDX and HMX (Envirodyne Engineers, 1980). However, for TNT even extreme concentrations of 3000 mg/kg were observed in one wastewater lagoon bed that had been inactive for 20 years (Sanoki et al., 1976). RDX migrates only slowly in soils, but was nevertheless observed at levels from 20 to 700 µg/L in the vicinity of contaminated sites (Hale et al., 1979).

Currently, contaminated sites in Germany are still being assessed and detailed data on groundwater contamination is scarce. Soil contamination and subsequent groundwater contamination can be expected at many of these suspected sites. The German states of Thüringen, Baden-Württemberg and Sachsen-Anhalt have now assessed 70, 4 and 99 demilitarization sites, respectively (Garn, 1994; Flittner, 1994; Pflugradt, 1994). Haas et al. (1990) report a case of soil contamination at the German Stadtallendorf. The production

wastewaters and process waters from dismantling 30,000 tons of bombs in 1947 - 48 were collected in a channel next to the process water wells. Some of these wells are used today for drinking water. In 1988 RDX concentrations of up to 1.5 µg RDX/L were found in the groundwater in addition to other contaminants. These results indicate that the soil is contaminated to the depth of the wells, which are located 150 m below the surface.

RDX- and TNT containing wastewaters from explosives production are also reported in Australia where a munitions handling facility formerly produced 16 m<sup>3</sup>/day of a wastewater that contained 70 to 150 mg/L of both RDX and TNT (Semmens et al., 1984).

## **3.2 Possible Future Technologies**

### **3.2.1 Oxidative Treatment**

UV-radiation. The destruction of RDX and HMX by ultraviolet radiation (UV) was studied by Burrows et al. (1984). The wavelength applied in this investigation was 254 nm. Decomposition half-lives of 3.7 and 1.3 minutes were found for RDX and HMX, respectively. The respective wastewaters usually contain co-contaminants (e.g. acetic acid) which decrease the effectiveness of this energy-intensive process and may make industrial operation uneconomical.

Furthermore, the treatment of contaminated water with UV-radiation may lead to toxic intermediates (Rosenblatt et al., 1991; Yinon, 1990). This will need special attention for contaminated groundwater treatment, if the groundwater is used for a drinking water supply.

Ozone oxidation. Shelby et al. (1984) studied ozone oxidation for the treatment of a RDX-containing wastewater. It was possible to achieve a 43% reduction of the chemical oxygen demand (COD) within 6 hours using an Ozone-concentration of 20000 mg/L.

Hydrogen peroxide oxidation. Shelby et al. (1984) investigated treatment of a wastewater that contained RDX as the main compound with hydrogen peroxide oxidation. In the presence of an iron catalyst, at a pH of 4 to 4.5 and with a hydrogen peroxide dosage of 8,400 mg/L COD-removal from the wastewater was less than 40% and did not meet discharge grade. The study indicated that hydrogen peroxide in the presence of UV-radiation may be more appropriate.

UV/ozone oxidation. When ozone was combined with UV-radiation it was possible to remove the initial COD of 10,000 mg/L of a RDX-containing wastewater to less than 1 mg COD/L (Shelby et al, 1984). The ozone utilization rate at this point was above 80%. The Ozone dosage was 130 mg/min. That means a total of approximately 140 g Ozone was introduced into the system during the experiment.

UV/hydrogen peroxide oxidation. The results of Shelby et al. (1984) with hydrogen peroxide and UV indicate insufficient removal of the COD of a RDX-containing wastewater. Only 33% of the initial COD was removed and no improvement over hydrogen peroxide treatment alone could be found. This result was obtained with a hydrogen peroxide dosage of 4,200 mg/L, which is half of the dosage used for hydrogen peroxide-*only*-treatment in the same study.

Chlorination. Semmens et al. (1984) showed chlorine to be a possible oxidant for the removal of RDX and TNT from wastewater. Complete removal of 100 mg/L RDX and TNT

was achieved within 45 minutes at pH 9 to 10 in boiling water with 1.5 g  $\text{Ca}(\text{OCl})_2/\text{L}$ . The authors were concerned about possible toxicity of chlorinated products which they did not investigate.

### **3.2.2 Surfactant Technology**

Freeman and Colitti (1982) investigated the use of surfactant technology for the treatment of pink water which contains RDX, TNT and smaller amounts of HMX from the production of composition-B explosive. In an alkaline-surfactant environment TNT is precipitated and the hydrolysis of RDX and HMX is accelerated (see also Section 2.4.3; Croce and Okamoto, 1979). Almost complete TNT precipitation and destruction of RDX after 5 hours using the surfactant Duoquad T-50 were obtained at pH 11 and ambient temperature. The technology was actually a combination of pure surfactant technology for TNT precipitation and the known rate enhancement effect of surfactants for the alkaline hydrolysis of RDX. The possible enhancement effects of further increased hydroxide concentrations (pH 12) and elevated temperatures were discussed.

Freeman (1985) showed that the surfactant Duoquad T-50 in a two-stage continuous-flow reactor was able to remove virtually 100% of both RDX and TNT. The process was also shown to be effective for the removal of other pink-water compounds, e.g. HMX. He also reported improved analytical methods for HMX, RDX and TNT.

### 3.2.3 Biological Treatment

Early biodegradation studies on water containing RDX and TNT showed no evidence for degradation of RDX when enrichment cultures and supplemental yeast extract were used (Osmon and Klausmeier, 1972). McCormick et al. (1981) found almost complete anaerobic biodegradation of RDX in their study. The products of the biodegradation of RDX were found to be hexahydro-1-nitroso-3,5-dinitro-1,3,5-triazine, hexahydro-1,3,-dinitroso-5-nitro-1,3,5-triazine, hexahydro-1,3,5-trinitroso-1,3,5-triazine, hydrazine, 1,1-dimethylhydrazine, 1,2-dimethylhydrazine, formaldehyde, and methanol. Several of these compounds are carcinogenic and/or mutagenic and may present a higher health risk than RDX itself. Post-treatment, possibly aerobically, would therefore be necessary in commercial or industrial operation. Based on their findings McCormick et al. (1981) proposed a mechanism for the biodegradation of RDX.

In a more recent study Binks et al. (1995) identified an aerobic mixed culture that degraded RDX. A bacterium, *Stenotrophomonas maltophilia* PB1, that used RDX as its sole Nitrogen-source was isolated from this mixed culture. Surprisingly, this culture was also able to utilize s-triazine but not HMX for its growth.

Alatraste-Mondragon et al. (1995) also found an organism that utilized RDX for biological growth. An anaerobic, spore-forming gram positive rod was isolated and identified as *Clostridium putrificum*. Peptone, glucose and glycerol were used as co-substrates in this study. Furthermore, RDX-transformation could be observed in partially purified enzyme extracts.

Hesselmann et al. (1992) criticized the common method where the wastewater is treated directly biologically because large amounts of co-substrates need to be added to relatively clean water in the case of munitions industry wastewater. They therefore proposed a system where biodegradation is combined with activated carbon adsorption. In this study high explosives were extracted from activated carbon using solvent regeneration and then the liquid was introduced into a bio-reactor where the solvent was also used as a co-substrate for anaerobic biodegradation. A significant reduction in volume to be treated biologically can be achieved using this method. This proposal is complementary to the treatment scheme used in this study utilizing alkaline hydrolysis.

### **3.3 Adsorption**

Waters contaminated with high explosives generally have been treated by adsorption onto activated carbon (Schulte, 1973; Patterson et al., 1976a, b). The high explosives laden activated carbon that is produced during high explosives contaminated water treatment is a hazardous waste as defined by the US Code of Federal Regulations, particularly code 40 CFR, Part 261 (US-EPA, 1994).

Burning of spent activated carbon has now been banned because of more stringent air quality regulations. Thermal regeneration is problematic because of safety concerns (Andren et al., 1975). Walsh et al. (1973) reports a safety limit for high explosives laden activated carbon of 80 mg high explosives/g activated carbon. These limits are usually exceeded in fixed-bed adsorption because saturation of the activated carbon occurs at solid-phase

concentrations of approximately 200 - 250 mg/g. Incineration of the spent activated carbon may be unavailable because of the same reasons mentioned for burning of activated carbon.

The major disadvantage of the current treatment of high explosives contaminated water by activated carbon is the lack of an economical regeneration technology. For this reason the spent activated carbon is currently stockpiled while awaiting a practical regeneration technology.

### **3.3.1 Activated Carbon**

Even though adsorption of high explosives onto activated carbon is widely applied in the field of military explosives, only a few research studies exist on this treatment technology. Currently, high explosives laden activated carbon is either stored as hazardous waste or incinerated after a single use. Thermal regeneration is not possible due to safety concerns (see Section 3.4.1). The problem of an appropriate regeneration technology for high explosives laden activated carbon has yet not been addressed in the literature. Most of the existing research is limited to preliminary adsorption isotherm data.

Patterson et al. (1976c) studied the removal of RDX-, HMX- and TNT-mixed wastewaters in packed activated carbon columns. A column with a total volume of 57 L was fed with an average influent concentration of 5 mg RDX/L and 10 mg TNT/L. The empty-bed contact time ( $t_{re}$ ) was 3.3 minutes and 99.5% of RDX and TNT was removed using this system. The data were also compared with polymeric resin adsorption, but the resin could not achieve the same effectiveness, particularly for RDX where removal efficiency was as low as 30% due to the low adsorptive capacity of the resin.

Another effect discussed in this study was the competitive adsorption of compounds such as RDX, HMX and TNT. It was shown that RDX breakthrough occurs much earlier than TNT breakthrough which limits the complete process. Competitive adsorption of RDX, HMX and TNT, which often occur together at contaminated sites, will require special attention if activated carbon adsorption is used.

Shelby et al. (1984) studied the adsorption of RDX and other compounds on activated carbon. Unfortunately, their isotherm is based on COD-removal. They provide too little information to distinguish RDX adsorption and acetic acid adsorption. It is well known that acetic acid adsorbs very weakly onto activated carbon.

Burrows et al. (1984) investigated adsorption isotherms of RDX and HMX on the activated carbon Filtrasorb-300, and modeled their data with the *Freundlich*-equation (Table 6). The results for  $K$  are relatively high when compared to other studies. The negative effect of competitive adsorption when typical co-contaminants are adsorbed onto activated carbon at contaminated sites was also investigated. Adsorption of mixed contaminants from wastewaters was found to be less effective than single compound adsorption onto activated carbon.

Wujcik et al. (1992) identified *Freundlich*-isotherm parameters for RDX on various activated carbons (Table 6) in a pilot plant study on column activated carbon adsorption on various high explosives. The results vary significantly from the earlier study by Burrows et al. (1984). Unfortunately, both studies do not present enough background on their experimental methods. Therefore, the difference in data is hard to interpret.

Table 6 Results for the *Freundlich*-isotherm of RDX and activated carbon in the literature.

Study	Activated carbon brand	K (L/g) <sup>1/n</sup>	1/n ( )
Wujcik et al. (1992) - RDX	Filtrisorb-400	49	0.555
	Filtrisorb-300	31	0.413
	Filtrisorb-200	52	0.535
Burrows et al. (1984) - RDX	Filtrisorb-300	112	0.340
Burrows et al. (1984) - HMX	Filtrisorb-300	168	0.461

Wujcik et al. (1992) also studied column adsorption using a wastewater that contained RDX, HMX, TNT, DNT and some related compounds. An 11 liter column packed with Filtrisorb-300 (bed depth 1.2 m) was operated at an  $t_{re}$  of 4.2 minutes. None of the investigated compounds could be detected in the effluent for 17 days. The test was concluded before breakthrough occurred. In a second test the bed depth was 0.6 m and the  $t_{re}$  was 2 minutes. After one month breakthrough was evident and RDX and TNT were both detected in the effluent at 344 and 192  $\mu\text{g/L}$ , respectively.

### 3.3.2 Resin

In addition to activated carbon, synthetic resins show promise for the adsorption of high explosives. However, their capacity is usually lower than the adsorptive capacity of activated carbon and their price is usually higher. The classical advantage of resin adsorption is the absence of chemisorption. Adsorption on resins is believed to be governed by van der

Waals forces, only. Solvent regeneration of spent resins should be easy and should not lead to a decrease in capacity.

Andren et al. (1975) investigated Amberlite XAD-resins (Rohm and Haas) to remove RDX, HMX and TNT from pink water. They also successfully regenerated the spent resin with acetone. However, the regeneration liquid still presents a hazardous waste. In another study Hoffsommer and Kubose (1977a) used strongly basic ion-exchange resins to remove RDX from wastewater (see Section 3.4.4).

### **3.4 Adsorbent Regeneration**

Although few research studies exist on the regeneration of high explosives-laden activated carbon, the regeneration problem has been addressed in general for spent activated carbon loaded with a variety of toxic organics. Thermal regeneration of the spent activated carbon has been the method of choice for several years. Deficiencies of this process are the high investment cost of the regeneration furnace, possible toxic emissions, and the loss of approximately 10% activated carbon per regeneration cycle. Therefore, various chemical and biological regeneration technologies were investigated worldwide.

#### **3.4.1 Thermal Adsorbent Regeneration**

Thermal regeneration of spent activated carbon has long been the "state of the art"-regeneration technology in industrial adsorption applications. Thermal regeneration of high explosives laden activated carbon is, however, not an available technology due to safety

concerns. Andren et al. (1975) reported concentrations above a threshold concentration of 80 mg high explosives/g activated carbon to be unacceptable for thermal regeneration due to strict safety regulations in the military explosives industry. Operation of activated carbon treatment systems for the removal of high explosives from wastewater is not economical at these relatively low solid phase concentrations since loads of 200 - 250 mg high explosives/g activated carbon will be easily achieved, particularly when mixed adsorption occurs.

### **3.4.2 Biological Adsorbent Regeneration**

Bioregeneration of activated carbon was until now only demonstrated for well-degradable compounds such as phenolics (Hutchinson and Robinson, 1990). This process may not be available for regeneration of high explosives laden carbon, since biodegradation of compounds such as RDX, HMX and TNT is slow and only possible under very complex and usually anaerobic conditions (Alatrisc-Mondragon, 1995 submitted). Craveiro de Sa and Malina (1992) developed a model for the bioregeneration of activated carbon. Unfortunately, they only presented a schematic of the model and did not provide any modeling of experimental data.

A process using solvent regeneration of RDX laden activated carbon using ethanol was presented by Hesselmann et al. (1992). In this process RDX is adsorbed onto activated carbon from contaminated water. After exhaustion of the carbon the activated carbon is regenerated off-line by an aqueous ethanol solution and the solution is subsequently treated in an anoxic bio-reactor where the ethanol is used as a co-substrate.

### 3.4.3 Chemical Adsorbent Regeneration

Electrochemical regeneration. Recently the use of electrochemical methods was investigated by Narbaitz and Cen (1994). In this study phenol laden activated carbon was regenerated in a 1% NaCl solution (electrolyte) using anodic electrolysis which was found to be more effective than cathodic electrolysis. Maximum regeneration efficiencies of 95% were achieved when 100 mA were applied for 5 hours. Comparable efficiencies can be achieved when lower currents are used for longer duration. Multiple regeneration was found to reduce the regeneration efficiency by another 2% for each cycle.

Solvent regeneration. The use of solvents (organic or inorganic), acids (organic or inorganic) and alkaline solutions or a combination of the above for the regeneration of activated carbon were studied most extensively:

The use of a heated (100 - 110°C) alkaline regenerant solution was first mentioned by Rovel (1972). This study used activated carbon laden with numerous nitrated by-products from the synthesis of PTBB (Para-tertio-butyl-benzic acid). Here, the alkaline treatment was a process-stage preceded by initial hydrochloric acid treatment at room temperature and followed by solvent regeneration with ethanol at 80°C. Vapor at 120 - 140°C was used as the final treatment. If required, the activated carbon was neutralized with hydrochloric acid.

Beccari et al. (1977) investigated various organic and inorganic solvents as well as acid and alkaline treatment for the regeneration of spent activated carbon. They achieved a regenerative efficiency of peptone exhausted activated carbon of 50% when using a 6-M NaOH-solution at 80°C. When a subsequent extraction step with acetic acid was applied they achieved a regenerative efficiency of 100% with the combined method.

Martin and Ng (1985) investigated a wide variety of possible organic and inorganic regenerants. They found the molecule size of both the adsorbate and the regenerant to be the controlling factor in penetrating the activated carbon pores. The smaller the adsorbate the further it could penetrate into the micropore system of the adsorbent and therefore resist displacement by the regenerant.

They showed high regenerative efficiencies in subsequent work (Martin and Ng, 1987) with three adsorbates of significantly different molecular weight, Nitrobenzene, Rhodamine B and humic acid, when formic and acetic acid were used as regenerants. However, Newcombe et al. (1993a) criticized that surface charge effects were not interpreted in this study. The extraordinarily high regenerative efficiencies of 150% with humic acid were achieved without any prior removal of the adsorbed material during regeneration. Newcombe et al. extensively studied surface charge effects during the regeneration of activated carbon (1993a, 1993b, 1994). They concluded that the high regenerative efficiency was solely due to a charge effect. The pH in Martin and Ng's (1987) study was changed from 9 before regeneration to 3 after acid-treatment.

It is well known that the adsorption of organics generally increases at decreasing pH and *vice versa* decreases at high pH (Müller et al., 1980). By changing the pH the surface charge of the adsorbent can be altered so that the increase in adsorptive capacity after this change may be so significant that extraordinary regenerative efficiencies will be achieved. The term "regenerative efficiency" is hence problematic and its definition in the various studies needs special consideration. In the present study a different approach to regenerative efficiency was chosen (see Section 6.3.4).

Complementing the findings of Newcombe et al. (1993a, 1993b, 1994) and Sontheimer et al. (1988) concluded that the use of alkaline solutions alone leads only to poor desorption (20 - 30%) of adsorbates due to the charge effect that leads to a shift in equilibrium conditions and adsorptive capacity.

In all these studies the regeneratability with alkaline solutions was contributed solely to the shift in the adsorption equilibrium at the higher pH. It was not yet understood that hydrolysis at high or low pH could be a powerful process in the regeneration of adsorbents that are loaded with pollutants that undergo hydrolysis reactions at high or low pH.

#### **3.4.4 Alkaline Hydrolysis Regeneration**

The alkaline hydrolysis of RDX was first mentioned as a possible regeneration process for adsorbents in a study by Hoffsommer and Kubose (1977). In a previous study Hoffsommer et al. (1977) investigated the chemistry of the alkaline hydrolysis of RDX under aqueous homogeneous conditions. Their findings were then applied in the study on the alkaline hydrolysis of RDX as part of a regeneration process using strongly basic ion-exchange resins. The approach in the regeneration study was different than presented in the present dissertation.

In the first step, the  $\text{Cl}^-$ -groups of a polymeric ion-exchange resin (Amberlite 400 and 410) were exchanged with  $\text{OH}^-$ -groups using 1-M aqueous NaOH. The strongly basic resin ( $\text{OH}^-$ -form) was then used to adsorb RDX from contaminated water. Adsorbed RDX interacted and hydrolyzed in the presence of the  $\text{OH}^-$ -surface groups to the already known products (see Section 2.4.3). The spent resin had altering  $\text{NO}_2^-$  and  $\text{OCHO}$ -surface groups.

In the subsequent regeneration step the resin was returned to the  $\text{Cl}^-$ -form using 1-M aqueous NaCl yielding  $\text{NO}_2^-$  and  $\text{HCOO}^-$ . The other hydrolysis products  $\text{NH}_3$ ,  $\text{N}_2\text{O}$ ,  $\text{N}_2$ ,  $\text{CH}_2\text{O}$  did not adsorb onto the resin.

It remains unclear why the authors did not consider RDX adsorption onto a conventional nonpolar resin with subsequent regeneration of the resin with an alkaline solution. This approach, whether applied on a conventional adsorbent (activated carbon) or a resin, was chosen in this study because it combines the two processes: adsorption of the contaminant on an adsorbent, and subsequent regeneration by alkaline hydrolysis in the simplest way.

Spitzer et al. (1994) recently described a similar process with a different adsorbent-adsorbate system than presented in this work. Alkaline hydrolysis was used to regenerate exhausted activated carbon and adsorption resins (Wofatit Y 77) loaded with *o,o*-Dimethyl-*o*-(4-nitrophenyl)-thiophosphate, a phosphoric acid ester, that undergoes hydrolysis reactions at elevated hydroxide concentrations. Hydrolysis was studied under homogeneous conditions and on adsorbents. Regeneration was carried out at pH 11.7 and the hydrolysis reaction was found to be of pseudo first-order initiated by a nucleophilic attack at the phosphor. Even though almost indefinite regenerability of polymeric resins was claimed, after 6 adsorption-regeneration cycles a loss of the adsorptive capacity of 30% was found.

#### 4. OBJECTIVES OF THIS STUDY

RDX and HMX undergo complete hydrolysis reactions at higher pH and elevated temperatures to form  $\text{NO}_2^-$ ,  $\text{N}_2\text{O}$ ,  $\text{N}_2$ ,  $\text{NH}_3$ ,  $\text{HCOO}^-$  and  $\text{HCHO}$  (see Section 2.4.3). Direct treatment of contaminated water with alkaline hydrolysis is not economical because RDX and HMX are only sparingly soluble in water. The solubility limits at 25°C are: approximately 50 mg RDX/L (Gibbs and Popolato, 1980) and approximately 5 mg HMX/L (Rosenblatt, 1991). A concentration step prior to alkaline hydrolysis treatment can enhance the economy of the process by considerably reducing the amount of required NaOH.

Therefore, the main objective in this study was to define process conditions for a new treatment process using adsorption of RDX and HMX on granular activated carbon (GAC) and subsequent off-line-regeneration of spent GAC through alkaline hydrolysis (Figure 3):

- In the first step the contaminated water is treated through RDX- and HMX-adsorption onto GAC, which concentrates the contaminants on the activated carbon and reduces the volume of material to be treated with alkaline hydrolysis. Clean water is being discharged from the first stage.
- In the second step the spent activated carbon is regenerated off-line with a recirculating alkaline solution at an elevated temperature. The solution can be subsequently reused to treat another charge of contaminated water as explained in step 1. The products of the alkaline hydrolysis are water soluble.

Before the process can be applied in industrial or commercial plants more basic research and development are necessary.

This research was undertaken to answer the basic research and development questions. A series of process development questions were found and are listed in the following sections:

#### **Adsorption of RDX and HMX on Activated Carbon**

1. What are the adsorption equilibria of RDX and HMX on activated carbon (adsorption isotherms)?
2. How does the adsorption proceed as a function of time (adsorption kinetics)?

#### **Chemical Kinetics, Intermediates and End-Products**

1. Under what process conditions (temperature and pH) does the alkaline hydrolysis of RDX and HMX proceed to completion and how much time is needed to reach equilibrium under aqueous homogeneous conditions?
2. What are the stable intermediates and end-products of the alkaline hydrolysis of RDX and HMX and what is the time dependence of their formation?
3. Are any toxic and previously unknown intermediates or products being formed during the alkaline hydrolysis of RDX and HMX?
4. What are the molar yields of the products? How much carbon and nitrogen can be recovered (mass balances)?

### **Regeneration of Spent Activated Carbon**

1. How does the alkaline hydrolysis of RDX and HMX proceed on activated carbon in comparison to the results under aqueous homogeneous conditions? Do the products desorb completely?
2. Does repeated exhaustion and alkaline hydrolysis regeneration of activated carbon change the characteristics of activated carbon (regenerative efficiency)?

### **Application of the Process in a Fixed Bed Adsorber**

1. Is the process in principal feasible in continuously operated columns? How can the results from the previous parts of this work be used to design a continuous process setup in a fixed bed adsorber?
2. What are the empty-bed contact times ( $t_{re}$ ) needed for fixed-bed operation (breakthrough curves)?
3. What are the necessary regeneration conditions in fixed-bed mode in comparison to the results for batch mode?

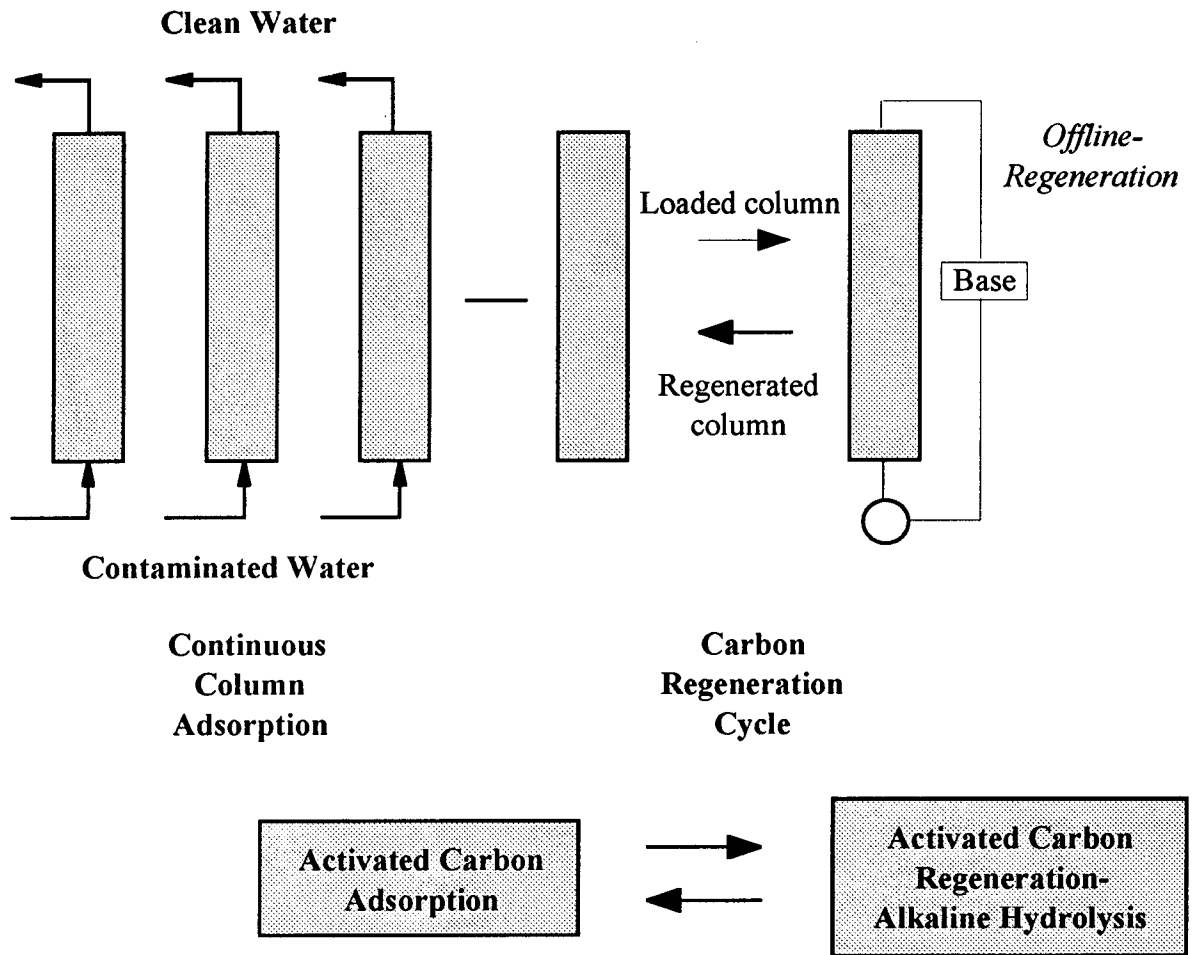


Figure 3 Proposed process scheme for the treatment of high explosives contaminated water using activated carbon adsorption and regeneration of laden activated carbon by alkaline hydrolysis.

## **5. MATERIALS AND METHODS**

### **5.1 Materials**

#### **5.1.1 High Explosives**

RDX (Hexahydro-1,3,5-trinitro-1,3,5-triazine; CAS: 121-82-4) and HMX (Octahydro-1,3,5,7-tetranitro-1,3,5,7-tetrazocine; CAS: 2691-41-0) were obtained from the Lawrence Livermore National Laboratory (LLNL) and the US Department of Energy's (DOE) Pantex Plant. LLNL-RDX had an impurity of approximately 9% HMX. Both LLNL and Pantex Plant HMX contained less than 1% of RDX. Pantex plant RDX contained less than 1% HMX. The LLNL-RDX and HMX were used in all experimental studies whereas the "pure" RDX and HMX were used mainly as analytical standards.

#### **5.1.2 Activated Carbon**

The activated carbon brands used were Filtrasorb-400 (Calgon Corporation, Pittsburgh, PA) and Alamo Brand Granular 30 (ABG-30, Alamo Water Refiners, San Antonio, TX). In commercial, technical and scientific applications Filtrasorb-400 is widely used. Therefore, research results with Filtrasorb-400 can be compared very well with other studies on activated carbon adsorption.

ABG-30 is a less known activated carbon mainly used for commercial applications. As part of the cooperation with DOE's Pantex Plant, spent ABG-30 from an actual production site was obtained. This had the advantage that the results with "synthetically" laden Filtrasorb-400 could be compared with a spent activated carbon that contained high

explosives from nuclear weapons dismantling as well as an unknown amount of background materials.

The manufacturer specifications for both activated carbons are shown in Table 7.

Table 7 Manufacturer specifications for activated carbons Filtrasorb-400 and Alamo Brand Granular ABG-30.

	Filtrasorb-400	ABG-30
Iodine Number (minimum)	1000	900
Abrasion Number (minimum)	75	75
Effective Size (mm)	0.8-1.0	1.5-1.7
Effective Size (mm)	0.8-1.0	1.5-1.7
US Standard Sieve Size Fraction	12x40	8X30
Surface Area, N <sub>2</sub> -BET (m <sup>2</sup> /g)	950-1050	900-1000
Density (g/cm <sup>3</sup> )	0.43	0.52

## 5.2 Analytical Methods

### 5.2.1 High Performance Liquid Chromatography (HPLC)

HPLC - Variable wavelength detection. Dissolved RDX and HMX were analyzed using High-Performance Liquid Chromatography with a variable wavelength UV-detector (HPLC/UV, Hewlett-Packard Series 1050) set to 236 nm. The mobile phase consisted of 40% water, 30% methanol and 30% acetonitrile (volume-%). The volumetric flow rate was 1 mL/min. All solvents were HPLC-grade (Fisher Scientific, Springfield, NJ).

An Adsorbosphere-C18-10 micron reversed-phase column (Alltech, Deerfield, IL) was used for the separation. A pre-filter element and guard column assembly (C18-5 micron, Alltech) was used to protect the analytical column. The injection volume was set to 20  $\mu$ L using the autosampler. The run-time was 6 minutes. Peaks were detected at retention times between 4.1 and 4.3 minutes (RDX) and 3.5 and 3.7 minutes (HMX), respectively.

The peak area was a linear function of the concentration between 0.1 - 40 mg/L (RDX) and 0.1- 5 mg/L (HMX), respectively. Standards were prepared for 0.9, 4.5, 9, 18 and 36 mg RDX/L and 0.5, 1, 2, 4 and 5 mg HMX/L. The amount of HMX-impurity contained in the RDX was quantified. A concentration of 0.1 mg/L was found to be the detection limit with this method. For the external calibration, at least three data points were gathered for each standard concentration. The mean was then used for the calibration curve.

All samples were filtered through sterile Acrodisc-13 0.2  $\mu$ m syringe-microfilters (Gelman Sciences, Ann Arbor, MI) before injection. Samples which were not run immediately were cooled in ice-water.

HPLC - Diode array detection. The wavelength for routine variable wavelength detection HPLC was verified with a Hewlett Packard 1050 HPLC equipped with a diode-array detector at the Lawrence Livermore Laboratory (all machine specifications as described above for variable wavelength HPLC). The UV-spectra of RDX and HMX are shown in Figure 4. It is evident that 236 nm is a good compromise for the routine detection of RDX and HMX in one HPLC-run.

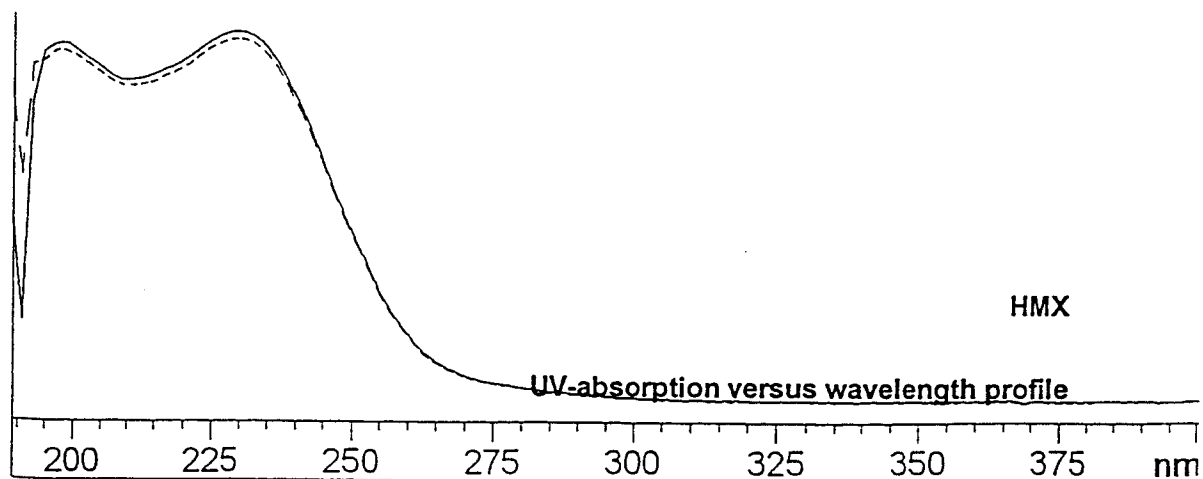
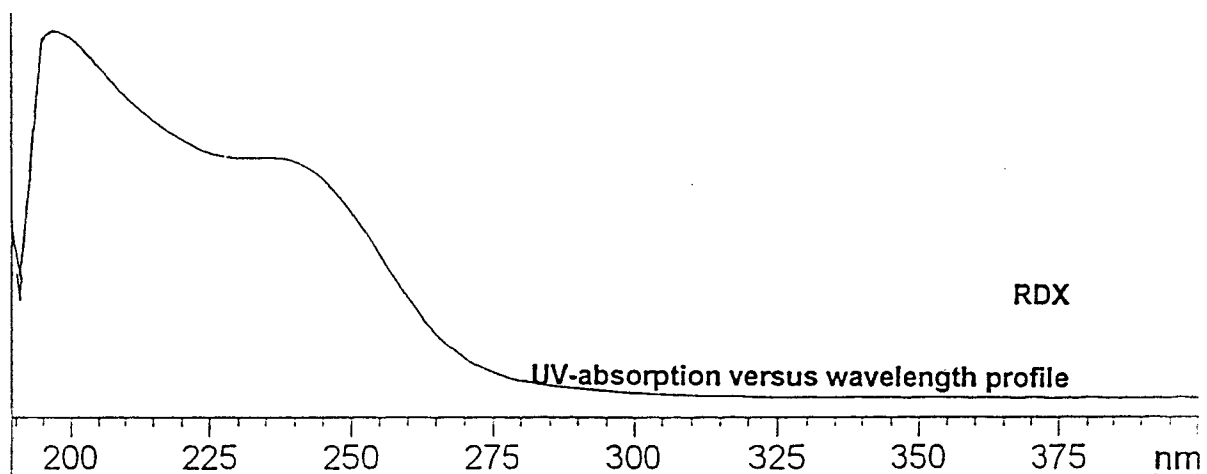


Figure 4 UV-spectra of RDX and HMX from HPLC-diode array detection.

### 5.2.2 Ion Chromatography (IC)

Ion chromatography-formate and nitrite. The anions  $\text{NO}_2^-$  (nitrite) and  $\text{HCOO}^-$  (formate) were analyzed using a Dionex Ion Chromatography (basic chromatography module CMB-2, gradient pump GPM-1; Dionex, Sunnyvale, CA). Suppressed conductivity detection was applied (conductivity detector CDM-1).

An Ion Pac AS9-SC analytical column (4 mm I.D.) was used with a subsequent suppressor column. The mobile phase consisted of 0.75 mM  $\text{NaHCO}_3$  and 2 mM  $\text{Na}_2\text{CO}_3$  dissolved per 1L of milli-Q water. The eluent flow rate was set to 2 mL/min. Samples were manually injected into a 50  $\mu\text{l}$  sample loop.

Peaks were detected at retention times between 1 and 1.1 minutes ( $\text{HCOO}^-$ ) and 1.7 and 1.8 minutes ( $\text{NO}_2^-$ ), respectively. The runtime was varied between 5 and 15 minutes depending on the samples and to provide complete elution of possible contaminants. The peak area was a linear function of the concentration between 0.33 and 13.24 mg/L ( $\text{HCOO}^-$ ) and 0.33 and 13.33 mg/L ( $\text{NO}_2^-$ ), respectively.

Standards were prepared for 0.33, 0.66, 3.3, 6.6 and 13.24 mg  $\text{HCOO}^-/\text{L}$  and 0.33, 0.67, 3.33, 6.67 and 13.33 mg  $\text{NO}_2^-/\text{L}$ . We found 0.01 mg/L to be the detection limit with this method at neutral pH. For the external calibration, at least three data points were gathered for each standard concentration. The mean was then used for the calibration curve. The pH influenced the determination of the  $\text{HCOO}^-$ - and  $\text{NO}_2^-$ -concentration. Therefore, standard curves were obtained for neutral pH and also pH 11 and 12.

All samples were filtered through sterile Acrodisc-13 0.2  $\mu\text{m}$  syringe-microfilters (Gelman Sciences, Ann Arbor, MI) and cooled in ice-water.

Ion chromatography-acetate. Acetate-ion ( $\text{CH}_3\text{COO}^-$ ) analysis was performed on a Dionex 2110i ion chromatograph with a AS10 analytical column and AG10 guard column (Dionex, Sunnyvale, CA). The mobile phase was 70 mM NaOH. The flow rate of the eluent was 1 mL/min. A suppressed conductivity detector was applied. The sample injection volume was 50  $\mu\text{L}$ . The retention time for acetate-ion with this method was 4.3 minutes. Standard curves were obtained for 2, 4, 6, 8, 12, 16 mg/L. The pH had no influence on the detection with this method in the observed pH-range from neutral to pH 12.

### **5.2.3 Gas Chromatography/Mass Spectrometry (GC/MS)**

#### *i. Sample Preparation: Liquid-Liquid-Extraction (LLE)*

Prior to GC/MS-analysis aqueous samples were extracted and concentrated with dichloromethane (Optima-grade, Fisher Scientific). 1000 mL of sample were contacted with 100 mL of dichloromethane in a Pyrex Accelerated One-Step Extractor Concentrator (Pyrex, Corning, Corning, NY). The concentrator tube was kept in a water bath at 80°C. Recondensation of the recirculating dichloromethane was achieved with a condenser on top of the extractor body that was operated at 2 - 4 °C (provided through recirculating coolant from a Fisher-Isotemp water bath and recirculator).

After 5.5 hours the extraction was complete and the bottoms were concentrated to 1 - 5 mL. The sample volume was further reduced by evaporation to 500  $\mu\text{L}$  with 99.999% Helium. The concentrated sample was transferred into an autosampler vial using a gas tight syringe with attached luer-tip needle. The vial was closed and sealed with a Teflon-lined cap. The final sample concentration was 1:2000 with this method.

## *ii. Gas Chromatography/Mass Spectrometry*

A Finnigan GC/MS-system, consisting of a Finnigan gas chromatograph model-9610 equipped with a Grob-type splitless injector and a Finnigan quadrupole mass spectrometer model-4000 with an INCOS model-2300 data system, was used (Finnigan, Sunnyvale, CA). The GC/MS was operated with an electron energy of 70 eV. The source temperature was 240°C. A scan speed of 1 s scan<sup>-1</sup> was used from 50 to 550 amu. A 30 m DB5-MS (0.25 mm I.D., 25 µm film thickness, J&W Scientific, Folsom, CA) fused silica column was used. The temperature was programmed for 4 minutes at 30°C, then up to 300°C at 6°C/min and hold at 300°C for 60 minutes. The carrier gas was Helium at a flow rate of 35 cm/s.

### **5.2.4 BET-Surface Area Measurements**

BET-surface area measurements of activated carbon were performed on a Gemini 2360 surface area analyzer. The multipoint BET and Langmuir surface area was determined. Only the BET-surface area is presented in this work. Pure nitrogen was used as the analysis gas. Helium was used for free space measurements to determine any volume difference between the reference and the sample tube. Liquid nitrogen was used to cool the samples during analysis. Prior to analysis the samples were degassed at 110°C using a Flow Prep 060 flowing gas (N<sub>2</sub>) degasser.

### **5.2.5 Gas Analysis**

Gas analysis of alkaline hydrolysis products was performed in a gas-tight stainless steel reactor (Parr-Instruments, Moline, IL). The total reactor volume was 465 mL. The

system was sealed and evacuated before a run with a vacuum system. Subsequently, the required amount of base was added into the sealed system. The solution was kept at a constant temperature ( $T = 90^{\circ}\text{C}$ ) and continuously stirred. The system pressure was measured. The gas samples were analyzed with a CEC 21-104 mass spectrometer (CEC, now Du Pont Corporation, Chicago, IL).

### 5.2.6 Miscellaneous Analytical Methods

#### *i. pH*

A Fisher Accumet (Model 25, Fisher Scientific) pH/Ion meter with a Fisher pH-electrode was used for all pH-measurements. The Fisher calibration solutions for pH 7 and pH 10 were used.

#### *ii. Ammonia*

The ammonia-concentration was measured with a Orion-95-12 (Orion Research, Boston, MA) ammonia-electrode. The electrode was calibrated using the Orion-951006 standard solution (0.1 M  $\text{NH}_4\text{Cl}$ ). A Fisher Accumet (Model 25, Fisher Scientific) pH/Ion meter was used.

#### *iii. Temperature*

Precision scientific thermometers ( $1/10^{\circ}\text{C}$  scaling;  $1^{\circ}\text{C}$  was equivalent to approximately 1 cm) were used for all kinetic studies. The criteria for a kinetic experiment

was constant temperature within the range  $\pm 0.1^{\circ}\text{C}$  of the target temperature at least one hour prior to a kinetic run.

## 5.3 Batch Experiments

### 5.3.1 Chemical Kinetics: Batch Studies

Homogeneous kinetics. Experiments were performed in a water bath (Haake E52) at 50, 60, 70,  $80^{\circ}\text{C}$ , which was held at constant temperature for at least one hour prior to the start of an experiment. From a stock solution (approximately 4 mg HMX/L or 36 mg RDX/L, respectively) 1000 mL were placed into a reaction vessel (1000-mL Erlenmeyer) and heated in the water bath until a constant temperature was reached. The mixture was stirred by an overhead motor stirring unit with stainless steel mixer.

The appropriate amounts of  $\text{OH}^{-}$  in order to reach a pH of 10 to 12 were added using a Eppendorf adjustable pipetter, or using a common pipette when 23 mM NaOH was added in the experiment with HMX. 1-M NaOH was used for the experiments with HMX (0.22, 2.1, 23 mM  $\text{OH}^{-}$ ). 1-M (1.5 and 2.1 mmol) and 10-M NaOH (10 and 20 mmol) was used with RDX. The volume change was evaluated for the experiments with 23 mmol.

A precision scientific timer was set simultaneously to the start of an experiment. Samples of 1 mL were taken at predefined times using 1 cc-microsyringes and attached needles. The time for sample collection was 2 seconds. The samples were then immediately filtered into cooled ( $0^{\circ}\text{C}$ ) HPLC vials and a HPLC-run or IC-run commenced as soon as possible after sample collection.

Quenching of the samples with acid was impracticable because of interactions of the acid with the sample. This was particularly true for IC-analysis where the  $\text{Cl}^-$  or the  $\text{SO}_4^{2-}$ -ions of hydrochloric and sulfuric acid overloaded the analytical column and covered all peaks of interest. Therefore, very rapid cooling to  $0^\circ\text{C}$  was chosen to quench the reaction.

### 5.3.2 Ammonia Experiments

The ammonia concentration could not be determined in the experiments above, because of the volatile character of ammonia (particularly at the elevated pH and temperature). In order to determine the ammonia production separate experiments were performed: 40 mL of an aqueous RDX-solution were placed into vials and 80  $\mu\text{L}$  of 10-M NaOH (pH 12) or 80  $\mu\text{L}$  of 1-M NaOH (pH 11), respectively, were added. The vials were immediately sealed with a Teflon-lined cap and put into a water bath (Haake E52) at constant temperature.

Selected vials were then taken from the water bath at precise time intervals and immediately cooled in an ice-water bath ( $T = 0^\circ\text{C}$ ). The ammonia concentration was then measured using an ammonia-electrode (see Section 5.2.6).

### 5.3.3 Activated Carbon Isotherms

#### *Virgin Activated Carbon Isotherms*

Granular activated carbon was ground to a fine powder in order to reduce the time until equilibrium. The 325 x 200 mesh-size fraction ( $45\ \mu\text{m} \times 75\ \mu\text{m}$ ) of virgin activated carbon Filtrasorb-400 was used. Aliquots of the activated carbon varying between 20 mg

and 600 mg were put into 1 L-Erlenmeyer flasks that contained an aqueous solution of RDX (approximately 36 mg RDX/L) and then stirred on a magnetic stirrer until equilibrium was reached. The same procedure was followed for the HMX-isotherm: activated carbon aliquots varied between 0.4 mg and 35 mg here and the solution contained approximately 3.6 mg HMX/L.

The virgin ABG-30 isotherm was obtained using a similar procedure; however, the complete ground fraction was used, because the ABG-30 isotherm data were not intended to be used for kinetic modeling with the HSDM-model.

#### *Isotherms for Regenerated Activated Carbon*

The same procedure as described above was used to evaluate the adsorption equilibria for activated carbon that was repeatedly spent and regenerated. However, the complete ground fraction was used because the results were not intended to be used for further kinetic modeling. Also, only four or five isotherm points were determined for regenerated activated carbon. This is appropriate since the focus of the regenerated isotherm study was not on maximum accuracy of the isotherm parameters but to determine regenerative efficiency over a wide concentration range.

## **5.4 Fixed Bed Adsorber Experiments**

Column adsorption studies were performed in Omni-glass columns (10 mm I.D., 250 mm length) with water jackets and low-pressure Omnifit-fittings (Rainin, Emeryville, CA).

The water jacket could be flushed with hot or cold thermostated water (depending on the process mode) from a recirculator (Fisher 9105-heater/cooler recirculator, Fisher 8005-heater recirculator). The height of the carbon bed was approximately 30 mm for 1 g of activated carbon Filtrasorb-400 and 70 mm for experiments with 2.4 g activated carbon Filtrasorb-400, resulting in height to diameter ratios of 1:3 and 1:7. The height of the activated carbon-beds was set with adjustable column end fittings and the bed was separated with a set of 53  $\mu\text{m}$  and 143  $\mu\text{m}$  nylon screens on both ends (Spectra/Mesh, Fisher Scientific, Springfield, NJ). In the experiments with 1 g activated carbon, glass beads (3 mm; Fisher Scientific) were used on both ends of the bed to finely adjust the bed-height and homogenize the volumetric flow. The height of the beads was approximately 15 mm.

Prior to an adsorption experiment the bed was rinsed with hot deionized water for at least 6 hours. The influent was pumped to the column from 100 L carboys that were continuously stirred on a magnetic stirrer. An inlet-filter was used (05-0141, Rainin). A peristaltic cartridge pump was used (pump-drive: 7524-00, pump-head: 7519-20, cartridge: 7519-65; Cole-Parmer, Niles, IL) with Masterflex tubing (silicone, size-13 and 14). Samples of the influent- and effluent concentration were taken at precise time intervals and analyzed with HPLC.

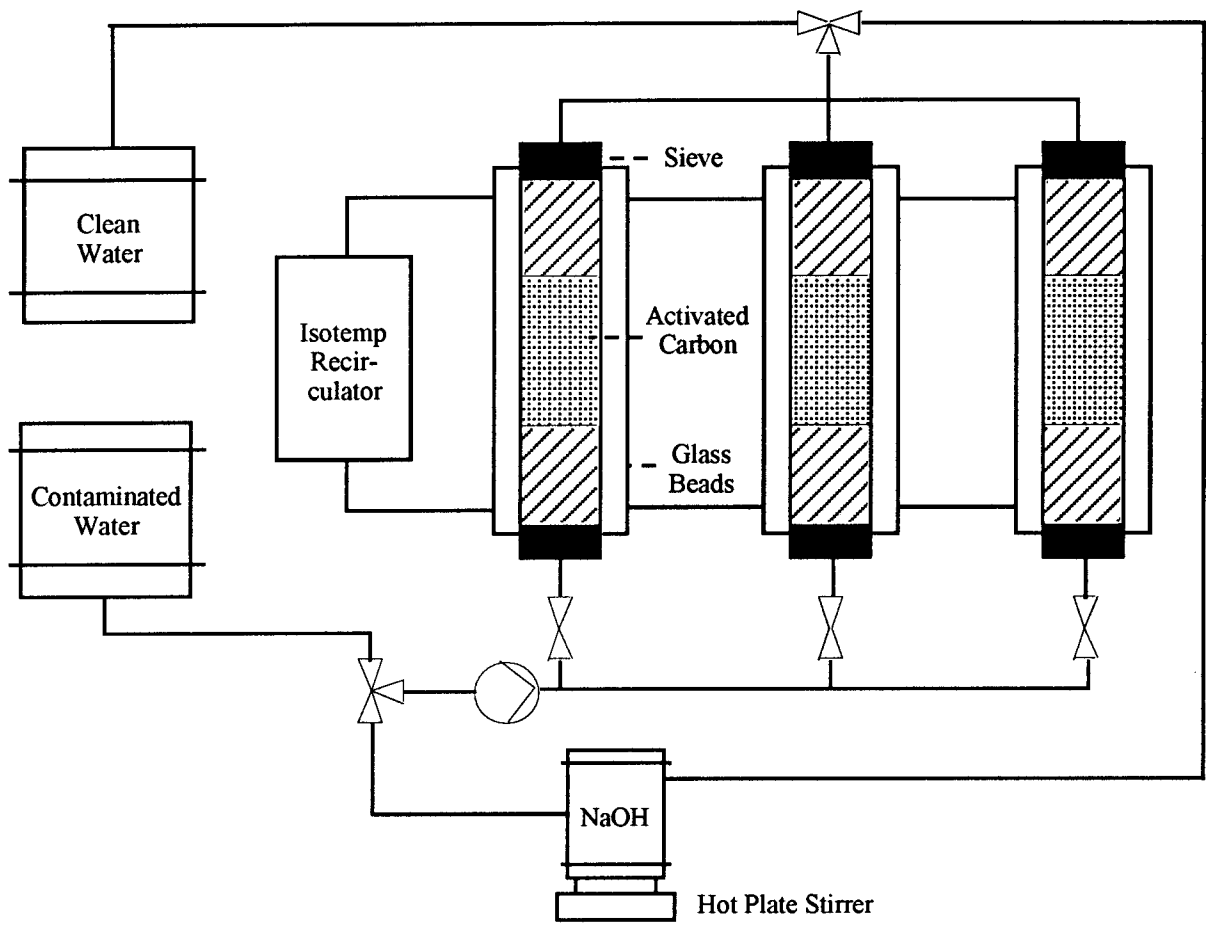


Figure 5 Fixed bed adsorber setup .

## **6. RESULTS AND DISCUSSION**

### **6.1 Aqueous Homogeneous Alkaline Hydrolysis**

#### **6.1.1 Objectives**

The batch studies of the aqueous homogeneous alkaline hydrolysis of RDX and HMX were conducted to determine basic chemical kinetics data. For future applications of the process the following information is needed:

- Rate constants of the alkaline hydrolysis of RDX and HMX at elevated pH and temperature are needed for applications of the process in high explosives contaminated water treatment and bulk high explosives treatment.
- To understand the mechanism of the alkaline hydrolysis of RDX and HMX, detailed chemical kinetics information (experimental activation energy, molar yields of the products in relation to substrate hydrolyzed, time needed to reach complete equilibrium under various process conditions) is needed.
- The chemical kinetics are also needed for the comparison of alkaline hydrolysis product desorption during alkaline hydrolysis regeneration of activated carbon with aqueous homogeneous alkaline hydrolysis kinetics under the same process conditions (pH, T).

#### **6.1.2 Chemical Kinetics**

##### *i. Kinetic Models*

In accordance to previous researchers (Hoffsommer et al., 1977) a second-order rate equation was used to fit the experimental data from batch experiments:

$$\frac{dc}{dt} = -k_2 \cdot c \cdot c_{OH^-} \quad (1)$$

Where  $c$  is the concentration of the respective high explosive compound,  $c_{OH^-}$  the hydroxide concentration and  $k_2$  the second-order rate constant. The second-order rate law can be reduced to a pseudo first-order rate equation for constant  $OH^-$ -concentration provided through excess base:

$$\frac{dc}{dt} = -k_1 \cdot c$$

with (2)

$$k_1 = k_2 \cdot c_{OH^-}$$

Pseudo first-order rate constants can be obtained through a linear least-squares fit of the sample data to the integrated pseudo first-order model equation:

$$\ln \frac{c(t)}{c(t=0)} = -k_1 \cdot t \quad (3)$$

Several experiments need to be performed at different but constant  $OH^-$ -concentrations and constant temperature. The second-order rate constant can then be evaluated from the pseudo first-order rate constants for constant temperature and different  $OH^-$ -concentrations using the equation  $k_2 = k_1/c_{OH^-}$ .

All error determination limits were obtained using the standard deviation from the mean. The linear regression correlation coefficient  $R^2$  is presented when applicable.

ii. *Kinetic Experiments*

Alkaline hydrolysis experiments were performed over a range of temperatures and hydroxide concentrations. Four different temperatures were used for both compounds (50°C, 60°C, 70°C, 80°C). Four different pHs were used for RDX and three were used for HMX.

Figure 8a shows the kinetic experiments with HMX at a hydroxide concentration of 0.22 mM/L (pH = 10). At 50°C alkaline hydrolysis of HMX is very slow. After more than 20 hours less than 10% of the initial HMX was hydrolyzed. For the intermediate concentration of 2.1 mM OH<sup>-</sup>/L (pH = 11) and a temperature of 80°C alkaline hydrolysis of HMX is significantly faster (Figure 8b) with less than 0.1 mg HMX/L remaining after 100 minutes. At the same hydroxide concentration and temperature, the RDX concentration was reduced from 36 mg RDX/L to less than 0.1 mg/L in about 20 minutes (Figure 6b). At the highest applied hydroxide concentrations (23 mM OH<sup>-</sup>/L for HMX; 20 mM OH<sup>-</sup>/L for RDX; pH = 12) and the highest temperature (T = 80°C) the alkaline hydrolysis is more rapid for both RDX and HMX. After 10 minutes less than 0.1 mg HMX/L remained (Figure 9) and after 2 minutes less than 0.1 mg RDX/L remained (Figure 7b).

A prerequisite for the use of the pseudo-first order model were relatively constant hydroxide concentrations. Significant variation from constant pH can be detected in two ways:

1. The concentration versus time profile deviates from straight lines (logarithmic y-axis assumed).
2. The measured pH at the end of the experiment varies significantly from the value at the beginning of the experiment.

Both prerequisites were satisfied in the experiments: The pH was monitored in all experiments and did not vary more than  $\pm 1\%$  over the duration of the experiments. The concentration versus time profile also did not vary significantly from linear shape (Figures 6 - 9).

The accurate linear least-squares fit of the experimental data is also reflected in the statistical analysis of the linear regression. The standard errors for the pseudo first-order rate constants vary between  $\pm 0.4\%$  (HMX:  $k_1$  for  $50^\circ\text{C}$  and  $23 \text{ mM OH}^-/\text{L}$ ) and  $\pm 3.1\%$  (RDX:  $k_1$  for  $80^\circ\text{C}$  and  $1.5 \text{ mM OH}^-/\text{L}$ ) of the respective rate constants with the majority of the error limits below 2% or 1% (Tables 8 and 9).

The correlation coefficients of the linear regression of the pseudo first-order model fit are also presented in Tables 8 and 9. All values of the regression coefficients were higher than 0.99 for HMX and RDX. These values indeed confirm excellent linear regression of the experimental data. Therefore, the pseudo first-order model is applicable and deviations from constant  $\text{OH}^-$ -concentration are negligible for the respective process conditions from pH 10 to 12 and  $50^\circ\text{C}$  to  $80^\circ\text{C}$ .

The subsequent calculation of the second-order rate constants from the pseudo first-order rates is presented in Table 10 and Figure 10a and 10b. The correlation coefficients ( $R^2$ ) are nearly equal to 1 (considering four significant digits). For HMX the correlation coefficients are higher than 0.9999 for  $50^\circ\text{C}$ ,  $60^\circ\text{C}$  and  $70^\circ\text{C}$ . The values for RDX are higher than 0.9999 for  $60^\circ\text{C}$  and  $80^\circ\text{C}$ . This is important because the calculation of second-order rate constants from pseudo first-order rate data magnifies the impact of the error on the

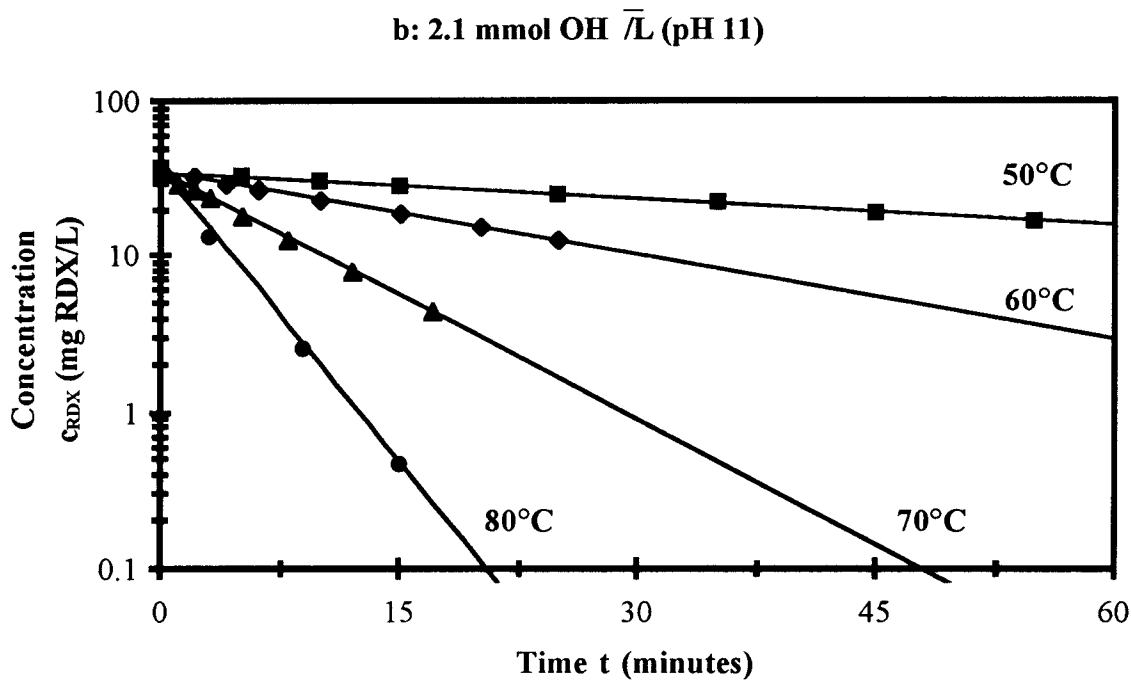
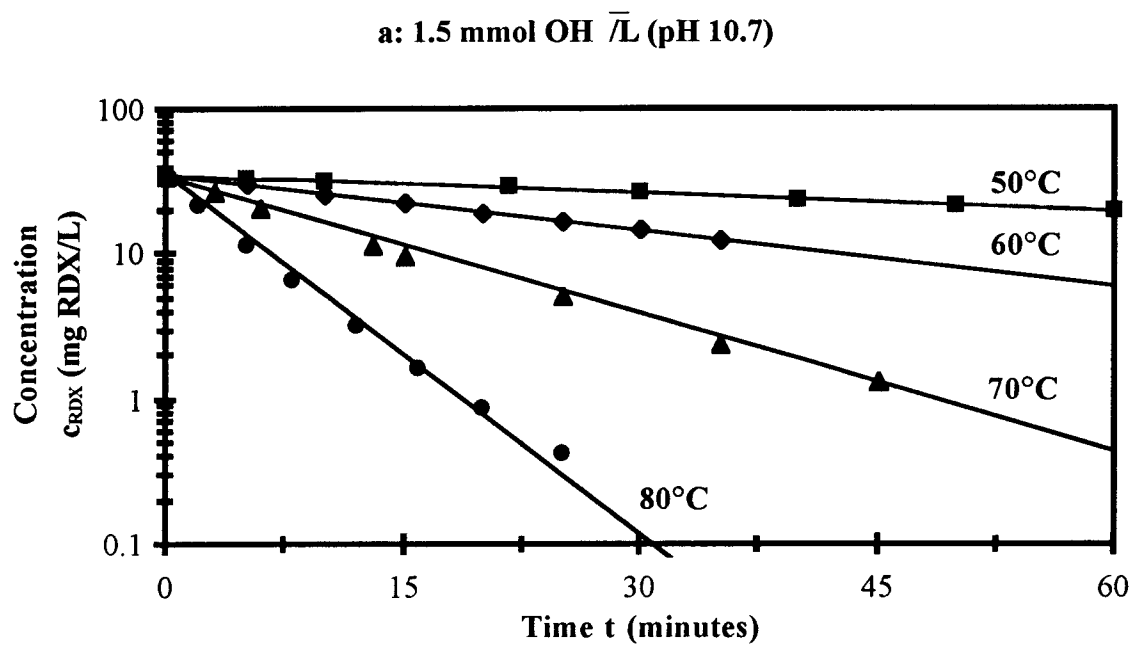
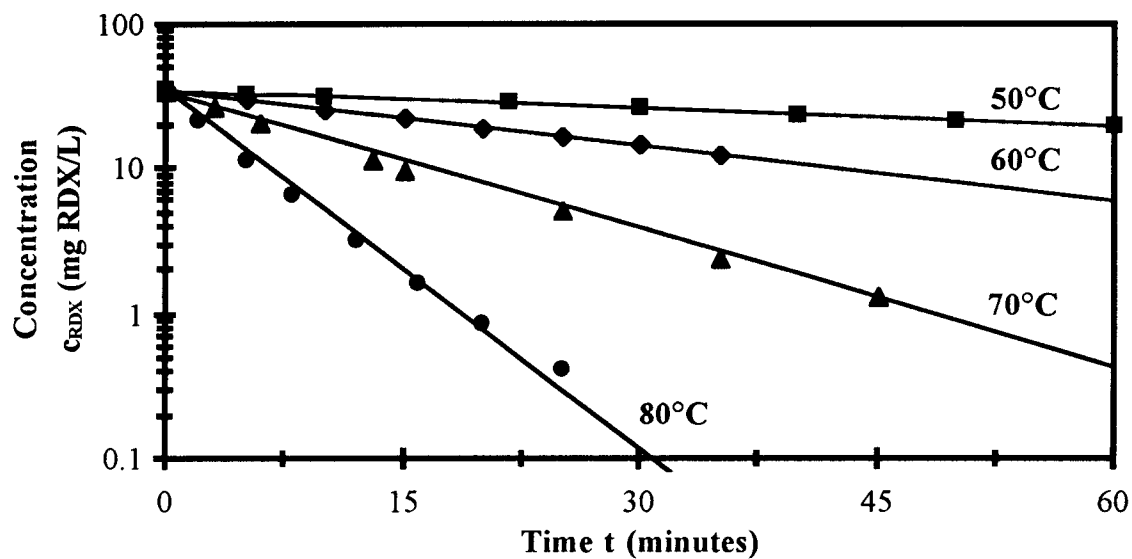


Figure 6 The aqueous homogeneous alkaline hydrolysis of RDX at pH 10.7 and 11.

a: 1.5 mmol OH<sup>-</sup> / L (pH 10.7)



b: 2.1 mmol OH<sup>-</sup> / L (pH 11)

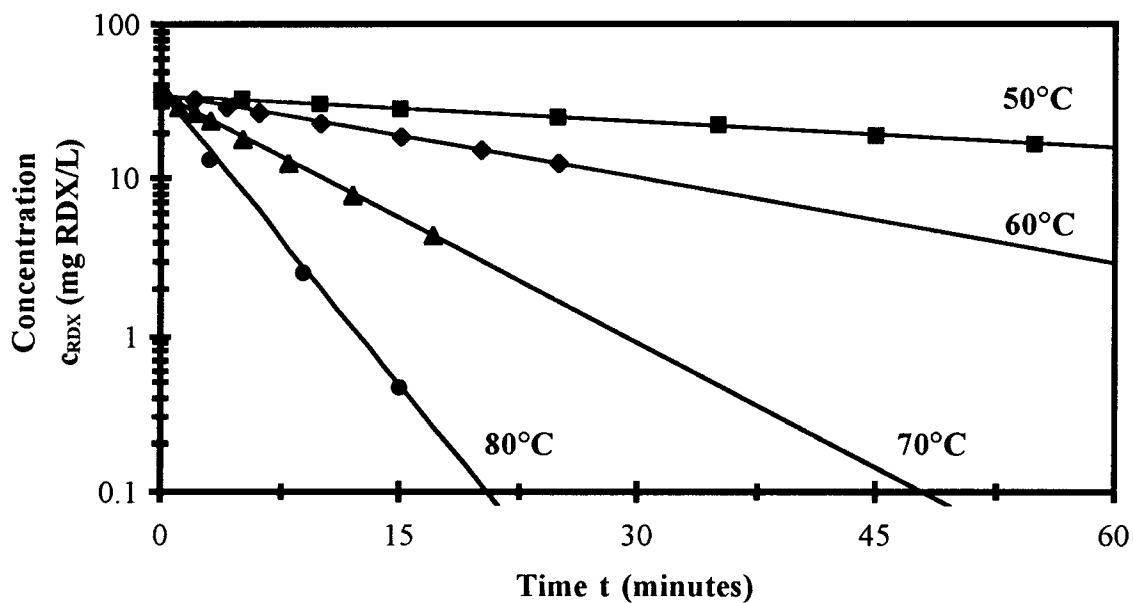


Figure 7 The aqueous homogeneous alkaline hydrolysis of RDX at pH 11.5 and 12.

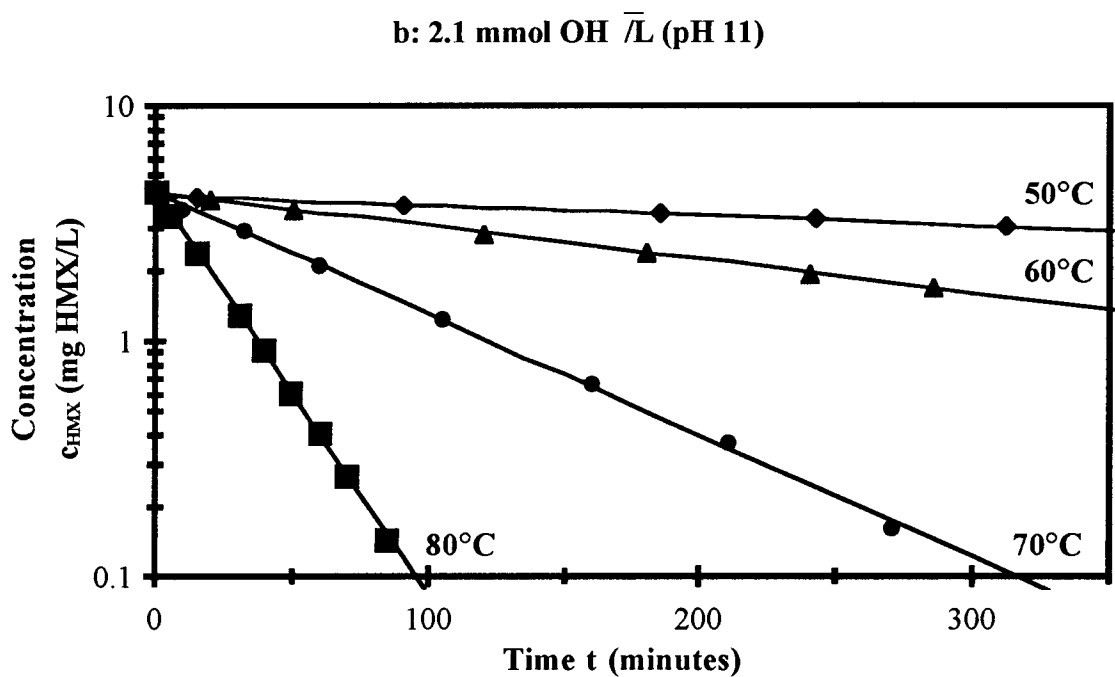
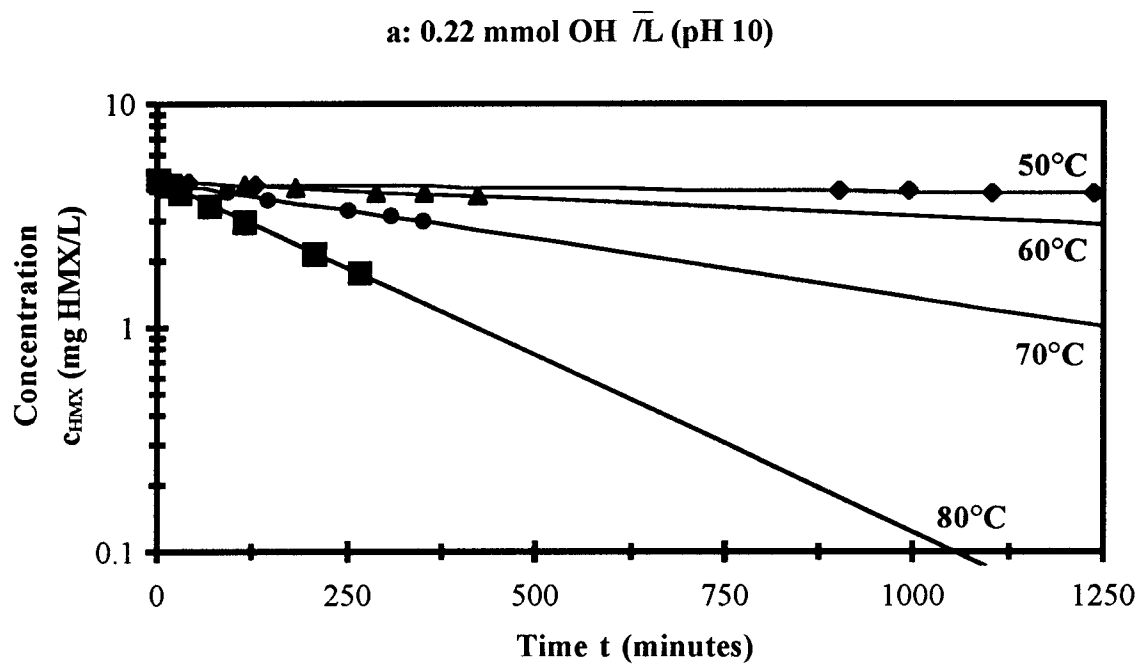


Figure 8 The aqueous homogeneous alkaline hydrolysis of HMX at pH 10 and 11.

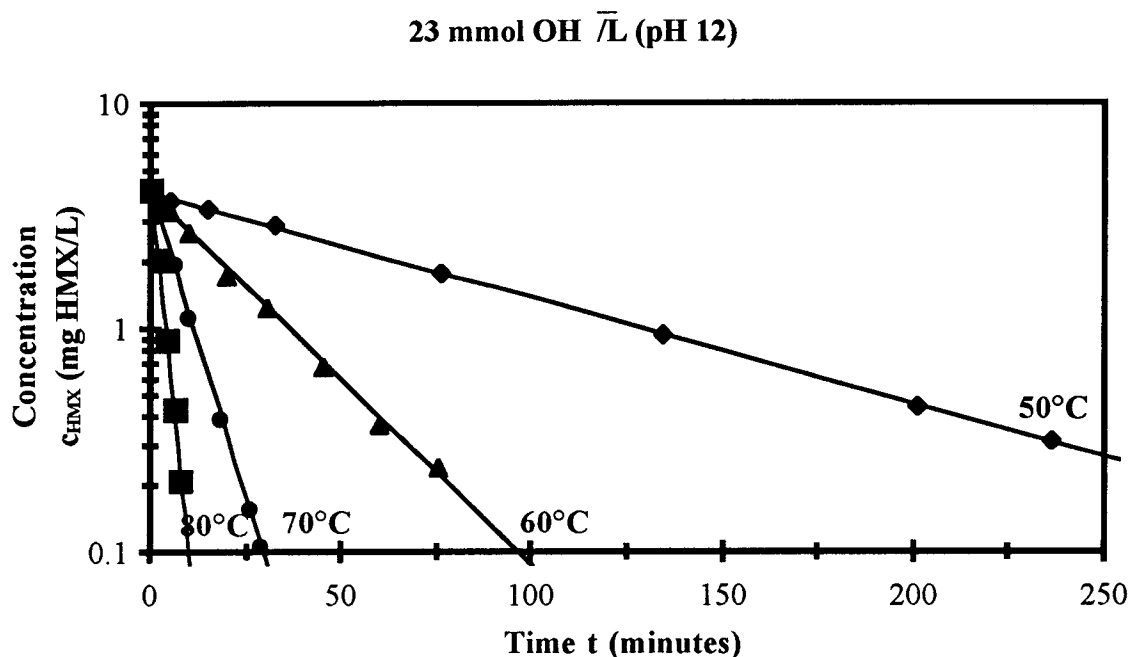


Figure 9 The aqueous homogeneous alkaline hydrolysis of HMX at pH 12.

Table 8 Pseudo 1st-order rate constants and correlation coefficients for the aqueous homogeneous alkaline hydrolysis of HMX.

T (°C)	$k_1$ ( $10^{-3} \cdot \text{min}^{-1}$ )		
	<i>0.22 mmol OH<sup>-</sup>/L</i> (pH 10)	<i>2.1 mmol OH<sup>-</sup>/L</i> (pH 11)	<i>23 mmol OH<sup>-</sup>/L</i> (pH 12)
50	$0.089 \pm 0.002$	$0.99 \pm 0.01$	$10.82 \pm 0.04$
60	$0.35 \pm 0.01$	$3.28 \pm 0.03$	$38.45 \pm 0.72$
70	$1.19 \pm 0.02$	$11.87 \pm 0.16$	$126.5 \pm 1.3$
80	$3.62 \pm 0.06$	$39.64 \pm 0.25$	$374.9 \pm 4.7$
$R^2$ (correlation coefficient)			
50	0.9972	0.9991	0.9999
60	0.9952	0.9997	0.9979
70	0.9980	0.9990	0.9995
80	0.9989	0.9997	0.9995

Table 9 Pseudo 1st-order rate constants and correlation coefficients for the aqueous homogeneous alkaline hydrolysis of RDX.

T (°C)	$k_1$ ( $10^{-3} \cdot \text{min}^{-1}$ )			
	1.5 mmol OH <sup>-</sup> /L (pH 10.7)	2.1 mmol OH <sup>-</sup> /L (pH 11)	10 mmol OH <sup>-</sup> /L (pH 11.5)	20 mmol OH <sup>-</sup> /L (pH 12)
50	9.25 ± 0.08	12.98 ± 0.09	58.2 ± 0.8	127.2 ± 1.2
60	29.52 ± 0.23	41.45 ± 0.38	204.3 ± 1.3	412.8 ± 3.3
70	72.97 ± 1.75	122.8 ± 1.5	607.9 ± 5.7	1162 ± 17
80	190.9 ± 5.9	288.5 ± 5.8	1484 ± 26	2977 ± 43
$R^2$ (correlation coefficient)				
50	0.9996	0.9997	0.9989	0.9995
60	0.9996	0.9995	0.9998	0.9995
70	0.9966	0.9992	0.9995	0.9988
80	0.9962	0.9992	0.9985	0.9992

Table 10 Calculated 2nd-order rate constants for the aqueous homogeneous alkaline hydrolysis of RDX and HMX and correlation coefficients.

T (°C)	HMX	RDX
	$k_2$ ( $L \cdot \text{mol}^{-1} \cdot \text{min}^{-1}$ )	
50	0.47 ± 0.0004	6.35 ± 0.22
60	1.68 ± 0.009	20.73 ± 0.05
70	5.50 ± 0.01	58.71 ± 1.33
80	16.19 ± 0.22	150.62 ± 0.48
$R^2$		
50	1	0.9977
60	1	1
70	1	0.999
80	0.9998	1

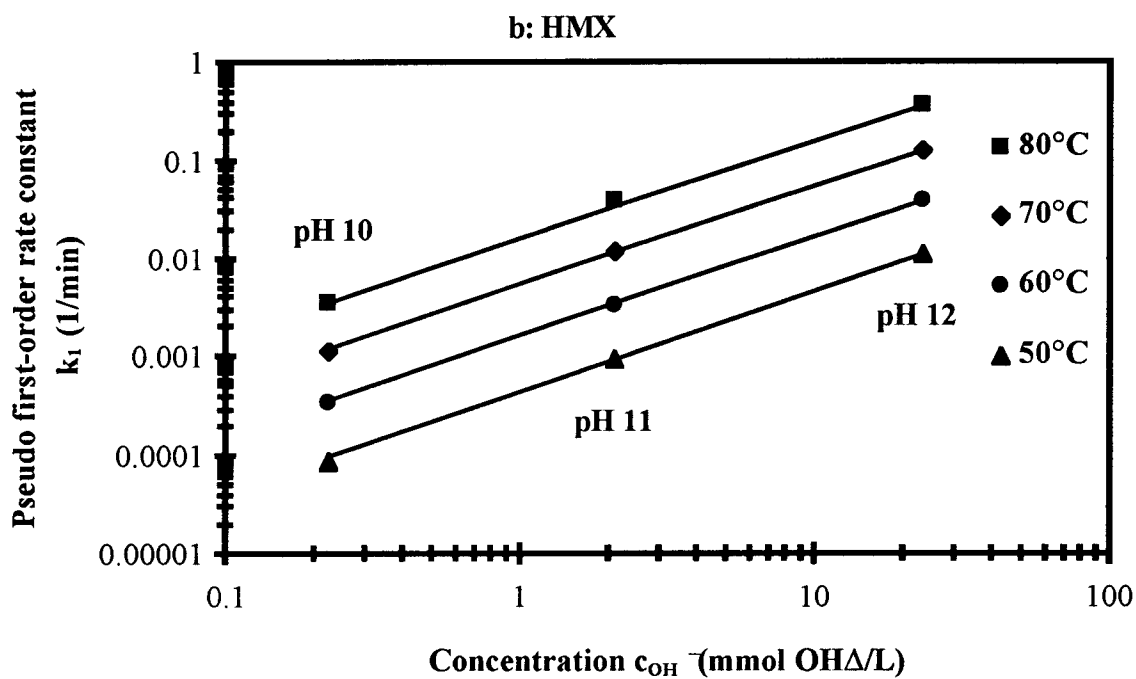
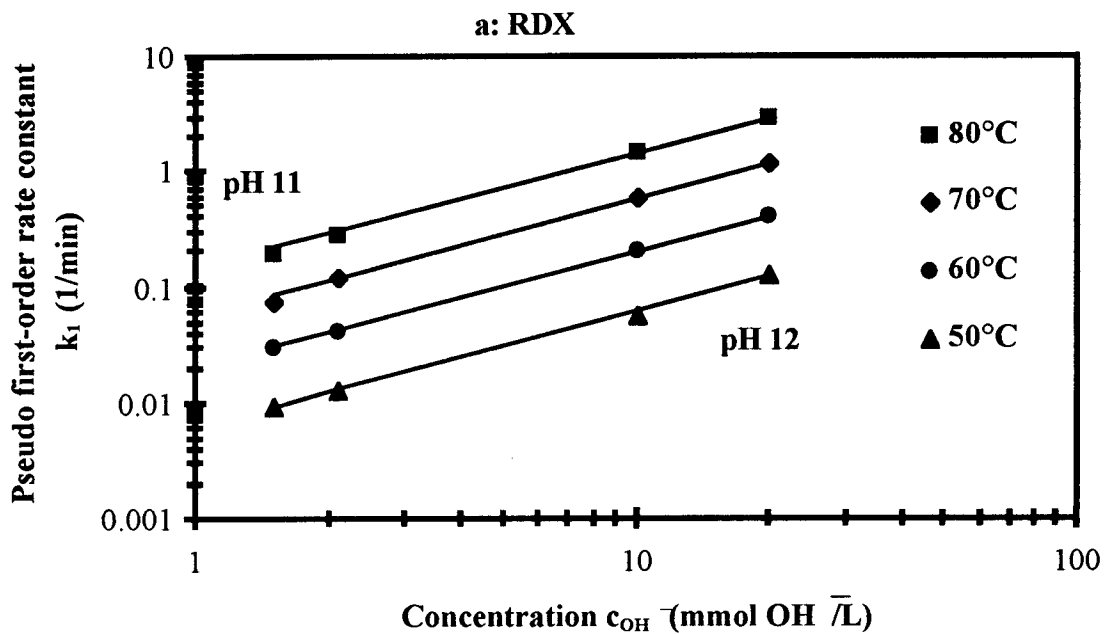


Figure 10 Pseudo first-order rate constants as a function of the OH<sup>-</sup>-concentration.

parameter estimates. It is evident in Table 10 and Figure 10a and 10b that the calculation of 2nd-order rate constants from pseudo first-order rate data is applicable under the investigated conditions.

The alkaline hydrolysis of RDX in the presence of hydroxide ions is approximately 10 times faster than the alkaline hydrolysis of HMX. Since HMX is a frequent contaminant in RDX, the compounds almost always occur together in explosives contaminated wastewater and at contaminated sites. Therefore, the rate of the alkaline hydrolysis of HMX may be rate limiting in the design of a treatment system using alkaline hydrolysis; however, the results also show that an increase in temperature has a higher influence on the rate of the alkaline hydrolysis of HMX than RDX. Higher temperatures (80°C) may therefore be preferable to further increased hydroxide concentrations (> 25 mmol/L) for treatment of RDX and HMX using alkaline hydrolysis.

### 6.1.3 Temperature Dependency of Rate Constants

The temperature dependency of the rate constants can be described using the *Arrhenius*-equation (Benson, 1982):

$$k_2(T) = A \cdot e^{-\frac{E_a}{R \cdot T}} \quad (4)$$

where  $A$  is the empirical *Arrhenius*-factor or pre-exponential factor;  $E_a$  is the empirical activation energy;  $R$  is the gas constant and  $T$  the absolute temperature. The *Arrhenius*-factor  $A$  and the constant  $E/R$  can be determined from a linear least square fit of the logarithm of the specific rate constants versus the reciprocal of the absolute temperature.

An increase in temperature of 10°C produced an increase in the rate of 3.6- to 2.9-fold for the alkaline hydrolysis of HMX and 3.3- to 2.6-fold for RDX over the investigated temperature range. The evaluation of the temperature dependency of the calculated second-order rate constants using the *Arrhenius*-equation is shown in an Arrhenius-plot (Figure 11). The activation energy  $E$  over the range from 50 to 80°C is constant as shown by the excellent correspondence between experimental and model data. The correlation coefficients of 0.9999 for HMX and 0.9993 for RDX confirm this.

Values for the activation energies of

- RDX:  $E_a = 99.9 \pm 1.9 \text{ kJ}\cdot\text{mol}^{-1}$
- and
- HMX:  $E_a = 111.9 \pm 0.8 \text{ kJ}\cdot\text{mol}^{-1}$

were found in the present work (Table 11). These results are accurate, since deviations of  $\pm 4 \text{ kJ}\cdot\text{mol}^{-1}$  are acceptable in common practice (Baerns et al., 1992). The Arrhenius-parameter for RDX [ $\ln A = 39.09 \pm 0.67 \ln(\text{L}\cdot\text{mol}^{-1}\cdot\text{min}^{-1})$ ] was found to be very close to the one of HMX [ $\ln A = 40.93 \pm 0.27 \ln(\text{L}\cdot\text{mol}^{-1}\cdot\text{min}^{-1})$ ]. This fact along with close activation energies for the two compounds suggests a similar basic reaction mechanism for the hydrolysis of RDX and HMX.

Table 11 Temperature dependence of the 2nd-order rate constants for the aqueous homogeneous alkaline hydrolysis of RDX and HMX (*Arrhenius*-parameters).

	$\ln A$ [ $\ln(\text{L}\cdot\text{mol}^{-1}\cdot\text{min}^{-1})$ ]	$E_a$ ( $\text{kJ}\cdot\text{mol}^{-1}$ )	$R^2$
HMX	$40.93 \pm 0.27$	$111.9 \pm 0.8$	0.9999
RDX	$39.09 \pm 0.67$	$99.92 \pm 1.87$	0.9993

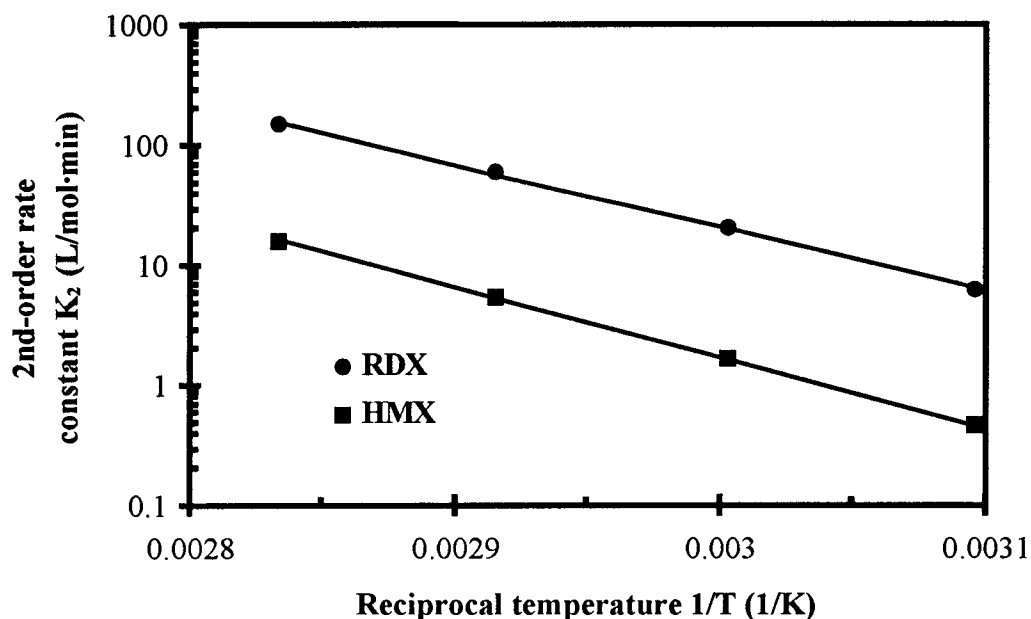


Figure 11 Temperature dependence of the 2nd-order rate constants ( $k_2$ ) of the aqueous homogeneous alkaline hydrolysis of RDX and HMX (*Arrhenius*-plot).

Kinetic coefficients at 50°C and 80°C, extrapolated from previous research over the range of 25°C to 45°C (Hoffsommer et al., 1977; Croce and Okamoto, 1979), are 20% to 22% lower for RDX and 3% to 27% lower for HMX than measured in this investigation. The values of the experimental activation energies found in this study are close to the values found by previous researchers at lower temperature (Jones, 1953; Hoffsommer et al., 1977; Croce and Okamoto, 1979; see Section 2.4.3). The difference is 6% for the experimental activation energy of RDX and 9% for HMX.

The isokinetic temperature, at which the rates of the alkaline hydrolysis of RDX and HMX are equal can be extrapolated using the *Arrhenius*-equation. It is approximately

510°C. The accuracy of this estimate is limited, because of the large difference between the investigated temperature region and the extrapolated temperature.

#### 6.1.4 Intermediates and End-Products

For the study of product formation similar experiments as discussed in Section 6.1.2 were conducted. The emphasis was on the detection of the concentration of  $\text{NO}_2^-$  and  $\text{HCOO}^-$  with Ion Chromatography (IC). These two compounds were chosen because they are believed to be the fastest produced product ( $\text{NO}_2^-$ ) and the slowest produced product ( $\text{HCOO}^-$ ). Therefore, they present kinetic information over the complete duration of the hydrolysis reaction. They can also be analyzed in a single IC-run.

For all other products the interest was mainly in their concentration at equilibrium. This information is needed for a material balance of carbon and nitrogen. Some of the products are volatile or gaseous products ( $\text{NH}_3$ ,  $\text{N}_2$ ,  $\text{N}_2\text{O}$ ). Special experiments were performed to determine the equilibrium concentrations of these compounds.

##### *i. Product Formation and Equilibrium Composition*

The kinetics of  $\text{NO}_2^-$  and  $\text{HCOO}^-$ -formation are shown in Figure 12 and 13. Equilibrium is reached in approximately 6 hours only at  $T = 80^\circ\text{C}$  and pH 12 (Figure 13b). In all other cases the formation of  $\text{HCOO}^-$  was incomplete after 360 minutes. In order to obtain information about the equilibrium concentration all experiments were continued until a final equilibrium was reached, which may have been several days or weeks for the slower process conditions. The equilibrium concentrations are shown in Table 12.

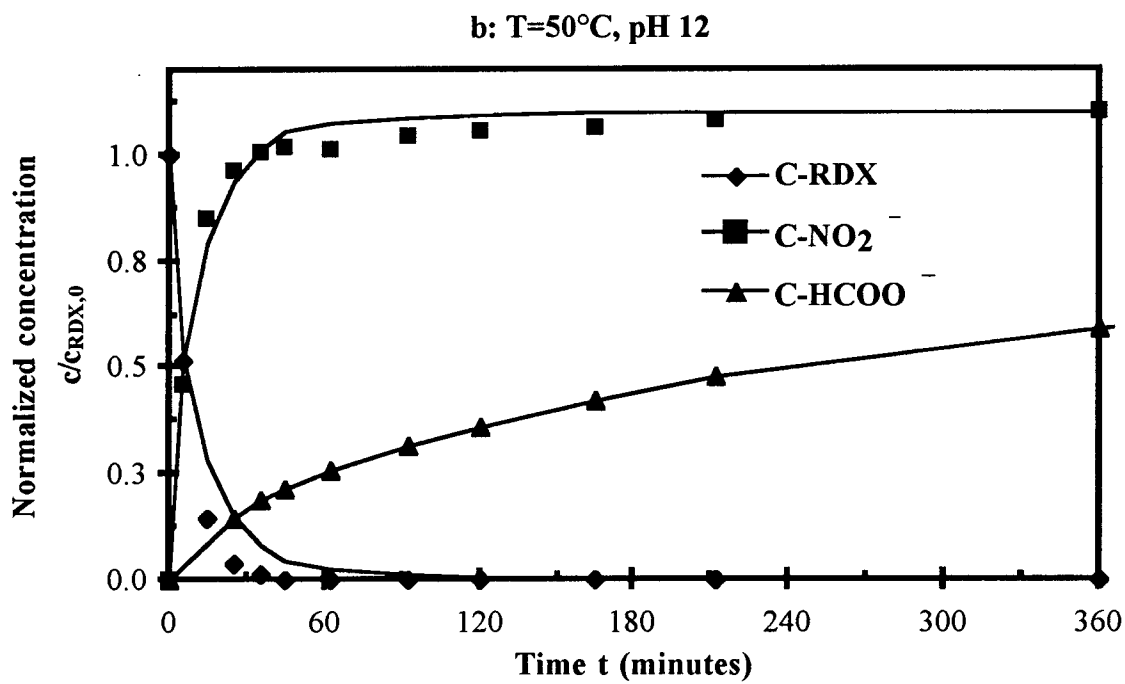
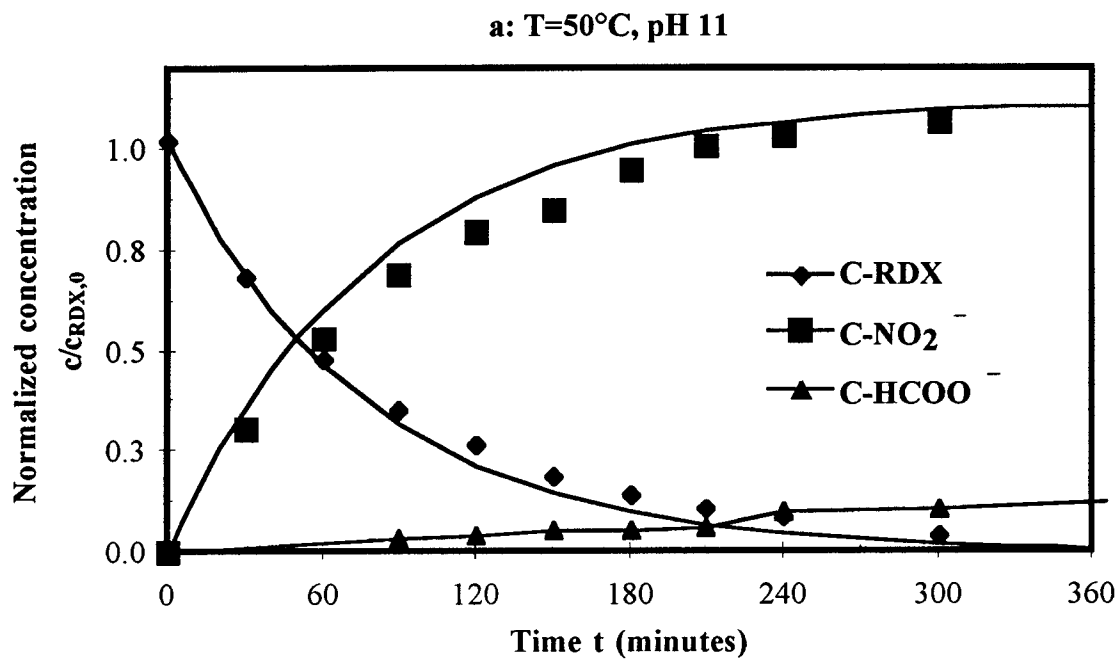


Figure 12 Product formation kinetics of the alkaline hydrolysis of RDX at 50°C;  $c_0 = 0.16$  mmol RDX/L.

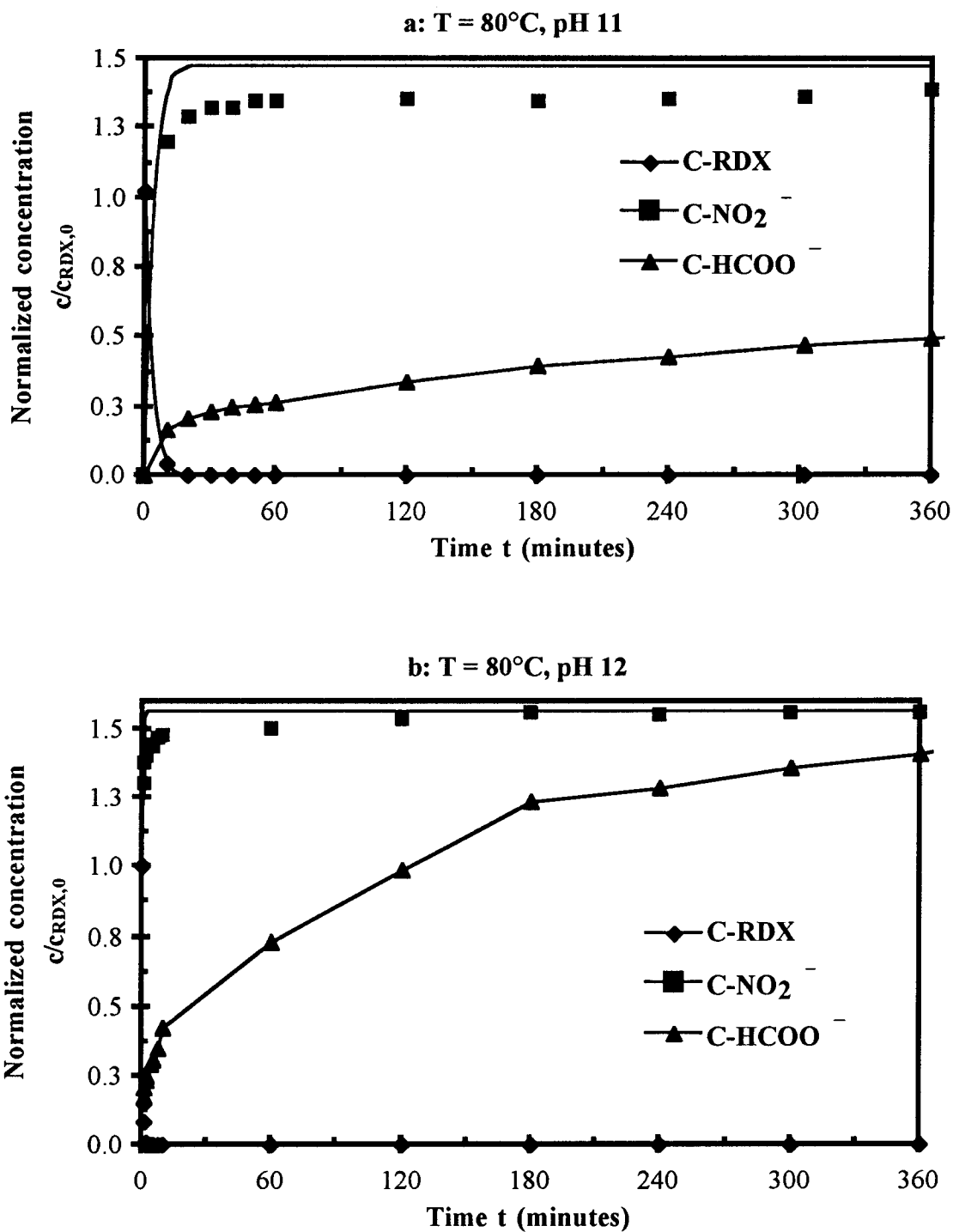


Figure 13 Product formation kinetics of the alkaline hydrolysis of RDX at 80°C;  $c_0 = 0.16$  mmol RDX/L.

The formation of  $\text{HCOO}^-$  is obviously slow in comparison with RDX-degradation and  $\text{NO}_2^-$ -formation. This is due to the production of formate from both the ring-cleavage and subsequently from the fourth-order *Canizarro*-reaction of formaldehyde ( $\text{HCHO}$ ) at the elevated pH (Hoffsommer et al., 1977), the latter one being slow (Sykes, 1981; Birstein and Lobanow, 1927; Euler and Lovgren, 1925).

It is also evident for all four conditions (Figures 12 and 13) that  $\text{NO}_2^-$  is a direct product from RDX formed during the first reaction step in accordance with RDX-degradation. The  $\text{NO}_2^-$ -formation principally follows the same rate as RDX. However, the experimental  $\text{NO}_2^-$ -concentration slightly lags behind the model-generated concentration versus time profile in all four cases. This indicates a small variation from constant yield values over the duration of the hydrolysis reaction.

The molar yields are approximately 1.5 M  $\text{HCOO}^-$  and 1.5 M  $\text{NO}_2^-$  formed per M of RDX hydrolyzed. These results are significantly higher than those reported in previous research. Hoffsommer et al. (1977) reported molar yields of 1.1 M  $\text{NO}_2^-/\text{M RDX}$  and 0.7 M  $\text{HCOO}^-/\text{M RDX}$ . However, they conducted their study at lower temperatures. In the present study it was found that at the slowest process conditions (pH 11,  $T = 50^\circ\text{C}$ ) the time needed to reach equilibrium was several weeks. These conditions are still more elevated than in Hoffsommer et al.'s (1977) study who investigated temperatures only as great as  $45^\circ\text{C}$ . Unfortunately, the experimental section of their study does not give evidence after how much time the final samples were taken. The results indicate the possibility that the normalized molar yields may have been calculated before complete equilibrium was reached.

For all other compounds equilibrium concentrations were determined, only (Tables 12 and 13). The normalized molar yield of  $\text{NH}_3$  is 0.9 M/M RDX hydrolyzed for pH 12 at 50 and 80°C as well as pH 11 and 80°C. Not surprisingly, beside  $\text{HCOO}^-$ , acetate-ion ( $\text{CH}_3\text{COO}^-$ ) was identified as an additional and previously unknown compound of the alkaline hydrolysis of RDX (Epstein and Winkler, 1951; Jones, 1953; Hoffsommer et al., 1977; Croce and Okamoto, 1979). The yield of 0.1 M  $\text{CH}_3\text{COO}^-$ /M RDX is less than 10% of the yield of  $\text{HCOO}^-$  and comparatively small. A quantifiable trend with pH or temperature could not be found in the molar yields.

Table 12 Normalized molar yields for the products of the alkaline hydrolysis of RDX (results from liquid analysis).

	pH 11		pH 12	
	T = 50°C	T = 80°C	T = 50°C	T = 80°C
(M product formed/M RDX hydrolyzed)				
$\text{NO}_2^-$	1.5	1.5	1.3	1.6
$\text{HCOO}^-$	1.3	1.5	1.5	1.5
$\text{CH}_3\text{COO}^-$				0.1
$\text{NH}_3$		0.9	0.9	0.9

Table 13 Normalized molar yields for the products of the alkaline hydrolysis of RDX (results from gas analysis: 5 g RDX in 50 mL 1.5-M NaOH).

Normalized Molar Yield (M product formed/M RDX hydrolyzed)	
$\text{N}_2\text{O}$	1.1
$\text{N}_2$	0.34

The analysis for gaseous products was performed at DOE's Pantex Plant. 5 g of RDX (0.0225 M) were contacted with 50 mL of 1.5-M NaOH. The temperature was held constant at  $T = 90^{\circ}\text{C}$ . The reaction produced a system pressure of 240.1 kPa at equilibrium. The total head space volume was 0.412 L.

The gas analysis using mass spectrometry showed 75%  $\text{N}_2\text{O}$  and 23%  $\text{N}_2$ . The remaining 2% included small amounts of argon, oxygen, ammonia (1.5%), as well as water and methanol (0.1%).

Using the ideal gas law:

$$N = \frac{P \cdot V}{R \cdot T} = 0.033M \quad (5)$$

the total moles are calculated to 0.033 M. With the results from the gas analysis the molar yields are calculated to 0.025 M  $\text{N}_2\text{O}$  and 0.0075 M  $\text{N}_2$ . The normalized molar yields are then 1.1 M  $\text{N}_2\text{O}$  and 0.34 M  $\text{N}_2$  per M of RDX hydrolyzed, respectively (Table 13).

RDX-h5, the intermediate of the initial step of the alkaline hydrolysis of RDX does not accumulate and could not be observed at any time on the HPLC-system. In the same step  $\text{NO}_2^-$  is produced and all RDX is destroyed. Since  $\text{HCOO}^-$  is produced much slower along with other products a time must exist where the material balance is not closed if the known products and intermediates are to be balanced. Therefore, the initial step of the alkaline hydrolysis of RDX must be followed by the formation of complex and unknown intermediates from ring cleavage.

These intermediates did not elute with any retention on the HPLC-system with a C18-reversed phase column using the water/methanol/acetonitrile-eluent. Nevertheless, some of

these intermediates showed UV-absorption. A "dirty" peak indeed existed at a retention time of approximately 1.7 minutes that increased during the initial phase of a hydrolysis experiment and decreased later on. It was not possible to further define this peak because  $\text{NO}_2^-$  also absorbs UV-light at 236 nm and does not elute with any retention on the applied HPLC-system. The further mineralization of these intermediates is slow and rate-limiting as evidenced in the formation of  $\text{HCOO}^-$ .

Considering the new results the reaction mechanism should be rewritten as shown in Figure 17.

ii. *Unknown Intermediates*

RDX- and HMX-hydrolysates were analyzed using liquid-liquid-extraction (LLE) and GC/MS-analysis. Any previously unknown organic intermediates, if present and extractable by dichloromethane and chromatographicable, are detected with this method. The samples were also concentrated from 1000 mL to 500  $\mu\text{L}$ . Additionally and in order to verify the origin of chromatographed compounds, a comprehensive set of blank samples was also extracted and concentrated with LLE (where applicable) and analyzed with GC/MS:

- GC/MS-system blanks. Pure Optima-grade dichloromethane (Fisher Scientific, Springfield, NJ) was injected into the GC/MS-system.
- LLE-system blanks. 100 mL of dichloromethane were recirculated without sample for 5.5 hours in the LLE-apparatus and then concentrated. The concentrated sample was injected into the GC/MS-system.

- Deionized water- and HPLC-grade water blanks. 1L of water (D.I. or HPLC-grade, respectively) were extracted and concentrated (LLE) and analyzed on the GC/MS.
- Base-water blanks. 1L of an alkaline solution (2 mL 10-M NaOH in 1000 mL D.I- water or HPLC-grade water, respectively) was extracted and concentrated (LLE) and then run on the GC/MS-system.
- Blanks of unhydrolyzed RDX and HMX. 1L of a solution of 40 mg RDX/L or 4 mg HMX/L in D.I.- or HPLC-grade water, respectively, were extracted and concentrated (LLE) and then injected into the GC/MS-system.

Eventually, RDX- and HMX-hydrolysis samples were prepared with deionized and HPLC-grade water (40 mg RDX or 4 mg HMX, respectively, were stirred for 6 hours in 1000 mL water with 2 mL 10-M NaOH at 80°C). The hydrolysate was then extracted and concentrated and analyzed on the GC/MS-system.

Figure 14 shows the chromatograms of the concentrated hydrolysates of RDX and HMX. Five major peaks were observed in both the RDX- and the HMX-hydrolysate samples. The retention times of these peaks were 416 (419), 1086 (1087), 1304 (1304), 2008 (2008) and 2522 (2519) seconds; the value in parentheses relates to the HMX-hydrolysate. The spectra of these peaks are presented in Figure 15 and 16. When comparing the spectra of the compounds at the same retention times for RDX and HMX it is evident that these compounds are identical. The chromatograms and spectra of the blanks are not presented here, but were compared with the hydrolysates. All of the five compounds could be repeatedly identified as impurities in the blank samples. They therefore do not relate to the hydrolysis of RDX or HMX.

The chemical identification of the spectra is irrelevant at this point because direct comparison of the spectra from hydrolysate-samples with blank-samples were used to determine if a compound relates to RDX- or HMX-hydrolysis reactions.

All other peaks with sufficient signals to produce a spectra were also compared with blank-sample data. The chromatograms and spectra are not presented here. All these compounds were repeatedly found in blank-samples and are therefore not related to the hydrolysis of RDX and HMX.

No previously unknown intermediates or end-products from the alkaline hydrolysis of RDX and HMX were discovered by GC/MS-analysis of LLE-concentrated hydrolysates of RDX and HMX.

### *iii. Mass Balance*

No additional or formerly unknown products were found using GC/MS-techniques. It is therefore reasonable to calculate a nitrogen- and carbon-balance using the previously discussed results (Table 14).

The recovery of carbon and nitrogen in the hydrolysis products was close to 100%: 94% of the carbon and 90% of the nitrogen from RDX were found in the described products. The material balance is significantly improved in comparison to earlier research by Hoffsommer et al. (1977). In the older study 60% carbon and 77% nitrogen were recovered. In the present work particularly the molar yields of  $\text{HCOO}^-$  and  $\text{NO}_2^-$  contributed to the enhancement of the material balance. Smaller corrections for the other products and the discovery of  $\text{CH}_3\text{COO}^-$  also improved the material balance.

Table 14 Carbon and nitrogen balance for the alkaline hydrolysis of RDX.

	Carbon	Nitrogen
	(M)	
RDX (C <sub>3</sub> H <sub>6</sub> N <sub>6</sub> O <sub>6</sub> )	<b>3</b>	<b>6</b>
Formate (HCOO <sup>-</sup> )	1.5	
Acetate (CH <sub>3</sub> COO <sup>-</sup> )	0.2	
Formaldehyde (HCHO)*	1.1	
Nitrite (NO <sub>2</sub> <sup>-</sup> )		1.6
Ammonia (NH <sub>3</sub> )		0.9
Nitrous Oxide (N <sub>2</sub> O)		2.2
Nitrogen (N <sub>2</sub> )		0.7
<b>Sum</b>	<b>2.8</b>	<b>5.4</b>
<i>Difference (RDX-Sum)</i>	<i>-0.2</i>	<i>-0.6</i>
<b>Recovery (%)</b>	<b>94</b>	<b>90</b>

\* data from Hoffsommer et al. (1977).

### 6.1.5 Conclusions

The kinetics of the aqueous homogeneous alkaline hydrolysis were investigated for the high explosives

- RDX (Hexahydro-1,3,5-trinitro-1,3,5-triazine) within the temperature range from 50°C to 80°C and the pH-range from 10.7 to 12.

and

- HMX (Octahydro-1,3,5,7-tetranitro-1,3,5,7-tetrazocine) within the temperature range from 50°C to 80 C and the pH-range from 10 to 12.

Previous researchers did not investigate the kinetics of the alkaline hydrolysis in the

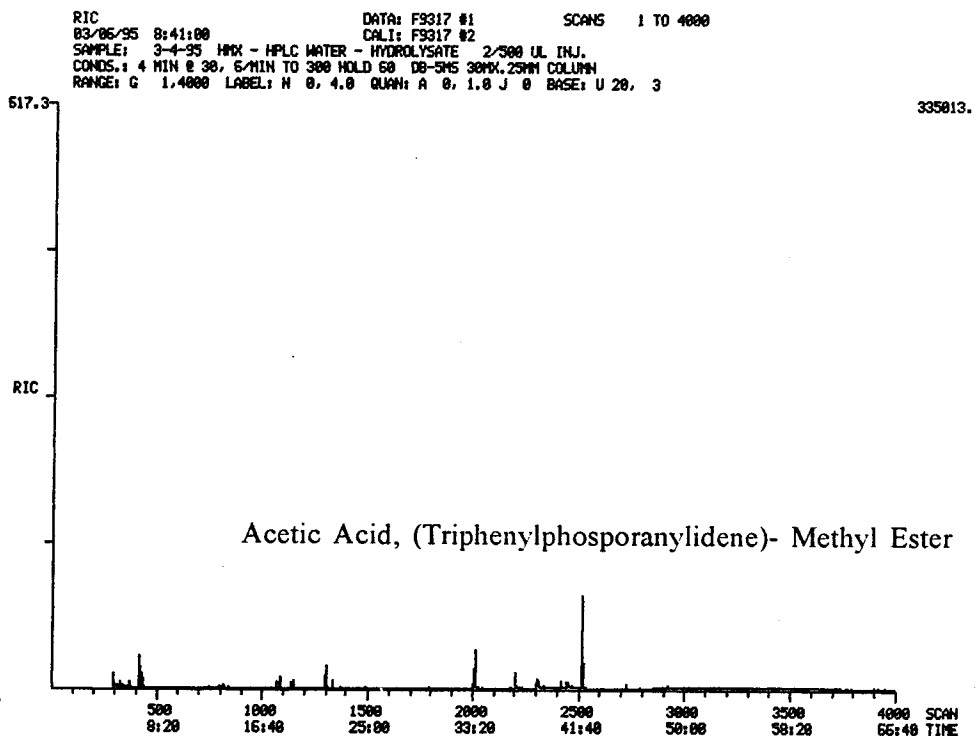
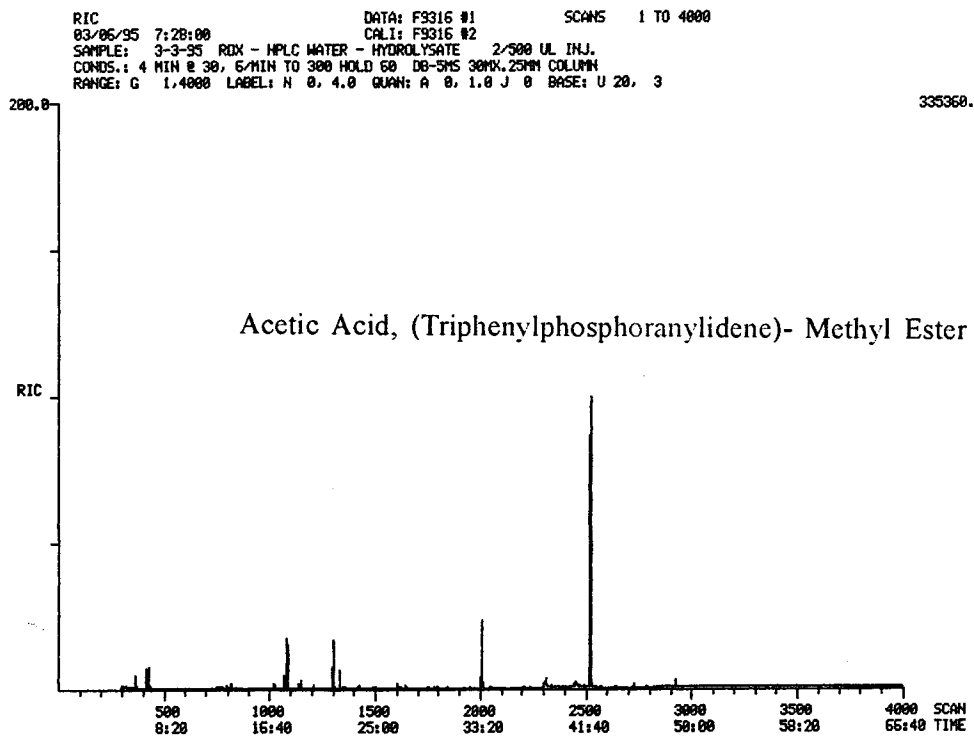
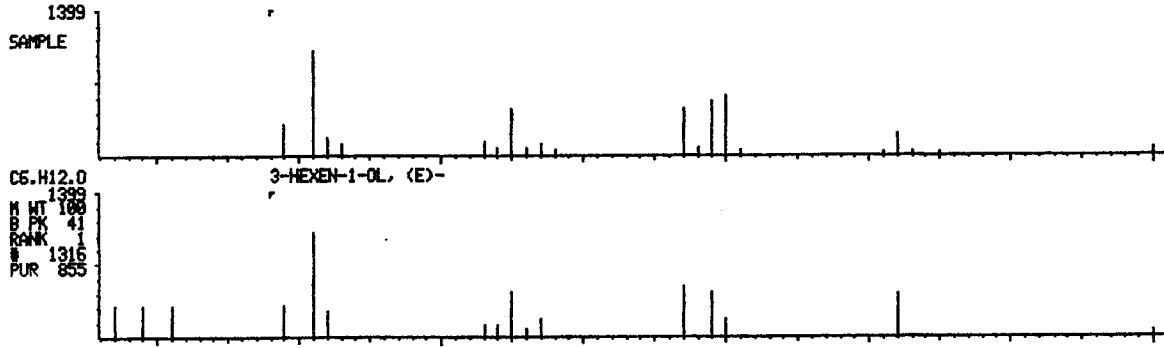


Figure 14 Chromatograms (GC/MS) of the alkaline hydrolysates of RDX and HMX.

LIBRARY SEARCH  
03/06/95 7:28:00 + 6:56  
SAMPLE: 3-3-95 RDX - HPLC WATER - HYDROLYSATE  
CONDS.: 4 MIN @ 30, 6/MIN TO 300 HOLD 60 DB-5MS 30MX.25MM COLUMN  
ENHANCED (S 158 2N 0T)

DATA: F9316 # 416  
CALI: F9316 # 2

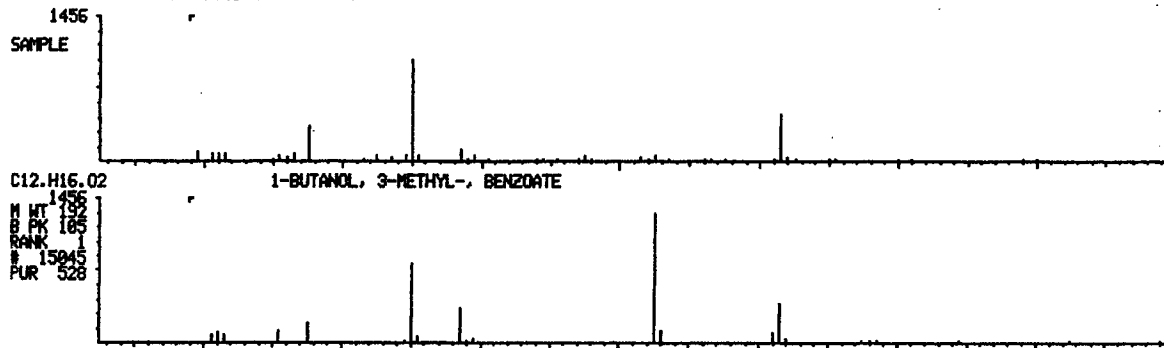
BASE M/Z: 41  
RIC: 7383.



LIBRARY SEARCH  
03/06/95 7:28:00 + 18:06  
SAMPLE: 3-3-95 RDX - HPLC WATER - HYDROLYSATE  
CONDS.: 4 MIN @ 30, 6/MIN TO 300 HOLD 60 DB-5MS 30MX.25MM COLUMN  
ENHANCED (S 158 2N 0T)

DATA: F9316 #1086  
CALI: F9316 # 2

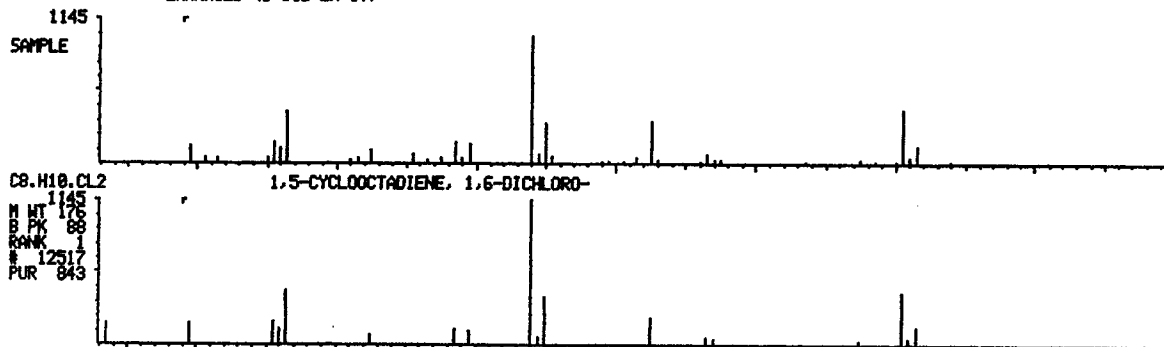
BASE M/Z: 70  
RIC: 23679.



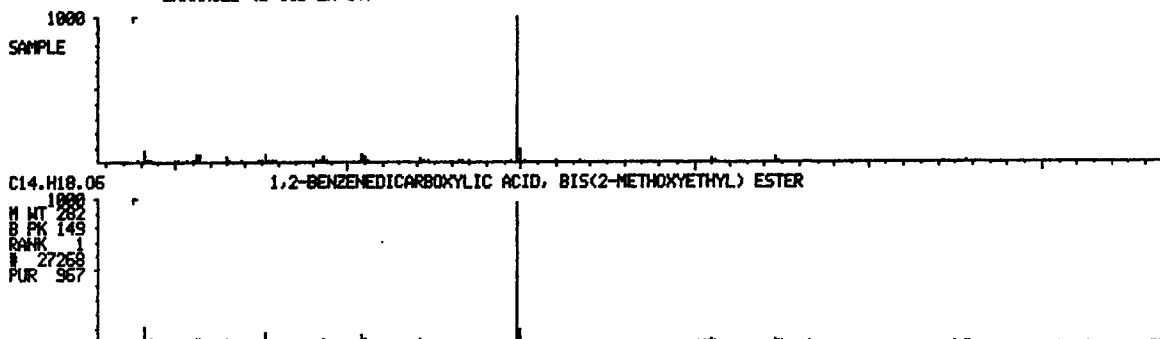
LIBRARY SEARCH  
03/06/95 7:28:00 + 21:44  
SAMPLE: 3-3-95 RDX - HPLC WATER - HYDROLYSATE  
CONDS.: 4 MIN @ 30, 6/MIN TO 300 HOLD 60 DB-5MS 30MX.25MM COLUMN  
ENHANCED (S 158 2N 0T)

DATA: F9316 #1304  
CALI: F9316 # 2

BASE M/Z: 88  
RIC: 23071.



LIBRARY SEARCH DATA: F9316 #2008 BASE M/Z: 149  
 03/06/95 7:28:00 + 33:28 CALI: F9316 # 2 RIC: 30559.  
 SAMPLE: 3-3-95 RDX - HPLC WATER - HYDROLYSATE 2/500 UL INJ.  
 CONDS.: 4 MIN @ 30, 6/MIN TO 300 HOLD 60 DB-5MS 30MX.25MM COLUMN  
 ENHANCED (S 158 2N 0T)



LIBRARY SEARCH DATA: F9316 #2522 BASE M/Z: 277  
 03/06/95 7:28:00 + 42:02 CALI: F9316 # 2 RIC: 130687.  
 SAMPLE: 3-3-95 RDX - HPLC WATER - HYDROLYSATE 2/500 UL INJ.  
 CONDS.: 4 MIN @ 30, 6/MIN TO 300 HOLD 60 DB-5MS 30MX.25MM COLUMN  
 ENHANCED (S 158 2N 0T)

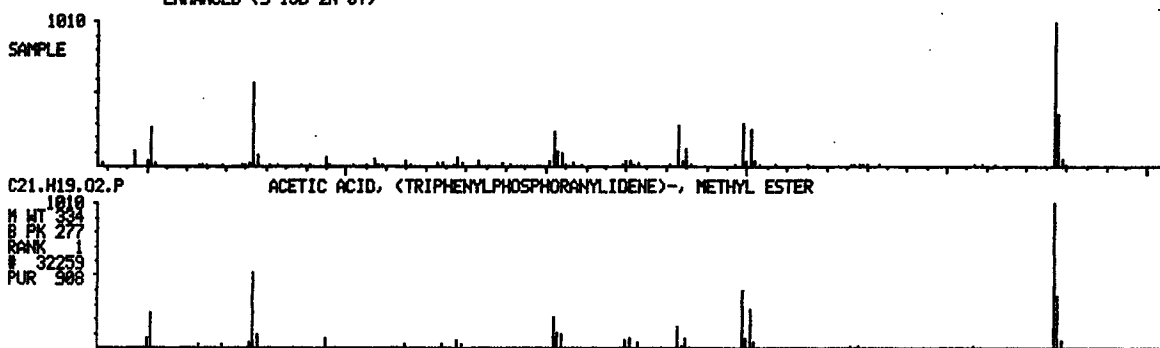
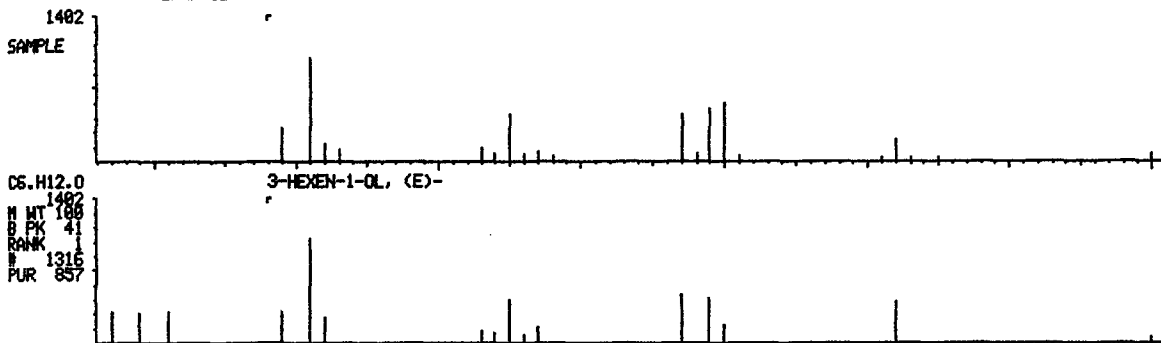


Figure 15 Mass-spectra of some compounds identified in the alkaline hydrolysates of RDX by GC/MS-analysis.

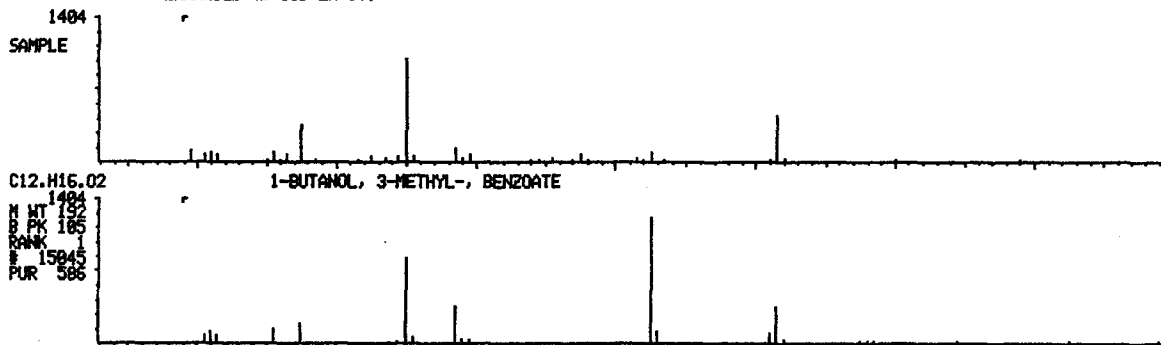
LIBRARY SEARCH DATA: F9317 # 419  
03/06/95 8:41:00 + 6:59 CALI: F9317 # 2  
SAMPLE: 3-4-95 HMX - HPLC WATER - HYDROLYSATE 2/500 UL INJ.  
CONDS.: 4 MIN @ 30, 6/MIN TO 300 HOLD 60 DB-SMS 30MX.25MM COLUMN  
ENHANCED (S 158 2N 0T)

BASE M/Z: 41  
RIC: 11743.



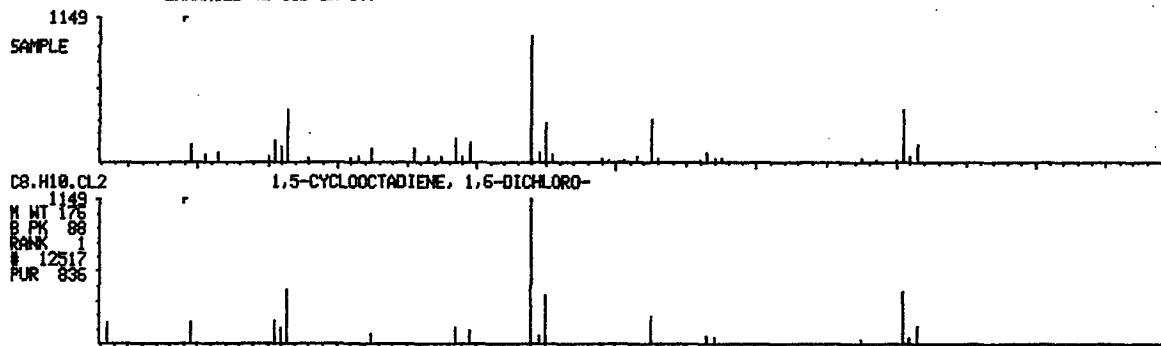
LIBRARY SEARCH DATA: F9317 #1087  
03/06/95 8:41:00 + 18:07 CALI: F9317 # 2  
SAMPLE: 3-4-95 HMX - HPLC WATER - HYDROLYSATE 2/500 UL INJ.  
CONDS.: 4 MIN @ 30, 6/MIN TO 300 HOLD 60 DB-SMS 30MX.25MM COLUMN  
ENHANCED (S 158 2N 0T)

BASE M/Z: 70  
RIC: 5631.



LIBRARY SEARCH DATA: F9317 #1304  
03/06/95 8:41:00 + 21:44 CALI: F9317 # 2  
SAMPLE: 3-4-95 HMX - HPLC WATER - HYDROLYSATE 2/500 UL INJ.  
CONDS.: 4 MIN @ 30, 6/MIN TO 300 HOLD 60 DB-SMS 30MX.25MM COLUMN  
ENHANCED (S 158 2N 0T)

BASE M/Z: 88  
RIC: 12527.



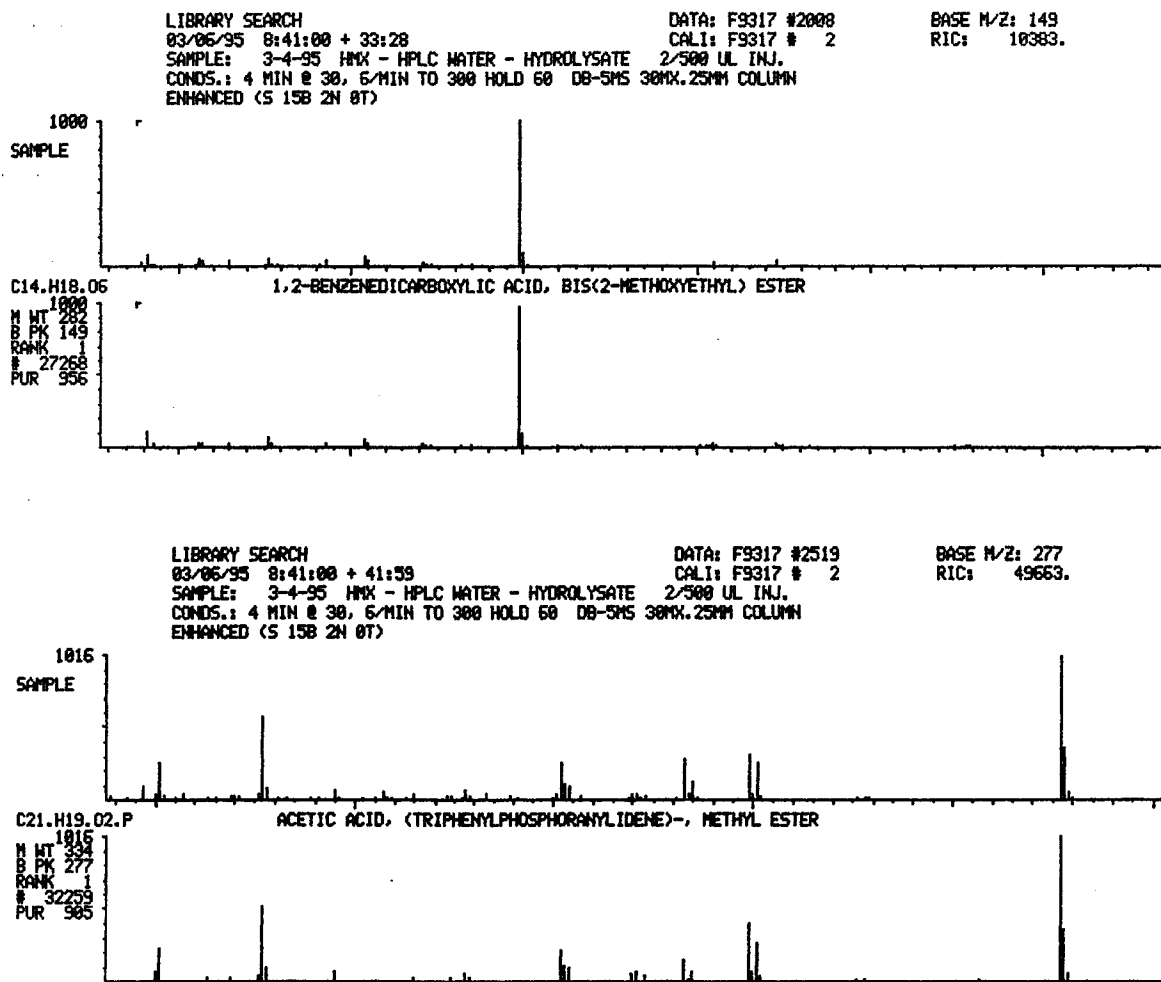


Figure 16 Mass-spectra of some compounds identified in the alkaline hydrolysates of HMX by GC/MS-analysis.

higher temperature range. Therefore, the following conclusions will have an important impact on the future research and development of the process.

The kinetic experiments and the modeling of the RDX- and HMX-degradation kinetics show:

1. HMX hydrolyzes slower than RDX. At the most rapid conditions (pH 12 and 80°C) HMX disappeared after approximately 10 minutes, whereas no RDX could be detected after only 2 minutes. The difference in the rates decreases with increasing temperature.
2. The experimental data accurately fit a pseudo first-order kinetic model at constant pH. The rates of the alkaline hydrolysis of RDX are approximately the tenfold of the rates of the alkaline hydrolysis of HMX.
3. Subsequent calculation of second-order rates from pseudo first-order rate data at constant pH was also precise. The dependence of the rates on the pH can conclusively be described using the pseudo first-order rate equation.
4. The temperature dependence of the rates was modeled using the *Arrhenius*-equation. The model accurately corresponds with the calculated second-order rates. The experimental activation energies differed only slightly suggesting a similar basic reaction mechanism:

$$\text{RDX: } E_a = 99.9 \pm 1.9 \text{ kJ}\cdot\text{mol}^{-1}$$

$$\text{HMX: } E_a = 111.9 \pm 0.8 \text{ kJ}\cdot\text{mol}^{-1}$$

Statistical analysis of the kinetic modeling confirms the excellent correspondence of experimental results and model.

5. Kinetic coefficients at 80°C, extrapolated from previous research over the range of 25°C to 45°C (Hoffsommer et al., 1977a; Croce and Okamoto, 1979), are 22% lower for RDX and 27% lower for HMX than measured in this investigation.

The kinetics of product formation were studied. The concentration-time data of  $\text{NO}_2^-$ , the only stable product of the first reaction step, and  $\text{HCOO}^-$ , which is believed to be produced most slowly, were investigated as representatives for the complete reaction mechanism:

6. The rate of  $\text{NO}_2^-$ -production is in accordance with the rate of RDX-disappearance. The other product of the first reaction step, RDX-h5, is not stable and could not be observed at any time.
7. The rate of  $\text{HCOO}^-$  formation is slow. Even at the most rapid conditions (pH 12 and  $80^\circ\text{C}$ ) the time to reach the equilibrium  $\text{HCOO}^-$ -concentration was more than 6 hours. This is due to the production of  $\text{HCOO}^-$  from both ring cleavage and the fourth-order *Canizarro*-reaction of formaldehyde at the elevated pH.
8. The reaction proceeds via a second reaction step where complex intermediates must be formed. Using GC/MS-analysis of the hydrolysates of RDX and HMX it was found that none of these complex intermediates are stable.
9. The carbon- and nitrogen mass balances were improved using new molar yield data for the products of the alkaline hydrolysis of RDX. 94% of the carbon and 90% of the nitrogen were found in the products.
10. Based on the results from the study of the product formation and composition a modified reaction pathway is proposed (Figure 17).

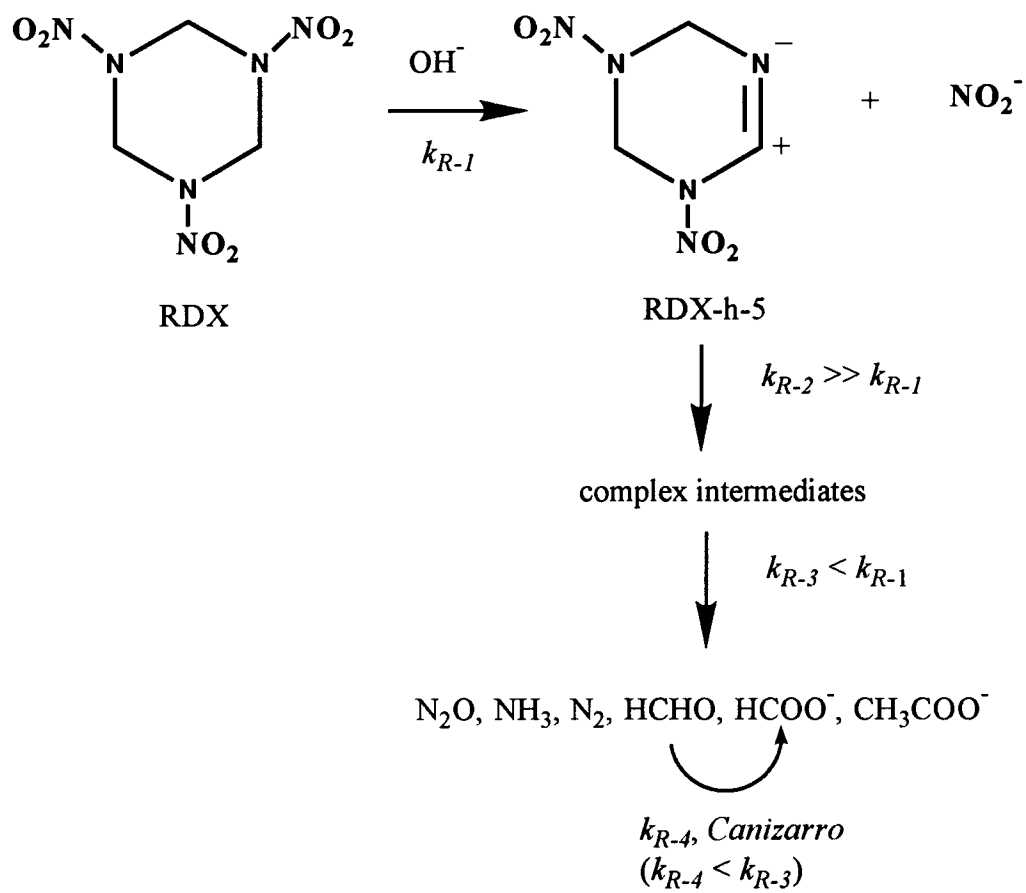


Figure 17 Proposed new reaction pathway of the alkaline hydrolysis of RDX.

## 6.2 Adsorption

### 6.2.1 Objectives

In order to determine if activated carbon can be repeatedly loaded and regenerated, the adsorptive behavior of virgin activated carbon must be evaluated. These data are needed as a benchmark to which all data from regenerated activated carbon can be compared. The

initial studies were conducted in batch reactors. The data can be used in later fixed-bed-adsorber design.

For the design of adsorption processes the following basic data are needed:

1. Adsorption equilibria: Isotherm experiments of virgin activated carbon are required. The experimental data can be fit to an isotherm equation.
2. Adsorption kinetics: In order to model breakthrough curves in fixed-bed adsorbers the diffusion coefficient needs to be determined. Adsorption kinetics experiments can be conducted in batch mode. Using the isotherm data and the concentration-time profile the kinetics can be modeled using the appropriate model. The diffusion coefficient can be estimated by fitting the experimental data to the model.

## **6.2.2 Isotherms of Virgin Activated Carbon**

### *i. Experimental*

All isotherm experiments were carried out with powdered activated carbon in order to minimize the time needed to reach equilibrium in the isotherm experiments. For the experiments with virgin Filtrasorb-400, the 325 x 200 mesh-size fraction (see Section 5.3.3) was used because the data were to be used for kinetic modeling. The equilibrium was reached between one and two days in all experiments. Concentration measurements were obtained after one, two and three days. No further concentration changes could be detected after two days in all experiments. Almost the entire concentration ranges of aqueous solubility of both compounds RDX and HMX were investigated. The lower limit was the HPLC-detection limit of 0.1 mg/L in this study; the upper limit was close to the solubility

limit of the compounds (approximately 50 mg RDX/L and approximately 5 mg HMX/L, see Section 2.1.1).

An equilibrium liquid phase concentration range from approximately 0.2 mg RDX/L to 30 mg RDX/L was investigated with the virgin Filtrasorb-400/RDX. It must be noted that the points at the upper end of the concentration range are difficult to obtain, and the possibility of experimental error rises drastically. This is due to the extremely small amounts of activated carbon that must be used to obtain these concentrations. In principal one could increase the volume of the experimental vessel; 4L-Erlenmeyer flasks were used here for the upper end of the concentration range and larger vessels could not be sufficiently agitated anymore.

The system virgin ABG-30/RDX was investigated from 0.6 mg RDX/L to approximately 15 mg RDX/L. A smaller concentration range was used for ABG-30 because the data were not to be used in kinetic modeling.

## ii. *Results and Model*

The *Freundlich*-equation, although empirical, has been successfully used to model the adsorption isotherms for a vast variety of adsorbate/adsorbent-systems:

$$q_e = K \cdot c_e^{1/n}$$

or

$$\ln q_e = \ln K + \frac{1}{n} \cdot \ln c_e \quad (6)$$

where  $q_e$  is the equilibrium adsorbent phase concentration and  $c_e$  the equilibrium bulk liquid phase concentration. The *Freundlich*-isotherm capacity constant  $K$  and *Freundlich*-isotherm

intensity constant  $1/n$  can be obtained from a linear least squares fit (linear regression) of  $\ln q_e$  over  $\ln c_e$  yielding  $1/n$  as the slope and  $\ln K$  as the intersection. The advantage of using the *Freundlich*-isotherm are the vast quantities of adsorption data in the literature that can be used for comparisons and model development. Particularly, in the field of adsorption of organics, the *Freundlich*-equation has been used extensively. Unfortunately, competitive multi-component adsorption effects can not be considered using the *Freundlich*-equation.

The isotherm for RDX on virgin Filtrasorb-400 shows a slightly higher capacity than the virgin isotherm for ABG-30 (Figure 18). This is also reflected in the different *Freundlich*-parameters (Table 15). The higher capacity constant  $K$  accompanied by somewhat similar intensity constants ( $1/n$ ) accounts for the higher adsorptive capacity of Filtrasorb-400 for RDX. In order to verify these results the isotherm experiments were repeated and the results confirm the earlier experiments (Table 15). The verified isotherms are also shown in Figure 18.

The system virgin Filtrasorb-400/HMX was studied within the concentration range from approximately 0.15 mg HMX/L to 3 mg HMX/L. It was noted before that the amounts of activated carbon needed to reach high equilibrium liquid phase concentrations are small. This was an even higher concern with HMX, since smaller initial concentrations exist due to HMX's low solubility. Very careful experimental procedures were used, and precise results were obtained.

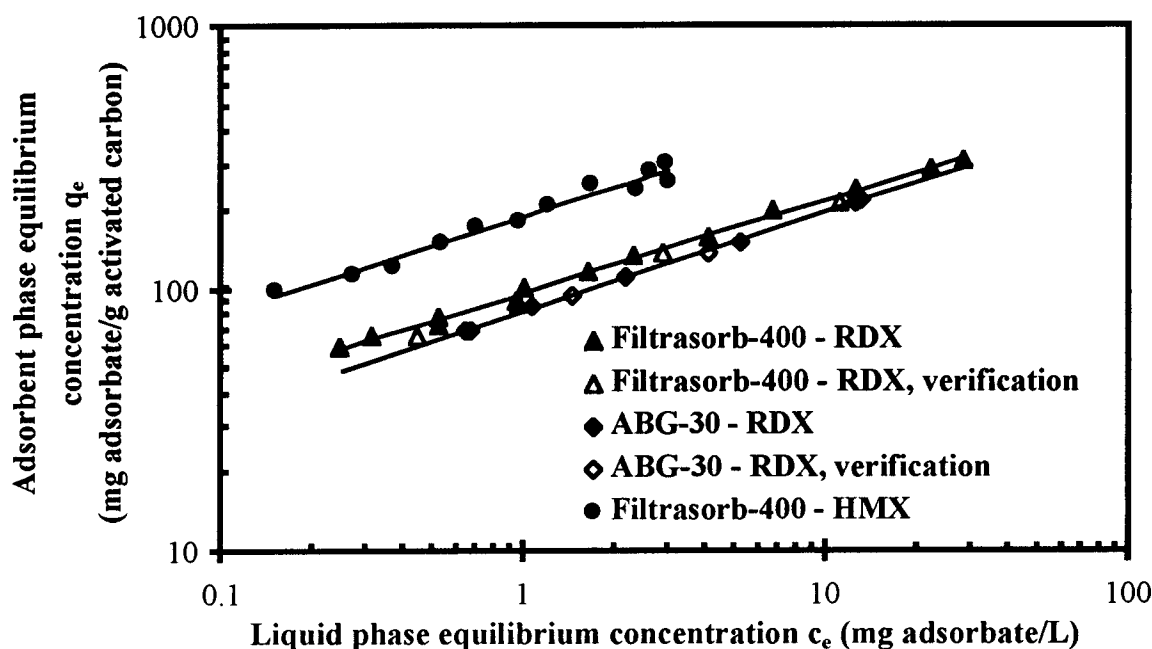


Figure 18 Virgin isotherms of RDX and HMX on activated carbon.

Table 15 *Freundlich*-constants and correlation coefficients for virgin activated carbon.

Adsorbent/Adsorbate System	$K (L/g)^{1/n}$	$1/n ( )$	$R^2$
Filtrisorb-400, RDX	$97 \pm 1$	$0.35 \pm 0.007$	0.9956
verification	$92 \pm 1$	$0.36 \pm 0.008$	0.9990
Filtrisorb-400, HMX	$190 \pm 1$	$0.37 \pm 0.019$	0.9742
ABG-30, RDX	$83 \pm 1$	$0.38 \pm 0.008$	0.9988
verification	$81 \pm 1$	$0.38 \pm 0.003$	0.9999

HMX adsorbs more strongly on Filtrasorb-400 than RDX (Figure 18), which is particularly indicated in the higher value of  $K$  (Table 15). This result was expected because HMX is less soluble in water and therefore has a greater affinity to adsorb onto activated

carbon. It is interesting that the isotherms for both carbons, Filtrasorb-400 and ABG-30, and both RDX and HMX show a somewhat similar slope, which is expressed in nearly equal values of the *Freundlich*-isotherm intensity constant  $1/n$ .

Burrows et al. (1984) determined the isotherms of RDX and HMX on Filtrasorb-300. Their results are in a 15%-variation range of the data presented here (see Section 3.3). Wujcik et al. (1992) published isotherms for RDX on Filtrasorb-200, -300 and -400 which vary by approximately 50% (capacity constants and intensity constants) from the results presented here. It is beyond the scope of this dissertation to determine the reasons for the differences.

Competitive adsorption, which was beyond the scope of this research, was not investigated. The fact that HMX adsorbs significantly stronger on activated carbon, however, will have important implications when industrial or commercial facilities are constructed. Additionally, the presence of other explosives and organic compounds in contaminated water will need consideration. TNT often accompanies RDX- and HMX-adsorption. In a study by Patterson et al. (1976c) activated carbon columns were found to break through before the capacity for TNT was achieved because RDX adsorbed more strongly on the activated carbon and limited the whole process.

### **6.2.3 Adsorption Kinetics**

#### *i. Experimental*

It should be stressed that very accurate results of the isotherm-tests are needed for valuable model predictions of the adsorption kinetics. The experimental procedures which

considered Hand et al.'s (1983) experimental protocol were presented earlier (see Section 5.3.3).

The necessary dosage of granular activated carbon to reach a particular equilibrium concentration ( $c_e/c_0 = 0.5$  is required for the user-oriented solution of the Homogeneous Surface Diffusion Model (HSDM), see next subsection) can be calculated based on a different formulation of the *Freundlich*-equation:

$$m_o = \frac{c_0 - c_e}{Kc_e^{1/n}} \quad (15)$$

The experimental normalized end concentration should not vary significantly from the desired value. A range of tolerance for different values of  $1/n$  is presented by Hand et al. (1983).

In an 1L-Erlenmeyer flask 0.067 g of Filtrasorb-400 were contacted with an RDX solution of 36.35 mg RDX/L. The solution was stirred by a stainless steel propeller-type stirrer driven by an overhead motor at different speeds. Timing commenced simultaneously with the beginning of an experiment and 1-mL-samples were drawn at precise time intervals. Based on the *Freundlich*-parameters this dosage should lead to a 50% reduction of the liquid concentration at equilibrium. The actual equilibrium concentration was 17.95 mg/L, yielding a  $c_e/c_0$  of 0.49, which is well in the acceptable range, as defined for the model by Hand et al. (1983).

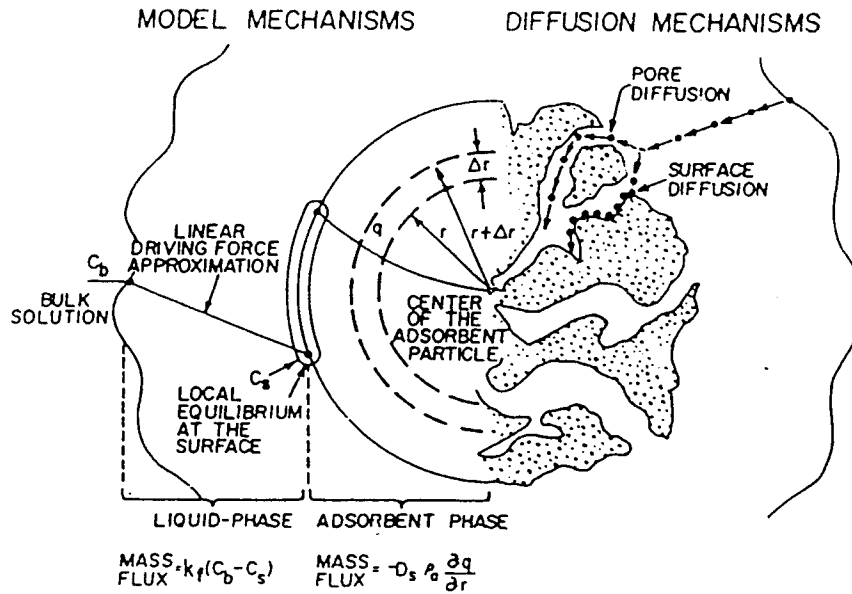
ii. *Results and Model*

In order to be able to calculate breakthrough-curves and understand the basic mass transfer mechanism of the adsorption of RDX on activated carbon the adsorption kinetics need to be studied and modeled. The surface diffusion coefficient  $D_s$  which can be obtained from modeling the adsorption kinetics under special conditions (surface diffusion, only; no external mass transfer resistance) represents the intraparticle mass transport processes during adsorption. The coefficient  $D_s$  is needed for simulations of adsorption processes and the design of fixed-bed adsorption systems. No data for  $D_s$  for the system activated carbon/RDX or other high explosives is available in the literature.

Batch adsorption kinetics data for the adsorption of RDX on activated carbon Filtrasorb-400 were obtained using a procedure suggested by Hand et al. (1983). The experimental data are presented in Figure 20.

Hand et al. (1983) present a user-oriented solution to the HSDM. The basic model assumptions for the HSDM are presented in Figure 19a. Hand *et al.* (1983) assume a spherical particle for the model mechanism. In earlier studies (Brecher et al., 1967; Crittenden, 1976; Furusawa and Smith, 1973; Komiyama and Smith, 1974; Suzuki and Kawazoe, 1975) it was shown that the surface diffusion flux is many times greater than the pore diffusion flux for strongly adsorbed species. Therefore, pore diffusion was neglected in the HSDM-model. External mass transfer resistance can be neglected when appropriate agitation is provided.

**a: Model mechanisms**



**b: Model sensitivity**

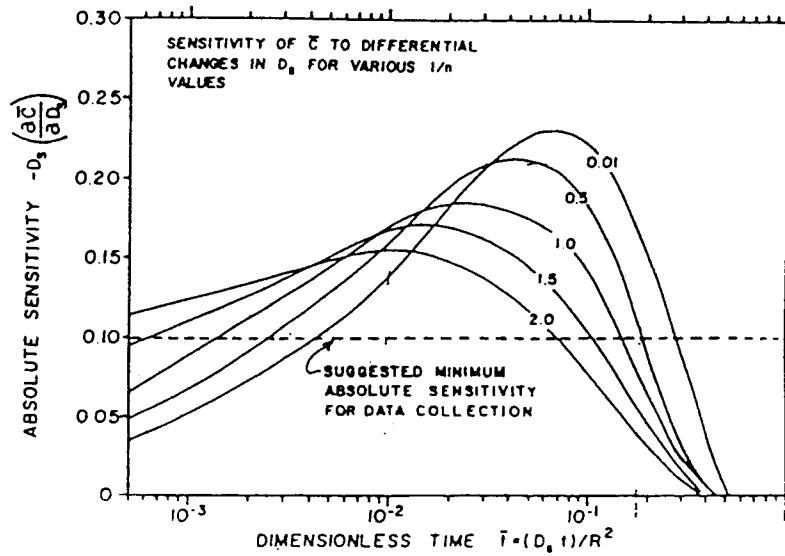


Figure 19a, b Homogeneous Surface Diffusion Model (after Hand et al., 1983).

c: Model solutions

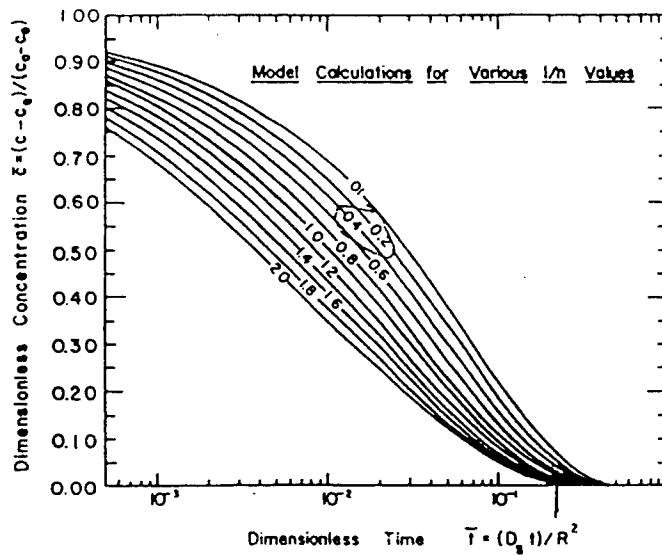


Figure 19c Homogeneous Surface Diffusion Model (after Hand et al., 1983).

The differential equation for the overall mass balance is (a more complete derivation of the model equations is given in the appendix):

$$\frac{\partial \bar{C}(\bar{t})}{\partial \bar{t}} = \frac{-3D_g}{(1 - \frac{c_e}{c_0})} \frac{\partial}{\partial \bar{t}} \int_0^1 \bar{q}(\bar{r}, \bar{t}) \bar{r}^2 d\bar{r}$$

where

$$\bar{r} = \frac{r}{R}$$

$$\bar{t} = \frac{t \cdot D_s}{R^2}$$

$$\bar{C}(\bar{t}) = \frac{c(\bar{t}) - c_e}{c_0 - c_e}$$

$$\bar{q}(\bar{r}, \bar{t}) = \frac{q(\bar{r}, \bar{t})}{q_e}$$

and

$$D_g = \frac{m_{AC} \cdot q_e}{V \cdot \varepsilon \cdot c_o} = \frac{(1 - \frac{c_e}{c_o})}{(\frac{c_e}{c_o})^{1/n}} \quad (7)$$

with the initial conditions:

$$\bar{C}(\bar{t} = 0) = 1$$

and (8)

$$\bar{q}(0 \leq \bar{r} \leq 1, \bar{t} = 0) = 0$$

The intraparticle mass balance is:

$$\frac{\partial \bar{q}(\bar{r}, \bar{t})}{\partial \bar{t}} = \frac{1}{\bar{r}^2} \frac{\partial}{\partial \bar{r}} \left( \bar{r}^2 \frac{\partial \bar{q}(\bar{r}, \bar{t})}{\partial \bar{r}} \right) \quad (9)$$

with the initial condition:

$$\bar{q}(0 \leq \bar{r} \leq 1, \bar{t} = 0) = 0 \quad (10)$$

and the boundary condition:

$$\frac{\partial \bar{q}(\bar{r} = 0, \bar{t} \geq 0)}{\partial \bar{r}} = 0 \quad (11a)$$

and for eliminated mass transfer resistance:

$$\bar{C}_s(\bar{t}) = \bar{C}(\bar{t}) \quad (11b)$$

The nonlinear equation which couples the differential equations is the *Freundlich*-isotherm

equation rewritten in dimensionless form:

$$q_e = K c_e^{1/n}$$

and

(12)

$$\bar{q}(\bar{r} = 1, \bar{t}) = \left[ \left(1 - \frac{c_e}{c_0}\right) \bar{C}_s(\bar{t}) + \frac{c_e}{c_0} \right]^{1/n}$$

Equation 11b simplifies Equation 12. The differential equations were solved using orthogonal collocation techniques. The HSDM-solutions are characterized by only two parameters:  $c_e/c_0$  and  $1/n$ . It is important to show in experiments that external mass transfer resistance could indeed be neglected.

In Hand et al.'s (1983) user-oriented solution the numerical solutions of the HSDM for eliminated liquid-phase mass-transfer resistance, a constant value of  $c_e/c_0 = 0.5$  and various values of  $1/n$  were fit to an empirical equation. The particular equilibrium concentration  $c_e/c_0 = 0.5$  was chosen, because the concentration-time profile may be difficult to measure accurately at large values of  $c_e/c_0$ . For small values of  $c_e/c_0$  the surface diffusion coefficient that is estimated may be for lower concentrations than normally encountered in fixed-bed adsorber operation. The empirical equation is:

$$\ln \bar{t} = \ln\left(\frac{t \cdot D_s}{R^2}\right) = A_0 + A_1 \bar{C}(\bar{t}) + A_2 \bar{C}(\bar{t})^2 + A_3 \bar{C}(\bar{t})^3 \quad (13)$$

Hand et al. (1983) provide the polynomial coefficients  $A_0$  to  $A_3$  for various values of the *Freundlich*-parameter  $1/n$  and  $c_e/c_0 = 0.5$  (see Table 16 for  $1/n=0.4$ ). They also showed for all values of  $1/n$  that the fit of the empirical equation to the numerical model solution is accurate and that model-fits obtained with this method are valid. They provide a second empirical equation and coefficients for the calculation of model-solutions using the surface diffusion coefficient  $D_s$  from above for simulation:

$$\bar{C}(\bar{t}) = B_0 + B_1(\ln \bar{t}) + B_2(\ln \bar{t})^2 + B_3(\ln \bar{t})^3 \quad (14)$$

The polynomial coefficients are provided by Hand et al. (1983) for various values of  $1/n$  and  $c_e/c_0 = 0.5$  (see Table 16). Model solutions can then be obtained for different values of the surface diffusion coefficient. The best fit surface diffusion coefficient is obtained from the model fit with the smallest average sum of the squares of the residuals.

Table 16 Polynomial coefficients [from Hand et al. (1983)].

$1/n$	$A_0$	$A_1$	$A_2$	$A_3$
0.4	-1.14297	-9.14255	13.2803	-11.982
	$B_0$	$B_1$	$B_2$	$B_3$
0.4	-0.15229	-0.08166	0.035631	0.003788

The batch adsorption kinetics of RDX on Filtrasorb-400 can be modeled using the HSDM (Figure 20a). For very short and very long model times, however, the model delivers invalid results. This can be seen in the singularity of the model solution between 0 and 10 minutes (see also next paragraph). This has nevertheless no influence on the calculation of the surface diffusion coefficient. Very long model times are also irrelevant for the model solution; they are presented for illustrative reasons (Figure 20b).

According to Hand et al. (1983) the surface diffusion coefficient is the average of the local coefficients for a specific model time window of high model sensitivity which is

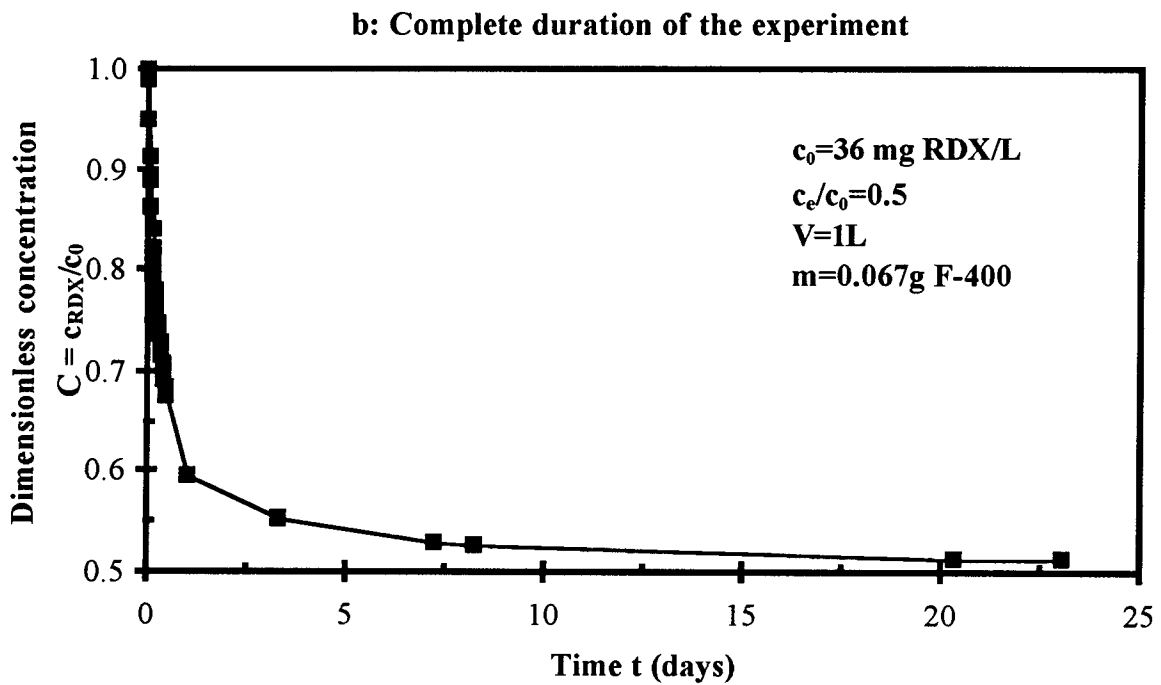
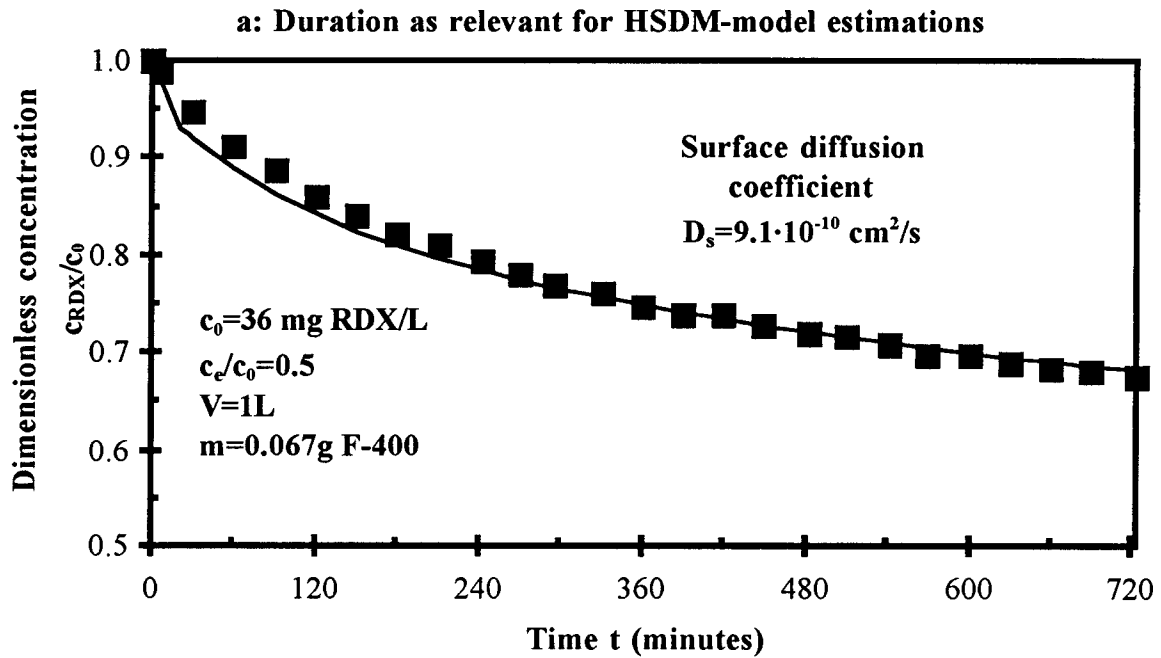


Figure 20 Adsorption of RDX on activated carbon Filtrasorb-400.

between 180 and 723 minutes in this study (Figure 19c). Based on the initial HSDM-model solution a surface diffusion coefficient of  $D_s = 9.8 \cdot 10^{-10} \text{ cm}^2/\text{s}$  was calculated. This value is indicated as "original" in Table 17 which presents a parameter optimization based on the minimization of the average sum of the squares of the residuals between the model and experimental data. The minimum of the average sum of the squares of the residuals was observed for 93% of the original value of the surface diffusion coefficient; the optimized value is  $D_s = 9.11 \cdot 10^{-10} \text{ cm}^2/\text{s}$ . The square root of  $S^2$  of the best model fit is the standard deviation  $S = 0.04$ . According to Hand et al.'s (1983) criteria, this is a good to excellent model fit. They distinguish between excellent fits ( $S = 0 - 0.04$ ), good fits ( $0.04 - 0.08$ ) and satisfactory fits ( $0.08 - 1$ ). Values of the standard deviation  $S$  above the value of 1 would indicate that the surface diffusion coefficient should not be used for column model predictions.

Table 17 Evaluation of the best-fit surface diffusion coefficient  $D_s$ .

percent of original estimate %	surface diffusion coefficient $D_s$ ( $\text{cm}^2/\text{s}$ )	sum of the squares of the residuals $S^2$	standard deviation $S$
100 (original)	9,8E-10	0,001767	0,042034
75	7,35E-10	0,003122	0,055873
85	8,33E-10	0,001877	0,043325
90	8,82E-10	0,001641	0,04051
<b>93 (optimized)</b>	<b>9,11E-10</b>	<b>0,001602</b>	<b>0,04002 (<math>S_{\min}</math>)</b>
95	9.3E-10	0.001614	0.040173
110	1,08E-09	0,00252	0,050204
125	1,22E-09	0,004507	0,067133

In order to verify eliminated external mass transfer resistance a special set of rate tests was carried out at different stir speeds. Ideally, the adsorption kinetics will be the same for different stir speeds if external mass transfer is eliminated. Stir speeds between 400 and 2000 rpm were investigated.

The rate tests were conducted using the same experimental protocol as described earlier, but samples were only drawn at four times. The results are presented in Figure 21 and Table 18. The kinetic curves for 400 to 1350 rpm show no significant differences. It is therefore clearly visible that in the observed agitation range mass transfer could be eliminated. In fact stir speeds of 400 rpm were already sufficient. The data presented earlier which were used for the modeling of the adsorption kinetics were obtained at 1350 rpm and are therefore valid. Results with 2000 rpm can be explained with particle attrition leading to different adsorption kinetics: Indeed, the activated carbon was ground partly at 2000 rpm by the stirrer. At the end of this experiment almost all formerly granular activated carbon was ground resulting in a colloidal solution of activated carbon and water. On the other hand, at all other agitation rates the granular activated carbon kept its shape over the entire duration of the experiment. All granular activated carbon was rinsed with deionized water repeatedly before the experiments. This removes all ground material from the virgin granular activated carbon.

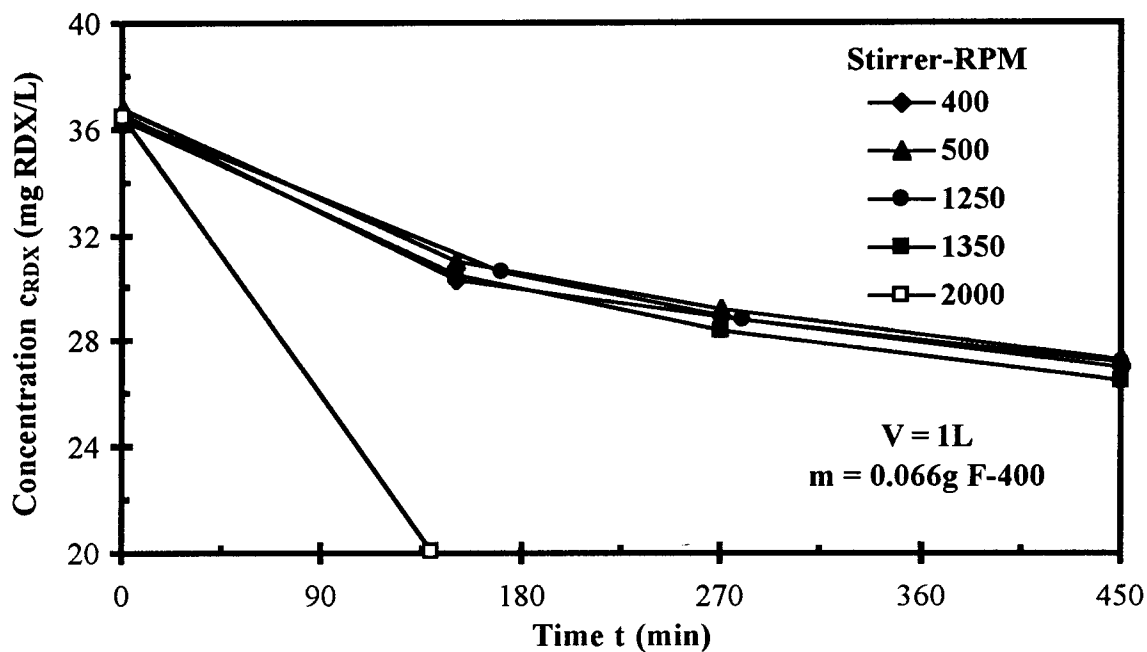


Figure 21 Influence of agitation on HSDM batch rate data.

Table 18 Adsorption kinetics of RDX on activated carbon Filtrasorb-400 at different stir speeds.

Stirrer RPM	400	500	1250	1350
$c_0$ (t = 0 min) (mg/L)	36.6	36.8	36.5	36.4
$c_e$ (t = 450 min) (mg/L)	27.0	27.3	27.2	26.5

$m_{AC} = 0.066 \pm 0.001$  g; V = 1000 mL

#### 6.2.4 Conclusions

The adsorption of the high explosives RDX and HMX on virgin activated carbon from the aqueous phase was investigated. Two activated carbon brands were studied: Filtrasorb-400 and ABG-30.

The adsorption equilibria were described using the *Freundlich*-equation:

1. The adsorptive capacity of Filtrasorb-400 for RDX is slightly higher ( $K = 97 (L/g)^{1/n}$ ) than the capacity of ABG-30 for RDX ( $K = 83 (L/g)^{1/n}$ ). The isotherms for both systems show almost similar slopes (RDX/F-400:  $1/n = 0.35$  and RDX/ABG-30:  $1/n = 0.38$ ) explaining the almost similar adsorptive characteristics of the isotherms.
2. HMX ( $K = 190 (L/g)^{1/n}$ ) adsorbs more strongly on Filtrasorb-400 than RDX ( $K = 97 (L/g)^{1/n}$ ). However, the intensity constant for HMX  $1/n = 0.37$  shows an almost similar slope of the isotherm than the two investigated systems with RDX ( $1/n = 0.35$  and  $1/n = 0.35$ ).

The adsorption of high explosives from the aqueous phase follows a similar mechanism independently of the studied adsorbent/adsorbate system as evidenced in the similar slopes of the isotherms. Nevertheless, significant differences in the adsorptive capacities exist for all studied systems.

The adsorption kinetics in a completely mixed batch reactor were studied and modeled with the homogeneous surface diffusion model (HSDM). The experiments were conducted for a  $c_e/c_0 = 0.5$  concentration versus time profile. Based on the model the surface diffusion coefficient which is needed for the design and modeling of fixed-bed adsorption systems was determined:

3. External mass transfer could be neglected and therefore the only model parameters were the *Freundlich*-isotherm intensity constant  $1/n$  and  $c_e/c_0$ . The surface diffusion coefficient  $D_s$  was found to be  $9.1 \cdot 10^{-10}$  cm<sup>2</sup>/s for the system Filtrasorb-400/RDX .
4. According to statistical analysis of the data and following the procedure suggested by Hand et al. (1983) the model fit was good to excellent.

## 6.3 Batch Regeneration of Activated Carbon

### 6.3.1 Objectives

There are no standard procedures for defining regenerative efficiency of activated carbon. In most of the available studies on activated carbon regeneration (Rovel, 1972; Beccari et al, 1977; Martin et al, 1985 and 1987; Hutchinson et al., 1990; Narbaitz and Cen, 1994) only single isotherm points were compared before and after regeneration. The variation in the values was used to define a regenerative efficiency. Newcombe (1993a, b; 1994) criticized this common concept to define regenerative efficiency because no information is collected to document desorption of adsorbed species. They found that due to surface charge effects, the capacity of exhausted activated carbon can increase during regenerative treatment without any desorption of adsorbates. Values of more than double the adsorptive capacity of the virgin material were found after regeneration.

Therefore, various methods were combined in the present work to assess the regenerative efficiency of the alkaline hydrolysis process in more detail:

- Batch regeneration kinetics were obtained and can be compared with aqueous homogeneous alkaline hydrolysis kinetics to evaluate completeness of desorption.

- Isotherms of regenerated activated carbon were obtained using the same experimental protocol as for virgin activated carbon and can therefore be easily compared with the isotherms for virgin activated carbon.
- The characteristics of the activated carbon surface before and after regeneration were assessed using BET-surface data.

With this combined method the actual desorption of products, as well as the adsorptive capacity and characteristic of the regenerated activated carbon, are comprehensively investigated over a wide concentration range.

### 6.3.2 Regeneration Kinetics

The batch aqueous homogeneous kinetics of the alkaline hydrolysis of RDX can be compared with batch desorption kinetics during alkaline hydrolysis regeneration of activated carbon. However, because the adsorbed RDX is rapidly destroyed during the regeneration process at elevated pH and temperature, its concentration cannot be used to determine desorption kinetics. Therefore,  $\text{NO}_2^-$  and  $\text{HCOO}^-$  were chosen as appropriate parameters to indicate desorption rates during regeneration.  $\text{NO}_2^-$  is the first product formed during the alkaline hydrolysis of RDX, while  $\text{HCOO}^-$  is more slowly produced because of its dual formation from the ring cleavage and the fourth-order *Canizarro*-reaction of formaldehyde (Hoffsommer et al., 1977; Euler and Lövgren, 1925; Birstein and Lobanow, 1927). The normalized liquid concentrations of  $\text{NO}_2^-$  and  $\text{HCOO}^-$  can then be compared for solid phase hydrolysis accompanied by desorption, as well as under aqueous homogeneous conditions.

*i. Experimental*

Under homogeneous conditions, 20 mM OH<sup>-</sup> (pH = 12) were added to an aqueous RDX-solution (35 mg/L) that was stirred and heated at 80°C (see Section 5.3).

For the regeneration experiments 0.13 g of dried (24 h at 105°C) Filtrasorb-400 activated carbon were contacted with 1 L of RDX-solution (36 mg RDX/L) in an Erlenmeyer-flask until equilibrium was reached; the equilibrium solid phase concentrations were  $q_e = 187$  mg RDX/g activated carbon for the regeneration experiment at 80°C and  $q_e = 196$  mg RDX/g activated carbon for the experiment at 90°C. The bulk liquid was then discharged and the carbon was dried at ambient temperature. The dry loaded carbon was then added to an Erlenmeyer-flask containing 1L of a regeneration solution (20 mmol OH<sup>-</sup>/L; pH 12) that was kept at the respective constant temperature for at least one hour before the experiment. Timing commenced simultaneously. Samples were taken and analyzed for RDX-, HCOO<sup>-</sup>- and NO<sub>2</sub><sup>-</sup>-content.

*ii. Results*

Experimental results at 80°C show that NO<sub>2</sub><sup>-</sup> is produced much faster under homogeneous conditions than during regeneration (heterogeneous condition), which suggests limitation through diffusion (Figure 22). However, the HCOO<sup>-</sup>-concentration during regeneration seems to be diffusion limited only in the beginning of the experiment. At the end of the experiment the rates of regeneration and the homogeneous hydrolysis are almost

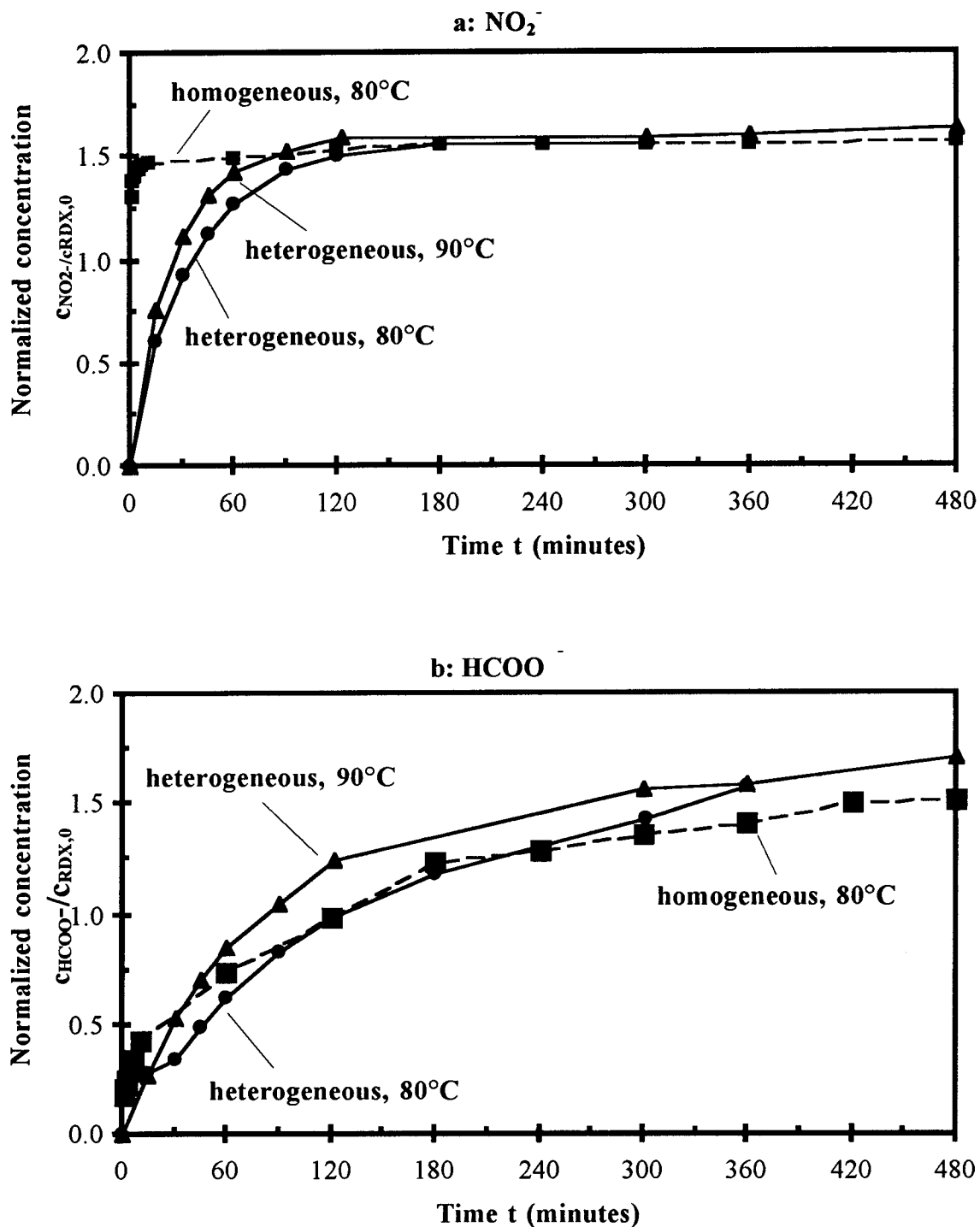


Figure 22 Product formation kinetics during the alkaline hydrolysis of RDX in an aqueous homogeneous system and on activated carbon for pH 12;  $c_0 = 0.16$  mmol RDX/L.

the same, which indicates chemical limitation at this stage of the process. RDX could not be detected in the liquid-phase at any time during the regeneration experiment. At 90°C the desorption proceeds more rapidly but follows the same basic pattern.

Most importantly, the final yields are virtually the same for homogeneous conditions and regeneration conditions. The homogeneous reaction yields 1.6 M  $\text{NO}_2^-$  and 1.5 M  $\text{HCOO}^-$  per mole of RDX. The regeneration experiments yielded 1.6 M  $\text{NO}_2^-$  and 1.6 M  $\text{HCOO}^-$  per mole RDX at 80°C and 1.6 M  $\text{NO}_2^-$  and 1.7 M  $\text{HCOO}^-$  per mole RDX at 90°C. The slight difference for  $\text{HCOO}^-$  is likely due to experimental error.

The regenerated activated carbon was furthermore contacted with 10 mL of acetonitrile in a 25 mL vial on a shaker table. No residual adsorbed RDX could be found in the bulk liquid after several weeks. This indicates that the alkaline hydrolysis of adsorbed RDX and subsequent desorption of hydrolysis products is complete.

### **6.3.3 Readsorption of Products**

The regeneration kinetics experiments were continued after complete desorption, in order to study readsorptive effects between the bulk regeneration liquid and activated carbon, as well as to determine any residual desorption from the activated carbon. After 24 h the bulk liquid of the experiment at pH 12 and 80°C was separated from the regenerated activated carbon. To the regeneration solution 0.18 g of virgin Filtrasorb-400 were added in order to determine any re-adsorption of the products on activated carbon. No reduction of the concentration of  $\text{NO}_2^-$  and  $\text{HCOO}^-$  could be detected.

The separated regenerated activated carbon was itself added to 1L of fresh D.I-water in order to determine if any further desorption would occur. No further desorption could be detected. Furthermore, after 2 hours 2 mL of 10 M NaOH were added to the mixture. After another 2 hours no further increase in the  $\text{NO}_2^-$ - and  $\text{HCOO}^-$ -concentration could be detected.

#### 6.3.4 Regeneration Cycles

Two activated carbon brands were investigated:

1. Filtrasorb-400
2. ABG-30

Spent ABG-30 from high explosives contaminated water treatment at a nuclear weapons dismantling site, the DOE's Pantex Plant in Amarillo, Texas, was shipped wet to UCLA for further analysis and experiments. The contaminated water there contains HMX and small amounts of RDX.

In order to determine the load of high explosives on the exhausted ABG-30, 0.2 g of the spent ABG-30 that was previously loaded at the Pantex Plant was extracted with 10 mL of acetonitrile for 24 h on a shaker table. The activated carbon contained 9 mg RDX and 45 mg HMX/g activated carbon and an unknown very small amount of background materials.

##### *i. Experimental*

1.4 g activated carbon were contacted with an RDX-solution (36 mg RDX/L) until all RDX was adsorbed on the activated carbon. The RDX-laden carbon was then contacted for 6

hours with an alkaline regeneration solution (1L water + 20 mL 10-M NaOH; pH 13) at 80°C in an 1L-Erlenmeyer-flask. The solution was stirred by a stainless steel propeller-type stirrer driven by an overhead motor at 900 rpm. This constituted an adsorption-regeneration cycle. This procedure (adsorption followed by regeneration) was repeated until the required number of regeneration cycles was achieved. The activated carbon was then ground and an isotherm was obtained using the same procedure as described earlier (see Section 5.3.3). Usually, four isotherm-points (aliquots of 0.1, 0.23, 0.37 and 0.5 g were contacted with 1L of a 36 mg RDX/L-solution) were obtained for regenerated activated carbon isotherms. In the case of ABG-30 the first adsorption-regeneration cycle was started directly with regeneration because the activated carbon was already exhausted.

ii. *Results*

Figure 23 shows isotherms of activated carbon that was regenerated with alkaline hydrolysis and repeatedly reloaded in up to 10 (Filtrisorb-400, Figure 23a) or 6 (ABG-30, Figure 23b) adsorption-regeneration cycles, respectively. Both activated carbons show only a small reduction in adsorptive capacity after several adsorption-regeneration cycles. This is also confirmed by the *Freundlich*-parameters in dependence of the numbers of regeneration cycles (Table 19). The intensity constant remains almost constant for both activated carbons. However, there is obviously a decrease in the values of  $K$ , the capacity constant. This is true for both Filtrisorb-400 and ABG-30.

In the case of ABG-30 the capacity constant first increases to a maximum value of

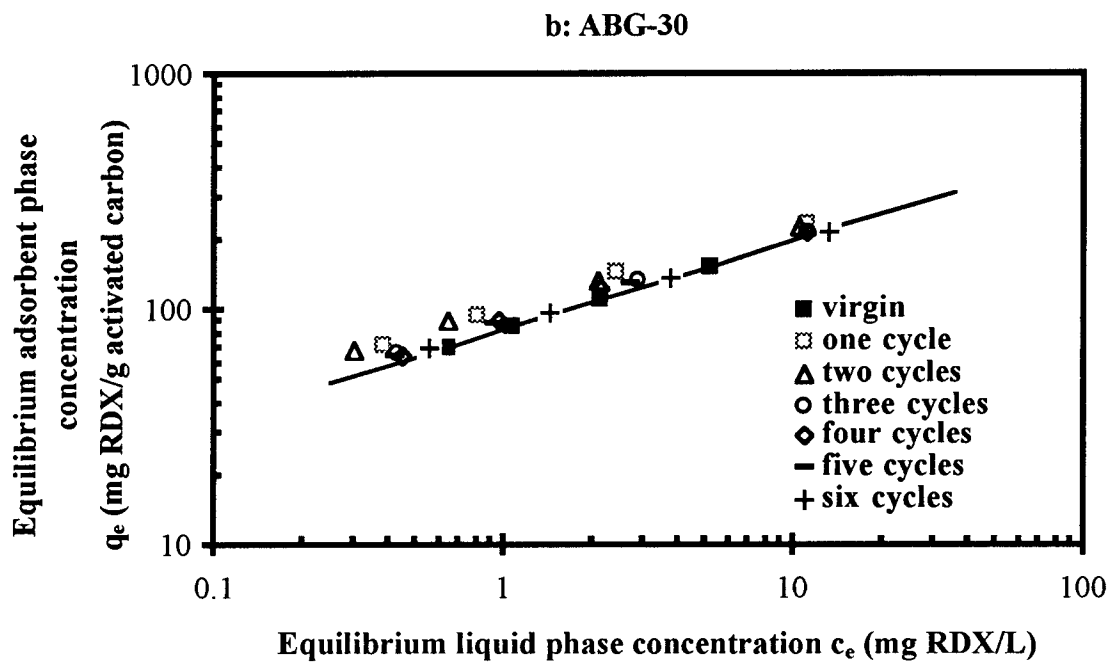
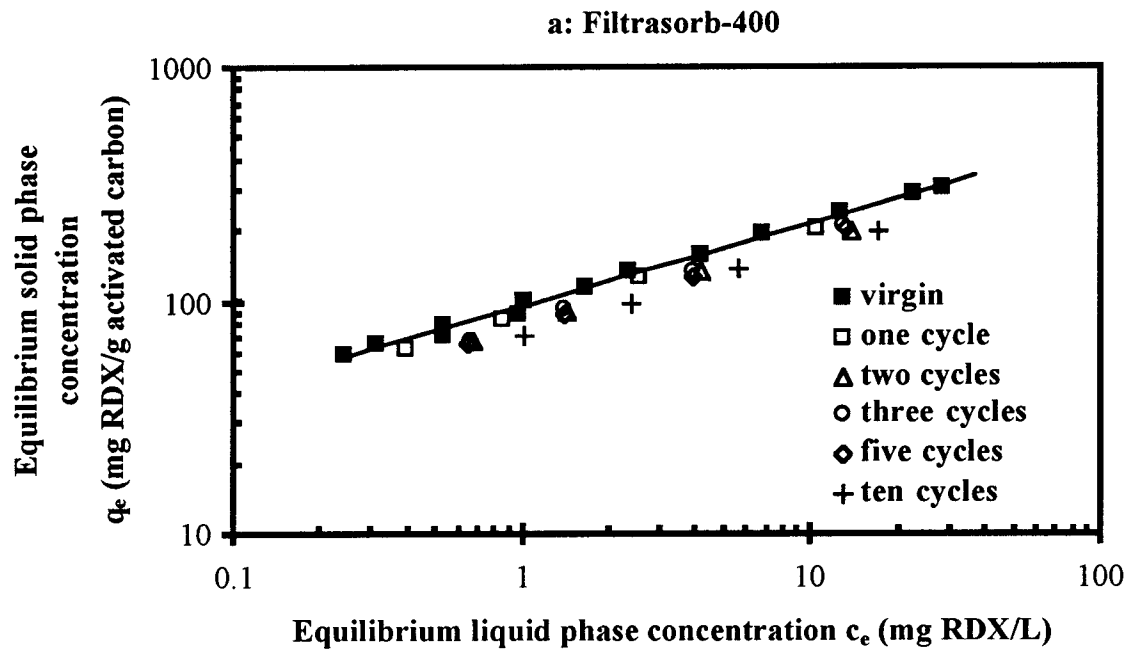


Figure 23 Isotherms of repeatedly regenerated activated carbon.

103 (L/g)<sup>1/n</sup> and then slowly decreases with higher numbers of regeneration cycles. The isotherm of virgin ABG-30 shows a lower adsorptive capacity for RDX than the virgin Filtrasorb-400 isotherm. After regeneration with alkaline hydrolysis the capacity of ABG-30 for RDX is higher than the capacity of virgin Filtrasorb-400 (Figures 18 and 23; Tables 15 and 18). Evidently, the alkaline hydrolysis regeneration process changes the parameters of the virgin ABG-30 much more than it changes those for Filtrasorb-400. This may be attributed to a "wash-effect"; by flushing the activated carbon with a hot alkaline solution some background contamination originating from the production of activated carbon is desorbed. Unfortunately, it is not possible to obtain detailed information about the production processes from the manufacturers because these information are usually trade secrets. It also indicates that virgin ABG-30 may have a higher background contamination than Filtrasorb-400. Newcombe et al. (1993a, 1993b and 1994) also discussed an effect of alkaline solutions on the surface charge distribution of activated carbon. The changed surface charge raised the adsorptive capacity after alkaline regeneration in their study. The change occurred, even though a mass balance had shown that complete desorption of the adsorbates did not occur during the alkaline treatment.

The experiments with commercially loaded ABG-30 were conducted in order to compare the data for synthetically loaded Filtrasorb-400 with an activated carbon (ABG-30) that may have additional background contamination from its commercial use. It is evident that ABG-30 shows a less predictable adsorptive behavior. Principally, the regeneration process works as well for ABG-30 as it does for Filtrasorb-400.

For both activated carbons a period exists when the capacity constants do not change significantly. This is between three and five (ABG-30) and two and five (Filtrisorb-400) cycles, respectively (Table 19). After additional adsorption-regeneration cycles the capacity constant decreases. This seems to be more dramatic for Filtrisorb-400. After 10 cycles the capacity decreases by 24%; this is still only 2.4%-points per adsorption-regeneration cycle. After a few numbers of adsorption-regeneration cycles a threshold concentration of residual adsorbates may be surpassed. This may lead to a slow but constant decrease in the adsorptive capacity. In future investigations this aspect should be considered.

All these regenerations were carried out for 6 hours at 80°C and pH 13. It may very well be possible that a regeneration time of 6 hours is not completely sufficient and desorption of alkaline hydrolysis products still proceeds at a very slow rate after 6 hours. This small residual of products on the carbon would then build up on the activated carbon with every adsorption-regeneration cycle and may lead to the small decrease in adsorptive capacity. Reviewing the desorption kinetics in Figure 22, this assumption may be supported, because at 80°C and pH 12 a small change in the  $\text{HCOO}^-$ -concentration is indeed still observable at the end of the experiment. The increase of the pH to 13 may not yet be sufficient to reach complete equilibrium during regeneration after 6 hours.

### **6.3.5 Acid Post Treatment**

High and low pH may significantly change the surface properties of activated carbon (Newcombe et al., 1993 a and b, 1994). This can have an effect on the adsorptive capacity and characteristics of the activated carbon. If a high pH changes the activated carbon surface

charge to a relatively negative charge, then it should be possible to reset this charge by post-treating an alkaline hydrolysis regenerated activated carbon with acid.

Table 19 *Freundlich*-isotherm constants for regenerated activated carbon.

<b>ABG-30, RDX.</b>							
Regeneration cycles	0	1	2	3	4	5	6
1/n	0.38±	0.35±	0.34±	0.37±	0.36±	0.35±	0.36±
	0.008	0.014	0.009	0.012	0.017	0.007	0.003
K (L/g) <sup>1/n</sup>	83 ± 1	102 ± 1	103 ± 1	89 ± 1	90 ± 1	89 ± 1	85 ± 1
R <sup>2</sup>	0.9988	0.9969	0.9986	0.9980	0.9958	0.9992	0.9998
Regeneration cycles	1 + acid						
1/n	0.36±						
	0.016						
K (L/g) <sup>1/n</sup>	112 ± 1						
R <sup>2</sup>	0.9962						
<b>Filtrisorb-400, RDX</b>							
Regeneration cycles	0	1	2	3	5	10	
1/n	0.35	0.37	0.36	0.38	0.37	0.37	0.37
	± 0.007	± 0.008	± 0.008	± 0.006	± 0.002	± 0.006	± 0.006
K (L/g) <sup>1/n</sup>	97 ± 1	89 ± 1	80 ± 1	81 ± 1	87 ± 1	73 ± 1	
R <sup>2</sup>	0.9956	0.9992	0.9991	0.9996	0.9999	0.9995	
Regeneration cycles	1 + acid						
1/n	0.37 ±						
	0.002						
K (L/g) <sup>1/n</sup>	87 ± 1						
R <sup>2</sup>	0.9999						

The effect of an acid-post treatment subsequent to alkaline hydrolysis regeneration was investigated for Filtrasorb-400 and ABG-30. Granular activated carbon that was regenerated once with alkaline hydrolysis was post-treated with hydrochloric acid in order to determine any improvement in the isotherm due to a reset of the surface charge after alkaline treatment:

- The activated carbon was separated from the alkaline solution after regeneration and rinsed with D.I. water and then put in an Erlenmeyer-flask containing a 0.01-M HCl-solution and put on a shaker table for 16 h.
- The results were compared with activated carbon that was regenerated once without post-treatment (Figure 24).

Although there is a small visible improvement due to acid-post treatment, the effect is not very large. The values of the capacity constants confirm this. The increase in adsorptive capacity is higher for ABG-30 than for Filtrasorb-400 (Table 19). It was noted earlier, that the increase in capacity of exhausted ABG-30 from the Pantex Plant after the first regeneration cycle was significant (see Section 6.3.4). The fact that ABG-30 also responds stronger to acid post-treatment confirms the assumption that surface charge effects may have a higher impact on ABG-30.

### **6.3.5 BET Surface Area Measurement**

A widely applied method to evaluate the surface characteristics of activated carbon and other adsorbents is the BET-surface area analysis. As a result of this analytical method the overall surface area of the adsorbent is determined.

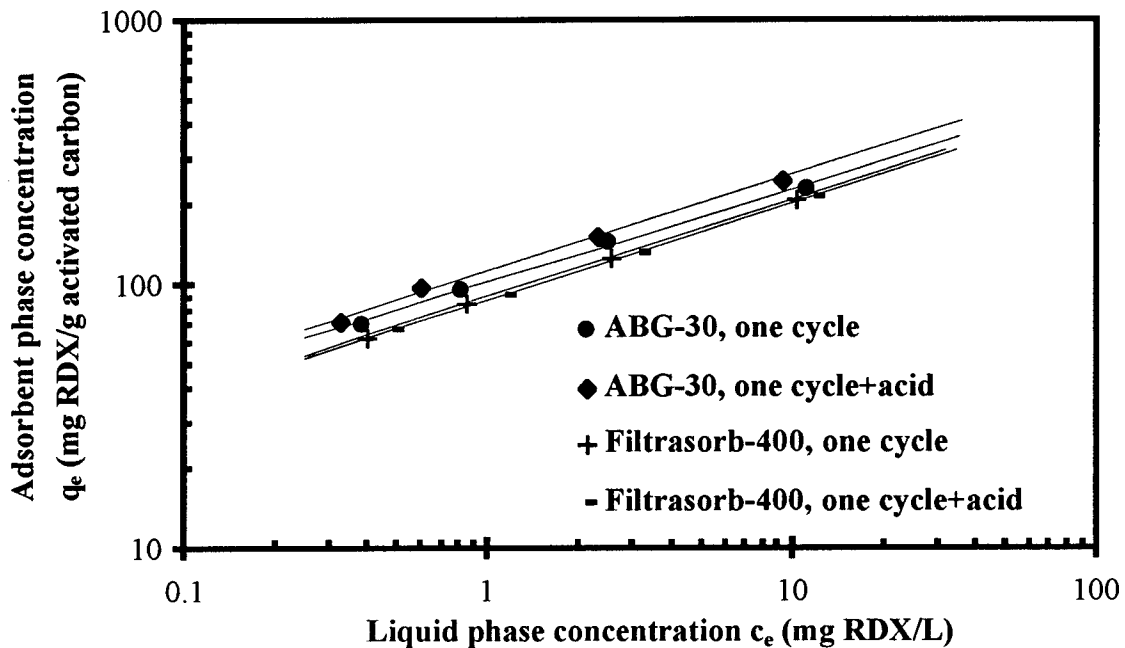


Figure 24 Isotherms of regenerated and acid post-treated activated carbon Filtrasorb-400.

Activated carbon samples that were exhausted and regenerated with the earlier described methods were analyzed for the BET-surface area in order to determine if the overall surface area changes after regeneration with alkaline hydrolysis. Three sets of samples were prepared:

1. Activated carbon Filtrasorb-400 was loaded to equilibrium solid phase concentrations of approximately  $q_e = 200$  mg RDX/g. The laden material was then regenerated using alkaline hydrolysis or alkaline hydrolysis followed by acid post-treatment, respectively.

2. A set of blanks was also prepared. Virgin activated carbon Filtrasorb-400 samples were treated with the same methods as above (1). The effect of the treatment method on virgin activated carbon can be determined and compared.
3. Virgin activated carbon with and without pre-treatment using hot DI water was also evaluated.

The previously discussed results (see Section 6.3.4) are confirmed in principal by BET-surface area analysis of activated carbon:

When virgin Filtrasorb-400 is rinsed with hot water the surface area increases only slightly over the value for untreated virgin Filtrasorb-400. The BET-surface area of exhausted Filtrasorb-400 ( $q_e = 180$  mg RDX/g) is approximately half of the surface area of virgin Filtrasorb-400 (Table 20). This indicates that significant unused surface spaces still exist even after exhaustion. After alkaline hydrolysis regeneration the surface area regains almost the value of virgin Filtrasorb-400.

A blank sample shows the effect on the surface area if virgin Filtrasorb-400 is treated with alkaline hydrolysis at the same conditions. Evidently, alkaline hydrolysis alone does not alter the surface of the activated carbon considerably. Rather the desorption of the previously adsorbed species must be responsible for the increase of the surface area after regeneration.

An acid-post treatment of the alkaline hydrolysis regenerated activated carbon further increases the value of the surface area to a value that is almost exactly the same as for virgin activated carbon (Table 20). Alkaline hydrolysis with subsequent acid-treatment of the virgin Filtrasorb-400 (blank sample) also increases the value of the surface area above that of

virgin Filtrasorb-400. The effect of acid on the surface of activated carbon is evident. The possible reasons for this behavior were already discussed (see Section 6.3.5).

Table 20 Results of the BET-surface area measurements of activated carbon.

Sample	Treatment applied on sample	BET-surface area (m <sup>2</sup> /g)	BET-surface area of blank (m <sup>2</sup> /g)*
Virgin Filtrasorb-400	no treatment	910	
Virgin Filtrasorb-400, pretreated	stirred in DI water at 80°C for 16 hours	917	
Filtrasorb-400 loaded	loaded to $q_e = 180$ mg RDX/g	488	
Filtrasorb-400 regenerated	loaded to $q_e = 195$ mg RDX/g, regenerated at pH 13 and 80°C for 6 hours	884	911
Filtrasorb-400 regenerated and acid-post treated	loaded to $q_e = 195$ mg RDX/g, regenerated at pH 13 and 80°C for 6 hours, then 16 hours on shaker in 0.01-M HCl	905	941

\* In order to evaluate the effect of alkaline treatment and acid-post treatment on the surface area of activated carbon alone, a blank experiment was defined for control purposes: Virgin activated carbon was contacted with a regeneration solution under the same conditions as the exhausted activated carbon. The BET-surface area was measured after the contact with the regeneration solution.

### 6.3.7 Residual Adsorbates After Regeneration

All activated carbon samples that were analyzed for the BET-surface area were also extracted with acetonitrile in order to determine any residual RDX content on the activated carbon:

- From each sample 0.2 g activated carbon were shaken for several days in 10 mL of acetonitrile.
- The bulk liquid was then analyzed on the HPLC for its RDX-content.

No residual RDX could be detected in any of the alkaline hydrolysis regenerated activated carbon samples.

### 6.3.8 Conclusions

A different method from those used in previous research studies was chosen to evaluate regenerative efficiency in the present work. Therefore, experimental data and modeling results from the following areas were combined:

- Kinetics of alkaline hydrolysis products desorption during regeneration of exhausted activated carbon were compared with data from aqueous homogeneous experiments under the same conditions (T, pH).
- Regenerated activated carbon was contacted with organic solvents to determine residual desorption. BET-surface area data was measured for regenerated activated carbon and compared with data for virgin activated carbon.
- Isotherms of repeatedly exhausted and regenerated activated carbon were investigated and can be compared with data for virgin activated carbon and as a function of regeneration cycles.

The investigation of the desorption kinetics during regeneration showed that:

1. The desorption of  $\text{NO}_2^-$  and  $\text{HCOO}^-$  was complete when compared to data from batch experiments on the aqueous homogeneous alkaline hydrolysis. Even though

$\text{NO}_2^-$ -formation was slower during regeneration,  $\text{HCOO}^-$ -formation was only initially slower than under aqueous homogeneous conditions.

2. Regenerated carbon was extracted with acetone to verify completeness of desorption. No residual RDX could be found on the regenerated activated carbon.
3. After the end of a batch regeneration experiment the bulk liquid and the regenerated activated carbon were separated. No further desorption off the activated carbon could be observed when the regenerated activated carbon was contacted with a fresh solution. Furthermore, no readsorption of  $\text{NO}_2^-$  and  $\text{HCOO}^-$  on activated carbon from the bulk liquid could be observed.

The dependence of the adsorption behavior of repeatedly exhausted and regenerated activated carbon was evaluated using isotherms and BET-surface area data:

4. After ten regeneration cycles the adsorptive capacity constant for Filtrasorb-400 and RDX was approximately 20% lower than for virgin activated carbon.
5. The isotherms for ABG-30 and RDX after 6 regenerations show a similar value to isotherms for virgin activated carbon. However, the value of the capacity constant increased after the initial regeneration with alkaline hydrolysis and from the peak value a loss of approximately 15% can be observed after 6 regeneration cycles.
6. A subsequent acid-wash after regeneration with alkaline hydrolysis did not improve the isotherms of regenerated activated carbon considerably.
7. BET-surface areas comparable to those for virgin activated carbon were observed after regeneration with alkaline hydrolysis.

8. Continued contact of activated carbon with alkaline solution (pH 12 and 13) does not effect the surface properties of activated carbon considerably; however, the adsorptive capacity decreases slowly due to alkaline treatment. It is not yet clear if this is due to contact with the alkaline solution alone or if a load of residual adsorbates or hydrolysis products accumulates with each regeneration cycle. This also raises the question if a residual load or change of the surface is reversible and if the process can be accordingly optimized.

## **6.4 Fixed Bed Studies**

### **6.4.1 Objectives**

Commercial or industrial adsorption technology usually employs fixed-bed adsorption columns. The basic physico-chemical results from batch studies therefore need to be verified in continuous process column operation. The work with the high explosives RDX and HMX presented special problems during the implementation of the adsorption/regeneration process in columns in lab-scale experiments. For safety reasons, only small amounts of RDX and HMX can be handled in a university laboratory. Therefore, the laboratory scale adsorbers had to be very small. To make later scale-up easier, height to diameter ratios common in industrial use were used in the experimental setup.

The objectives of the column studies which were developed from the findings of the previous three sections were:

1. To show in principal the feasibility of the alkaline hydrolysis regeneration process for activated carbon in fixed-bed adsorbers.
2. To determine empty-bed contact times for column adsorption of RDX on activated carbon.
3. To determine process conditions (T, pH, flow-rate of recirculating base) at which complete regeneration of the exhausted activated carbon can be achieved.

#### 6.4.2 Column Adsorption

The empty bed contact time, a formulation of a retention time for adsorbers, of an activated carbon bed is defined as:

$$t_{re} = \frac{V_b}{\dot{V}} \quad (16)$$

As the dimensionless time for an activated carbon fixed bed experiment the throughput in bed volumes fed is defined as:

$$\tau = \frac{\dot{V} \cdot t}{V_b} = \frac{t}{t_{re}} \quad (17)$$

All column studies were carried out with activated carbon Filtrasorb-400. Prior to an experiment the activated carbon was rinsed with DI water to remove all fines. Complete breakthrough curves, where the experiment was run until the effluent concentration reached the influent concentration, were only conducted when absolutely necessary. This had two reasons:

- High explosives inventory restrictions limited the stock of RDX and HMX to 1g.

- The main objective of the column adsorption studies in the present work was to generate exhausted columns for later column regeneration using alkaline hydrolysis while using the high explosives stock sparingly.

Figure 25a shows the results of a screening of different  $t_{re}$  in a column with a bed length of 70 mm (length to diameter ratio 7:1) filled with virgin activated carbon Filtrasorb-400. The experiments were stopped before complete breakthrough (effluent concentration = influent concentration) because the stock of high explosives was exhausted already earlier. As a consequence the bed length of 70 mm was not used for the regeneration experiments. Nevertheless, the three investigated  $t_{re}$  represent typical different breakthrough characteristics:

1.  $t_{re} = 0.88$  min;  $V = 5.5$  mL;  $m = 2.4$  g Filtrasorb-400; influent concentration = 19 mg RDX/L: The effluent concentration increases constantly from the beginning of the experiment.
2.  $t_{re} = 1.19$  min;  $V = 5.5$  mL;  $m = 2.4$  g Filtrasorb-400; influent concentration = 19 mg RDX/L: The effluent concentration stabilizes at a small but detectable value before it begins to increase after a throughput of approximately 1500 fed bed volumes.
3.  $t_{re} = 1.75$  min;  $V = 5.5$  mL;  $m = 2.4$  g Filtrasorb-400; influent concentration = 19 mg RDX/L: At the longest  $t_{re}$  the effluent concentration is stable below the detection limit for the entire duration of the experiment.

These results can be explained with classic fixed-bed adsorber theory: For the shortest  $t_{re}$  of 0.88 minutes the mass transfer zone cannot be fully established. The mass transfer zone

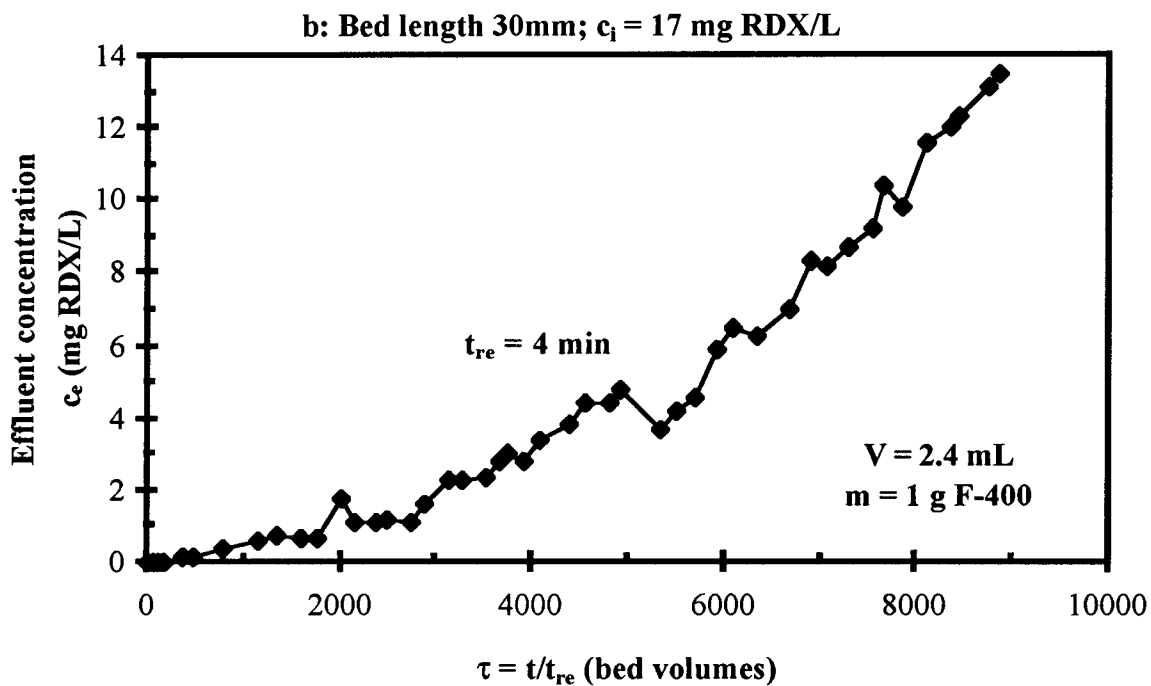
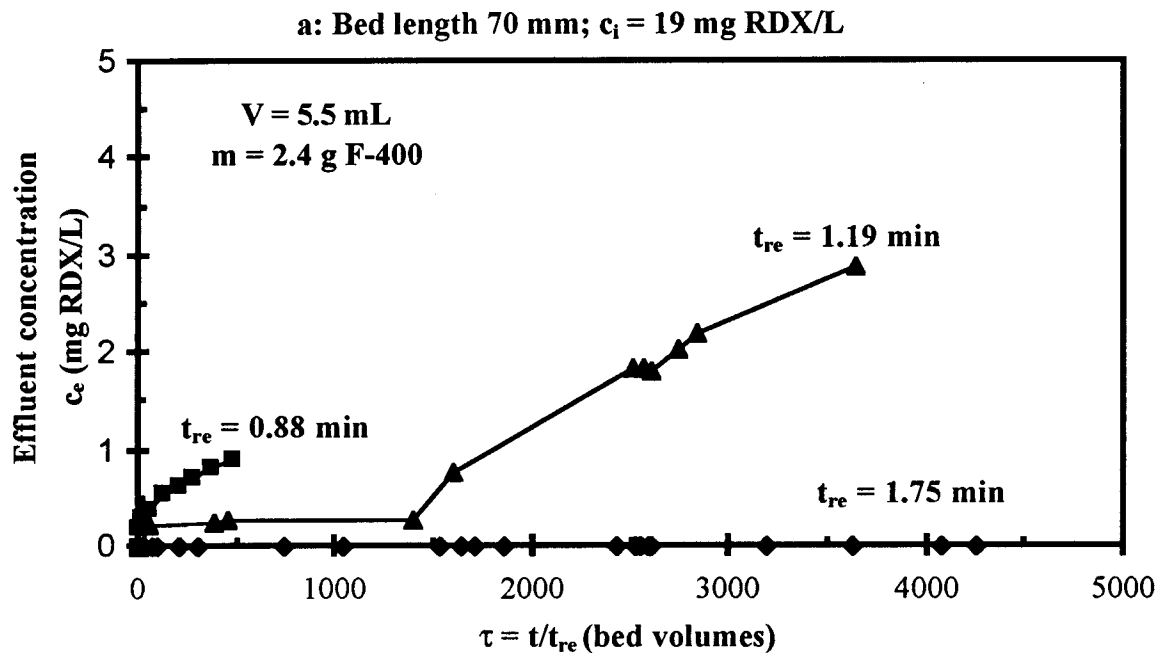


Figure 25 Adsorption of RDX on Filtrasorb-400 in continuous flow fixed-bed adsorbers.

spreads over a length that is longer than the length of the activated carbon bed. For an  $t_{re}$  of 1.19 minutes the mass transfer zone is established and travels through the column until reaching the end of the activated carbon bed at a throughput of approximately 1500 fed bed volumes. For the longest  $t_{re}$  of 1.75 minutes the mass transfer zone is established and does not reach the end of the activated carbon bed during the experiment.

Figure 25b shows a more complete breakthrough experiment in an adsorber with a bed length of 30 mm of virgin Filtrasorb-400 (length to diameter ratio 3:1;  $t_{re} = 4$  min;  $V = 2.4$  mL;  $m = 1$  g Filtrasorb-400; influent concentration = 17 mg RDX/L). A concentration below the detection limit could only be maintained for a throughput of approximately 150 fed bed volumes. The effluent concentration subsequently increased until reaching a value of approximately 14 mg RDX/L at a throughput of approximately 9000 fed bed volumes. At the end of the experiment a mean adsorbent phase concentration of  $q_e = 256$  mg RDX/g activated carbon was achieved. This breakthrough curve for virgin activated carbon will later be compared with breakthrough curves of repeatedly regenerated activated carbon.

### 6.4.3 Column Regeneration

The same system as above was used for the column regeneration studies:

1. In adsorption mode the activated carbon beds were exhausted until a sufficient mean adsorbent phase concentration was reached.
2. In regeneration mode the columns were kept at a constant temperature: the water jackets were fed with recirculated water by an Isotemp recirculator (Fisher Scientific 9105 or 8005, respectively).

3. For the regeneration 1 L of an aqueous alkaline regeneration solution (2 mL 10-M NaOH; pH = 12 or 2 mL 1-M NaOH; pH = 11, respectively) was heated and stirred in an 1L-Erlenmeyer flask. This regeneration solution was recirculated through the columns and samples from the regeneration solution were analyzed for RDX-,  $\text{NO}_2^-$ - and  $\text{HCOO}^-$ -content.

Figure 26 shows the formation of nitrite and formate from an exhausted activated carbon column (mean adsorbent phase concentration  $q_e = 123$  mg RDX/g activated carbon) during alkaline hydrolysis regeneration at a temperature of 80°C and pH 12. The regenerant solution was recirculated at a flow rate of 8.8 mL/min ( $t_{re} = 0.27$  min). The formation and yield of nitrite and formate can be compared with the formation kinetics and yields of the aqueous homogeneous and the regeneration batch studies under the same process conditions (see Sections 6.1 and 6.3).

The yields of nitrite and formate after a throughput of 2500 fed bed volumes (approximately 11 hours) are approximately 1.4 moles/mole RDX hydrolyzed for either compound. The nitrite concentration is already at equilibrium at this time and the formate concentration is increasing only slowly to an equilibrium yield of 1.5 after 6,000 fed bed volumes. These yields are comparable to the yields achieved in the batch studies. The time needed to reach equilibrium is longer than during batch regeneration where 6 - 8 hours were sufficient to reach equilibrium. Furthermore, the difference between the nitrite and formate formation kinetics is smaller. This indicates that, as expected, during column regeneration diffusion phenomena may have a higher influence on the overall rates.

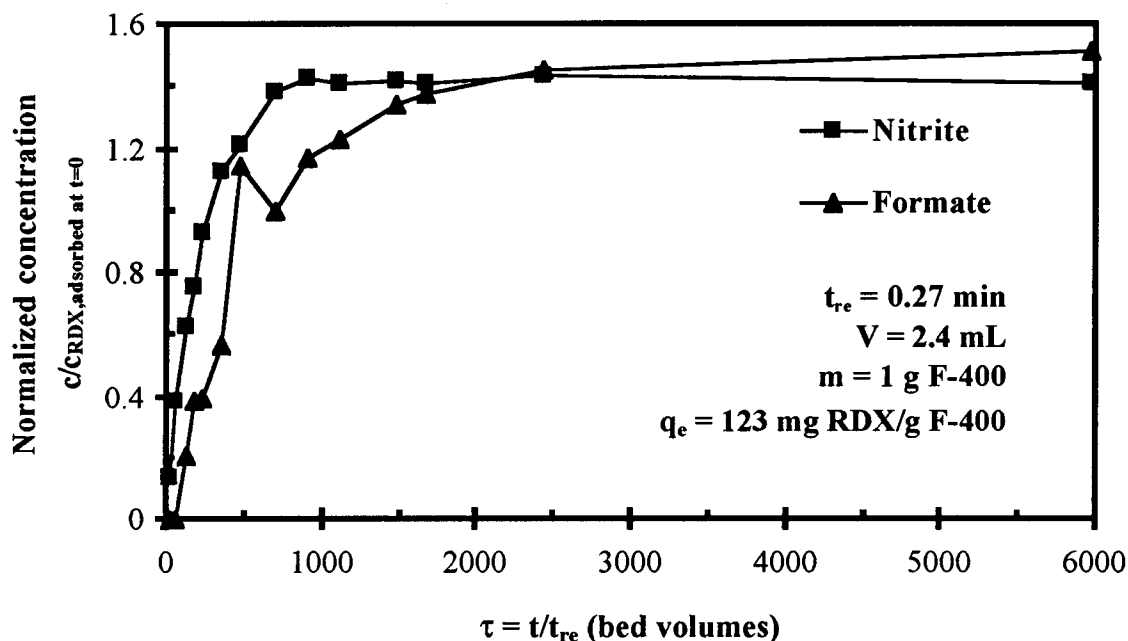
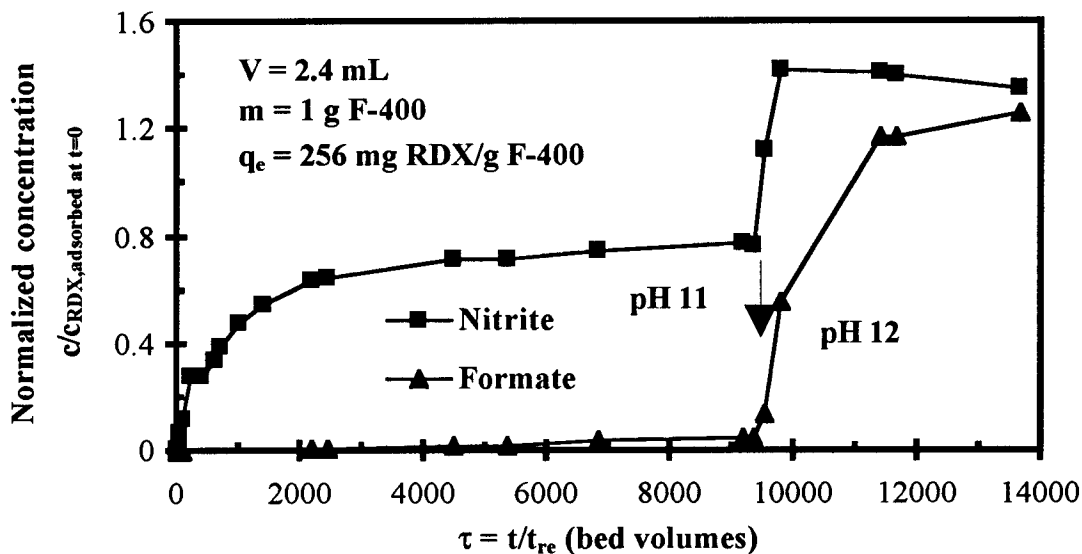


Figure 26 Regeneration of RDX-laden activated carbon at 80°C and pH 12.

Figure 27 shows the results of two column regeneration experiments that were started at pH 11. In the first experiment (Figure 27a; mean adsorbent phase concentration  $q_e = 256$  mg RDX/g activated carbon) the temperature was 70°C. The second experiment (Figure 27b; mean adsorbent phase concentration  $q_e = 198$  mg RDX/g activated carbon) was conducted at 80°C. The  $t_{re}$  was approximately 0.6 minutes in both experiments. In both cases the formation of formate was slow. Therefore, the pH was raised to 12 after a throughput of 9,000 or 4,000 fed bed volumes, respectively. In both cases the raise in pH accelerates the formate formation significantly. The rate change is also evident for the nitrite formation at 70°C (Figure 27a).

**a: Regeneration of an exhausted activated carbon column at 70°C;  $t_{re} = 0.64$  min**



**b: Regeneration of an exhausted activated carbon column at 80°C;  $t_{re} = 0.62$  min**

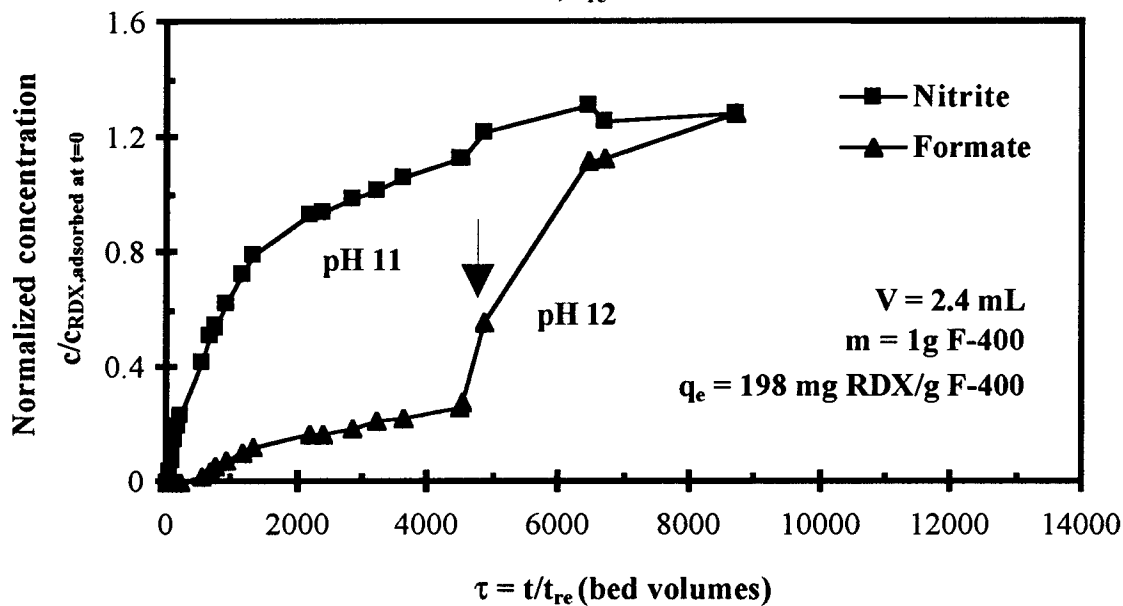


Figure 27 Regeneration of RDX-laden activated carbon from pH 11 to pH 12.

#### 6.4.4 Repeated Adsorption and Regeneration

Figure 28 shows complete breakthrough curves of virgin and repeatedly regenerated (two and three adsorption-regeneration cycles) activated carbon columns. The same process conditions ( $t_{re}$  = approximately 4 min;  $c_i$  = 17 mg RDX/L) existed for all columns. The regenerated activated carbon columns break through earlier than the virgin column. After a throughput of 5,000 fed beds the effluent concentration of the virgin activated carbon column is approximately 5 mg RDX/L. At the same time the regenerated activated carbon columns break through an effluent concentration of 8 mg RDX/L. Even though the regenerated activated carbon columns still show a considerable adsorptive capacity, the decrease is

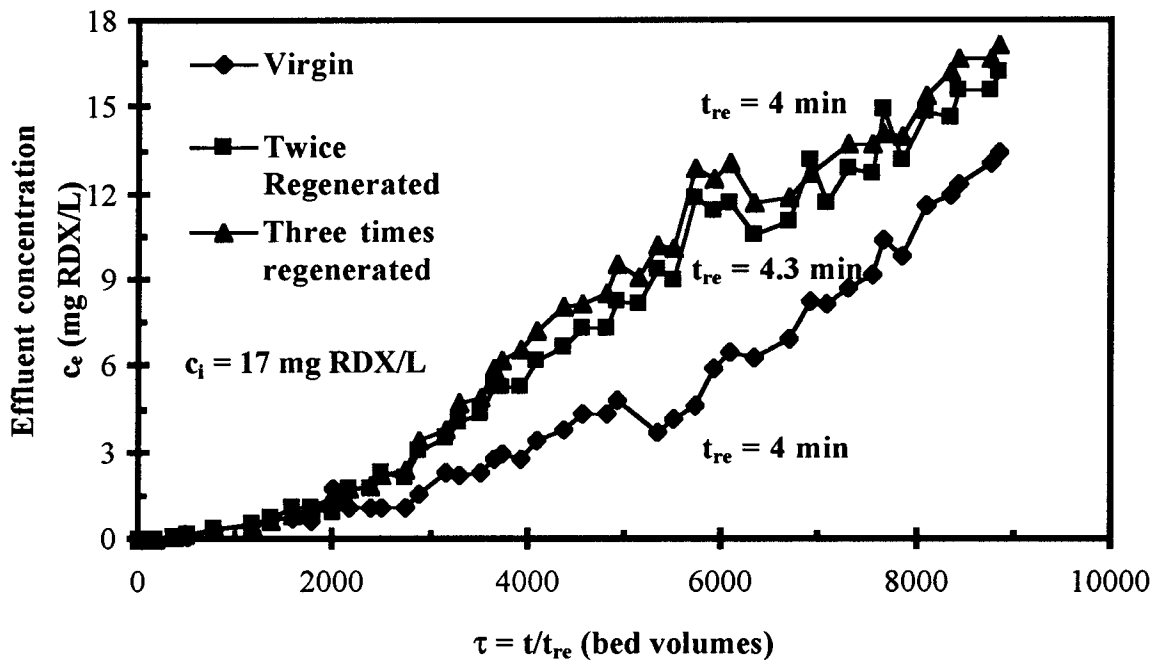


Figure 28 Breakthrough curves of virgin and repeatedly regenerated activated carbon F-400 in fixed-bed adsorbers.

evident. The earlier discussed surface charge effects (see Section 6.2) may be an explanation for this decrease. A subsequent acid-wash of the activated carbon may improve performance.

#### 6.4.5 Conclusions

The main objective of the fixed-bed adsorber studies was to show that the results from batch studies are principally valid and applicable for column operation. The results of the column studies show that activated carbon adsorption of high explosives from the aqueous phase and subsequent regeneration by alkaline hydrolysis in columns is feasible:

1. Empty-bed-contact-times ( $t_{re}$ ) in the approximate range from 1 to 4 minutes for adsorption were investigated and are in principal viable. The appropriate  $t_{re}$  values for column operation will also depend on the definition of a treatment objective. In the present work the definition of a treatment objective was not meaningful because the main objective was to exhaust activated carbon for regeneration.
2. The yields of  $\text{NO}_2^-$  and  $\text{HCOO}^-$  after regeneration are comparable to those found during batch regeneration and aqueous homogeneous batch studies. Column regeneration of activated carbon exhausted with RDX is viable.
3. Repeated exhaustion-regeneration studies show different breakthrough characteristics of activated carbon columns after regeneration. However, a considerable adsorptive capacity still exists. Further optimizations of the process, e.g. acid-post treatment were not investigated yet and may potentially improve performance.

## 7. SUMMARY

A new physico-chemical process for the treatment of water contaminated with the high explosives RDX and HMX was investigated. The process consists of high explosives adsorption on activated carbon and regeneration of the laden activated carbon using alkaline hydrolysis.

A. The aqueous homogeneous chemical kinetics of the alkaline hydrolysis of RDX and HMX were studied in the pH-range from 10 to 12 and the temperature range from 50 to 80°C. The kinetics of product formation and the product composition were also investigated. The following conclusions are made:

1. RDX hydrolyzes faster than HMX. At the most rapid conditions (pH 12 and 80°C) RDX disappeared after 2 minutes and HMX after 10 minutes. The rates of the alkaline hydrolysis of RDX are approximately ten times the rates of HMX.
2. The concentration versus time profiles could be modeled with a pseudo first-order rate equation. Second-order rates were calculated from data for various but constant hydroxide concentrations.
3. The temperature dependence of the rates was modeled using the *Arrhenius*-equation. The energies of activation are

$$\text{RDX: } E_a = 99.9 \pm 1.9 \text{ kJ}\cdot\text{mol}^{-1}$$

$$\text{HMX: } E_a = 111.9 \pm 0.8 \text{ kJ}\cdot\text{mol}^{-1}$$

4. Kinetic coefficients at 80°C, extrapolated from previous research over the range of 25°C to 45°C (Hoffsommer *et al.*, 1977a; Croce and Okamoto, 1979), are 22% lower for RDX and 27% lower for HMX than measured in this investigation.
5. Nitrite is produced in accordance with the rate of RDX-disappearance. Formate is produced more slowly; at the most rapid conditions (pH 12 and 80°C) more than 6 hours were needed to reach equilibrium.
6. No toxic and formerly unknown organic intermediates of the alkaline hydrolyses of RDX and HMX could be found with GC/MS-analysis.
7. The carbon- and nitrogen-balance for the alkaline hydrolysis of RDX could be improved. 94% of the carbon and 90% of the nitrogen were found in the products  $\text{NO}_2^-$ ,  $\text{HCOO}^-$ ,  $\text{CH}_3\text{COO}^-$ ,  $\text{HCHO}$ ,  $\text{NH}_3$ ,  $\text{N}_2\text{O}$ ,  $\text{N}_2$ .

**B.** The adsorption equilibria and kinetics of RDX and HMX on activated carbon were studied in batch experiments:

8. Batch adsorption equilibria of RDX and HMX on Filtrasorb-400 and ABG-30 could be modeled with the *Freundlich*-equation. The isotherms for all systems show similar slopes ( $1/n$  varies between 0.35 and 0.38). HMX adsorbs more strongly to activated carbon than RDX. The capacity constant  $K$  (HMX/Filtrisorb-400:  $190 (\text{L/g})^{1/n}$ ) is approximately two times the constant for RDX ( $97 (\text{L/g})^{1/n}$ ).

9. The batch adsorption kinetics of RDX on Filtrasorb-400 were modeled using the Homogeneous-Surface-Diffusion-Model (HSDM). A best-fit surface-diffusion coefficient of  $D_s = 9.1 \cdot 10^{-10} \text{ cm}^2/\text{s}$  was found with a parameter optimization.
- C.** The regeneration of high explosives-laden activated carbon using alkaline hydrolysis was studied in batch experiments:
10. The regeneration kinetics were compared with the kinetics of product formation under aqueous homogeneous conditions. Similar molar yields of nitrite and formate as under aqueous homogeneous conditions indicated complete regeneration of the laden activated carbon.
  11. No residual RDX was found when alkaline hydrolysis regenerated activated carbon was extracted with acetone.
  12. Isotherms of repeatedly regenerated activated carbon showed that the capacity decreases only slightly after repeated regeneration.
  13. Similar BET-surface areas were found for virgin activated carbon and alkaline hydrolysis regenerated activated carbon.
- D.** Results from the previous three sections were verified in continuous operation fixed-bed column experiments.
14. The molar yields of nitrite and formate during column regeneration with alkaline hydrolysis are similar to those found in aqueous homogeneous and batch regeneration studies.
  15. Repeated adsorption and regeneration of activated carbon in continuous column mode led to different breakthrough characteristics than with virgin activated

carbon. The regenerated activated carbon columns broke through earlier than a similar virgin activated carbon bed.

The principal result of this dissertation is: Alkaline hydrolysis at elevated pH and temperature is a feasible process to destroy the high explosives RDX and HMX in solution and on activated carbon.

## REFERENCES

- Alatrisme-Mondragon, F., Baresi, L., Stenstrom, M.K. and Mah, R.A. (1995). "Anaerobic Biotransformation of Hexahydro-1,3,5-trinitro-1,3,5-triazine (RDX)," *Submitted to Applied Microbiology and Biotechnology*.
- Andren, R.K., Nystrom, J.M., McDonnell, R.P. and Stevens, B.W. (1975). "Explosives Removal from Munitions Wastewater," *Proceedings of the 30th Purdue Industrial Waste Conference*, Purdue University, West Lafayette, Indiana, pp. 816-825.
- Ansell, E. (1993). "Department of Defense/Department of Energy (DOD/DOE) Research and Development of Techniques for Demilitarization," *Proceedings of the 12th International Incineration Conference*, Knoxville, Tennessee, May 3rd-7th, 1993, pp. 637-639.
- Baerns, M., Hofmann, H. and Renken, A. (1992). *Chemische Reaktionstechnik*, 2nd ed., Thieme, Stuttgart, Germany; pp. 205-207.
- Beccari, M., Paolini, A.E. and Variali, G. (1977). "Chemical Regeneration of Granular Activated Carbon," *Effluent and Water Treatment Journal*, Vol. 6, pp. 289-294.
- Benson, S.W. (1982). *The Foundations of Chemical Kinetics*, Corr (ed.), Krieger, Malabar, Florida, pp. 66-68.
- Bentley, R.E., Dean, J.W., Ells, S.J., Hollister, T.A., LeBlanc, G.A., Sauter, S. and Sleight, B.H. (1977). *Laboratory Evaluation of the Toxicity of Cyclotrimethylene Trinitramine (RDX) to Aquatic Organisms*. Final Report No. DAMD-17-74-C-4104/AD-A061730, EG Bionomics, Wareham, Massachusetts.
- Binks, P.R., Nicklin, S. and Bruce, N.C. (1995). "Degradation of Hexahydro-1,3,5-Trinitro-1,3,5-Triazine (RDX) by *Stenotrophomonas maltophilia* PB1," *Applied and Environmental Microbiology*, Vol. 61, No. 4, pp. 1318-1322.
- Birstein, G. and Lobanow, N. (1927). *Zeitschrift für Anorganische und Allgemeine Chemie*, Vol. 160, pp. 377-386.
- Borman, S. (1994). "Advanced Energetic Materials Emerge for Military and Space Applications," *Chemical & Engineering News*, Vol. 72, No. 3, pp. 18-22.
- Brecher, L.E., Frantz, D.C. and Kostecki, J.A. (1967). "Combined Diffusion in Batch Adsorption Systems Displaying BET Isotherms Part II," *American Institute of Chemical Engineers Symposium Series*, Vol. 63, p. 251.

- Burrows, W.D., Chyrek, R.H., Noss, C.I., Small, M.J. and Kobylinski, E.A. (1984). "Treatment for Removal of Munition Chemicals from Army Industrial Wastewaters," *Proceedings of the 16th Mid-Atlantic Industrial Waste Conference*, pp. 331-342.
- Burton, D.T., Turley, S.D. and Peters, G.T. (1994). "The Acute and Chronic Toxicity of Hexahydro-1,3,5-trinitro-1,3,5-triazine (RDX) to the Fathead Minnow (*Pimephales promelas*)," *Chemosphere*, Vol. 29, No. 3, pp. 567-579.
- Byrd Jr., J. and Humphreys, J. (1993). "Department of Defense/Department of Energy (DOD/DOE) Research and Development (R&D) of Incineration Techniques for Demilitarization," *Proceedings of the 12th International Incineration Conference*; Knoxville, Tennessee, May 3rd-7th, 1993, pp. 621-624.
- Clear, A.J. and Rinkenbach, W.H. (1945). *Procedures for Decomposing Waste High Explosives*, Final Report No. AD-495569, PA-TR 1556, Picatinny Arsenal, Picatinny, New Jersey
- Craveiro de Sa, F.A. and Malina, J.F. Jr. (1992). "Bioregeneration of Granular-Activated Carbon," *Water Science and Technology*, Vol. 26, No. 9-11, pp. 2293-2295.
- Crittenden, J.C. (1976). *Mathematical Modeling of Adsorber Dynamics - Single Components and Multi-Components*. Ph.D.-Dissertation, University of Michigan, Ann Arbor.
- Croce, M. and Okamoto, Y. (1979). "Cationic Micellar Catalysis of the Aqueous Alkaline Hydrolyses of 1,3,5-Triaza-1,3,5-trinitrocyclohexane and 1,3,5,7-Tetraaza-1,3,5,7-tetranitrocyclooctane," *Journal of Organic Chemistry*, Vol. 44, pp. 2100-2103.
- Dahn, A. (1993). "Chemisch-biologisches Verfahren zum Abbau von Treibmitteln auf Nitrozellulosebasis," Presented at *Wehrtechnisches Symposium: Biologie in Technik und Umwelt*. 6.9-8.9.1993, Mannheim, Bundesakademie für Wehrverwaltung und Wehrtechnik.
- Dobratz, B.M. (1981). *LLNL Explosives Handbook*; Technical Report No. UCRL-52997, Lawrence Livermore National Laboratory: Livermore, California.
- Envirodyne Engineers (1980). *Milan Army Ammunition Plant Contamination Survey*. Final report No. AD-B053362L, Ann Arbor, Michigan.
- Epstein, S. and Winkler, C. A. (1951). "Studies on RDX and Related Compounds," *Canadian Journal of Chemistry*, Vol. 29, pp. 731-733.
- Etnier, E. (1989). "Water Quality Criteria for Hexahydro-1,3,5-trinitro-1,3,5-triazine (RDX)," *Regulatory Toxicology and Pharmacology*, Vol. 9, pp. 147-157.

- Euler, H.v. and Lövgren, T. (1925). *Zeitschrift für Anorganische und Allgemeine Chemie*, Vol. 147, pp. 123-134.
- Flittner, M. (1994). "Stand der Bearbeitung von Rüstungsaltslasten in Baden-Württemberg," *Vortragsmanuskripte zur Tagung Militärische Altslasten am Umweltinstitut Offenbach*, January 1994.
- Freeman, D.J. and Colitti, O. (1982). "Removal of Explosives from Load-Assemble-Pack Wastewater (Pink Water) Using Surfactant Technology," *Proceedings of the 36th Purdue Industrial Waste Conference*, Purdue University, West Lafayette, Indiana, pp. 383-394.
- Freeman, D.J. (1985). "Continuous Fixation and Removal of Explosive Wastes from Pink Water Using Surfactant Technology," *Proceedings of the 40th Purdue Industrial Waste Conference*, Purdue University, West Lafayette, Indiana, pp. 659-676.
- Furusawa, T. and Smith, J.M. (1973). "Fluid-Particle and Intra-Particle Mass Transport Rates in Slurries," *Industrial Engineering and Chemical Fundamentals*, Vol. 12, p. 197.
- Garg, R., Grasso, D. and Hoag, G. (1991). "Treatment of Explosives Contaminated Lagoon Sludge," *Hazardous Waste and Hazardous Materials*, Vol. 8, No. 4, pp. 319-340.
- Garn, S. (1994). "Militärische und Rüstungsaltslasten in Thüringen," *Vortragsmanuskripte zur Tagung Militärische Altslasten am Umweltinstitut Offenbach*, January 1994.
- Gibbs, T.R. and Popolato, A. (eds.) (1980). *LASL Explosive Property Data*. University of California Press, Berkeley, California.
- Haas, R., Schreiber, I. v.Löw, E. and Stork, G. (1990). "Conception for the Investigation of Contaminated Munition Plants," *Fresenius Journal of Analytical Chemistry*, Vol. 338, pp. 41-45.
- Hale, V.Q., Stanford, T.B. and Taft, L.G. (1979). *Evaluation of the Environmental Fate of Munitions Compounds in Soil*, Final report No. AD-A082874, US-Army Medical Research and Development Command, Fort Detrick, Maryland.
- Hand, D.W. (1982). *User-Oriented Solutions to the Homogeneous Surface Diffusion Model for Adsorption Process Design Calculations: Batch Reactor Solutions*. Master thesis, Michigan Technological University, Houghton, Michigan.

- Hand, D.W., Crittenden, J.C. and Thacker, W.E. (1983). "User-Oriented Batch Reactor Solutions to the Homogeneous Surface Diffusion Model," *Journal of Environmental Engineering, Division ASCE*, Vol. 109, No. 1, pp. 82-101.
- Heilmann, H.M., Stenstrom, M.K., Hesselmann, R.P.X. and Wiesmann, U. (1994). "Kinetics of the Aqueous Alkaline Homogenous Hydrolysis of High Explosive 1,3,5,7-Tetraaza-1,3,5,7-tetranitrocyclooctane (HMX)," *Water Science and Technology*, Vol. 30, No. 3, pp. 53-61.
- Heilmann, H.M., Wiesmann, U. and Stenstrom, M.K. (1996). "Kinetics of the Aqueous Homogeneous Alkaline Hydrolysis of High Explosives RDX and HMX," *Environmental Science and Technology*, Vol. 30, pp. 1485-1492.
- Hesselmann, R. P. X., Alariste-Mondragon, F., Babcock, R. W., Knezovich, J. P., Daniels, J. I., Mah, R. A. and Stenstrom, M. K. (1992). Presented at the 1992 Waste Management and Environmental Sciences Conference, San Juan, Puerto Rico, April 9th-11th.
- Hoffsommer, J. C., Kubose, D. A. and Glover, D. J. (1977a). "Kinetic isotope effects and intermediate formation for the aqueous alkaline homogeneous hydrolysis of 1,3,5-triaza-1,3,5-trinitrocyclohexane," *Journal of Physical Chemistry*, Vol. 81, pp. 380-385.
- Hoffsommer, J. C. and Kubose, D. A. (1977b). *Chemical Degradation of RDX on Strongly Basic Ion-Exchange Resins*, Technical Report No. NSWC/WOL TR 77-30, Dahlgren, Virginia.
- Holl, G. and Schneider, M. (1993). "Conversion Products of Explosives During Combustion - Analysis for Risk Assessment of Open-Pit Burning Areas," In *Contaminated Soil '93*, Arendt, F., Annokkee, G. J., Bosman, R. and van den Brink, W. J. (eds), Kluwer: Netherlands, pp. 941-942.
- Holl, G. and Schneider, M. (1992). "Flüchtige Reaktionsprodukte beim Abbrand von Explosivstoffen," In *Management für die Sanierung von Rüstungs- und Militärischen Altlasten*, Thome-Kozmiensky, K.J., Spyra, W., Lohs, K.H., Preussner, M. and Rüden, H. (eds.), EF-Verlag, Berlin, pp. 353-370.
- Hutchinson, D.H. and Robinson, C.W. (1990). "A Microbial Regeneration Process for Granular Activated Carbon-II. Regeneration Studies," *Water Research*, Vol. 24, No. 10, pp. 1217-1223.
- Jones, W. H. (1953). "Mechanism of the Homogeneous Alkaline Decomposition of Cyclotrimethylenetrinitramine: Kinetics of Consecutive Second- and First-order

- Reactions. A Polarographic Analysis for Cyclotrimethylenetrinitramine," *Journal of the American Chemical Society*, Vol. 76, pp. 829-835.
- Kitchens, J.F., Harvard, W.E., Lauter, D.M., Wentsel, R.S. and Valentine, S.S. (1978). *Preliminary Problem Definition Study of 48 Munitions Related Chemicals. I, Explosive Related Chemicals*, Final Report No. AD-A0099733, Alexandria, Virginia.
- Komiyama, H. and Smith, J.M. (1974). "Surface Diffusion in Liquid-Filled Pores," *American Institute of Chemical Engineering Journal*, Vol. 20, p. 1110.
- Kooke, R.M.M., Lustenhouwer, J.W.A., Olie, K. and Huntzinger, O. (1981). "Extraction Efficiencies of Polychlorinated Dibenzo-p-dioxins and Polychlorinated Dibenzofurans from Fly Ash," *Analytical Chemistry*, Vol. 53, pp. 461-463.
- Layton, D., Mallon, B., Mitchell, W., Hall, L., Fish, R., Perry, L., Snyder, G., Bogen, K., Malloch, W., Ham, C. and Dowd, P. (1987). *Conventional Weapons Demilitarization: A Health and Environmental Effects Data-Base Assessment*. Lawrence Livermore National Laboratory, Livermore, California.
- Martin, R.J. and Ng, W.J. (1985). "Chemical Regeneration of Exhausted Activated Carbon-II," *Water Research*, Vol. 19, No. 12, pp. 1527-1535.
- Martin, R.J. and Ng, W.J. (1987). "The Repeated Exhaustion and Chemical Regeneration of Activated Carbon," *Water Research*, Vol. 21, pp. 961-965.
- McCormick, N.G., Cornell, J.H. and Kaplan, A.M. (1981). "Biodegradation of Hexahydro-1,3,5-trinitro-1,3,5-Triazine," *Applied and Environmental Microbiology*, Vol. 42, No. 5, pp. 817-823.
- McLellan, W., Hartley, W. R. and Brower, M. (1988a). *Health advisory for hexahydro-1,3,5-tetranitro-1,3,5-triazine*, Technical Report No. PB90-273533, Office of Drinking Water, US Environmental Protection Agency, Washington, DC.
- McLellan, W., Hartley, W. R. and Brower, M. (1988b). *Health Advisory for Octahydro-1,3,5,7-tetranitro-1,3,5,7-tetrazocine*, Technical Report No. PB90-273525, Office of Drinking Water, US Environmental Protection Agency, Washington, DC.
- Merck & Co. (1989). *The Merck Index*. 11th ed.
- Müller, G., Radke, C.J. and Prausnitz, J.M. (1980). "Adsorption of Weak Electrolytes from Aqueous Solution on Activated Carbon," *Journal of Physical Chemistry*, Vol. 84, pp. 369-375.

- Narbaitz, R.M. and Cen, J. (1994). "Electrochemical Regeneration of Granular Activated Carbon," *Water Research*, Vol. 28, No. 8, pp. 1771-1778.
- Newcombe, G. and Drikas, M. (1993a). "Chemical Regeneration of Granular Activated Carbon From an Operating Water Treatment Plant," *Water Research*, Vol. 27, No. 1, pp. 161-165.
- Newcombe, G., Hayes, R. and Drikas, M. (1993b). "Granular Activated Carbon: Importance of Surface Properties in the Adsorption of Naturally Occurring Organics," *Colloids and Surfaces A: Physicochemical Engineering Aspects*, Vol. 78, pp. 65-71.
- Newcombe, G. (1994). "Activated Carbon and Soluble Humic Substances: Adsorption, Desorption, and Surface Charge Effects," *Journal of Colloid and Interface Science*, Vol. 164, pp. 452-462.
- Osmon, J.L. and Klausmeier, R.E. (1972). "The Microbial Degradation of Explosives," *Developments in Industrial Microbiology*, Vol. 14, pp. 247-252.
- Patterson, J., Shapira, N. I., Brown, J., Duckert, W. and Polson, J. (1976a). *State of the Art Military Explosives and Propellants Industry Volume III. Wastewater Treatment*, Technical Report No. PB-265 042, US Environmental Protection Agency, Washington, DC, p. 92.
- Patterson, J., Shapira, N. I. and Brown, J. (1976b). "Pollution Abatement in the Military Explosives Industry," *Proceedings of the 31st Purdue Industrial Waste Conference*, Purdue University, West Lafayette, Indiana, pp. 385-394.
- Patterson, J., Shapira, N. I., Brown, J., Duckert, W. and Polson, J. (1976c). *State of the Art Military Explosives and Propellants Industry Volume II. Production Industry*, Technical Report No. PB-260 918, US Environmental Protection Agency, Washington, DC, p. 92.
- Patterson, W. E. and Phelan, P. F. (1993). *Proceedings of the 12th International Incineration Conference*, Knoxville, Tennessee, May 3rd-7th, 1993, pp. 625-629.
- Pflugradt, D. (1994). "Rüstungs- und Militärische Altlasten im Bundesland Sachsen-Anhalt," *Vortragsmanuskripte zur Tagung Militärische Altlasten am Umweltinstitut Offenbach*, January 1994.
- Pruneda, A., Mitchell, A.R. and Humphrey, J.R. (1993). "Reusing the High Explosives from Dismantled Nuclear Weapons," *Energy and Technology Review*, Nov-Dec 1993, pp. 19-26.

- Rosenblatt, D.H., Burrows, E.P., Mitchell, W.R. and Parmer, D.L. (1991). *The Handbook of Environmental Chemistry*, Vol. 3, Part G, Springer: Berlin, Germany; pp. 195-235.
- Rovel, J.M. (1972). "Chemical Regeneration of Activated Carbon," *Progress in Water Technology*, Vol. 1, pp. 187-197.
- Sanoki, S.L., Simon, P.B., Weitzel, R.L., Jerger, D.E. and Schenk, J.E. (1976). *Aquatic Field Surveys at Iowa, Radford, and Joliet Army Ammunition Plants, Vol. 1*. Final report No. AD-A036776, Ann Arbor, Michigan.
- Schulte, G.R., Hoehn, R.C., and Randall, C.W. (1973). "The Treatability of a Munitions-Manufacturing Waste with Activated Carbon," *Proceedings of the 28th Purdue Industrial Waste Conference*, Purdue University, West Lafayette, Indiana.
- Semmens, M.J., Barnes, D. and O'Hara, M. (1984). "Treatment of an RDX-TNT Waste from a Munitions Factory," *Proceedings of the 39th Purdue Industrial Waste Conference*, Purdue University, West Lafayette, Indiana, pp. 837-842.
- Shelby, S.E., Lankford, P.W. and McCollum, R.W. (1984). "A Case Study for the Treatment of an Explosives Wastewater from an Army Ammunition Plant," *Proceedings of the 39th Purdue Industrial Waste Conference*, Purdue University, West Lafayette, Indiana, pp. 821-836.
- Sontheimer, H., Crittenden, J.C. and Summers, R.S. (1988). *Activated Carbon for Wastewater Treatment* (2nd ed.), Engler-Bunte Institut, Karlsruhe, Germany.
- Spalding, R.F. and Fulton, J.W. (1988). "Groundwater Munition Residues and Nitrate Near Grand Island, Nebraska, USA," *Journal of Contamination and Hydrology*, Vol. 2, pp. 139-153.
- Spanggard, R.J. (1980). *Environmental Fate Studies on Certain Munition Wastewater Constituents, Phase II - Laboratory Studies*, Technical Report No. DAMD-17-78-C-808, US-Army Medical Research and Development Command, Fort Detrick, Maryland.
- Spitzer, P., Gosse, I. and Radeke, K.H. (1993). "Adsorption und Hydrolyse von Methylparathion an Aktivkohle und Adsorberharz," *Acta Hydrochimica et Hydrobiologica*, Vol. 21, No. 5, pp. 267-272.
- Spontarelli, T., Buntain, G. A., Sanchez, J. A. and Benziger, T. M. (1993). *Proceedings of the 12th International Incineration Conference*, Knoxville, Tennessee, May 3rd-7th, 1993, pp. 787-791.

- Stillwell, J.M., Eischen, M.A., Margard, W.L., Matthews, M.C. and Stanford, T.B. (1977). *Toxicological Investigations of Pilot Treatment Plant Wastewaters at Holston Army Ammunition Plant*. Final Report No. DAMD-17-74-C-4101, Wareham, Massachusetts.
- Sullivan, J.H., Jr., Putnam, H.D., Keirn, M.A., Pruitt, B.C., Jr., Nichols, J.C., McClave, J.T. (1979). *A Summary and Evaluation of Aquatic Environmental Data in Relation to Establishing Water Quality Criteria for Munitions-Unique Compounds*, Technical Report No. AD-A087683, US-Army Medical Research and Development Command, Fort Detrick, Maryland.
- Suzuki, M. and Kawazoe, K. (1975). "Effective Surface Diffusion Coefficients of Volatile Organics on Active Carbon During Adsorption from Aqueous Solution," *Journal of Chemical Engineering (Japan)*, Vol. 8, p. 379.
- Sykes, P. (1981). *A Guidebook to Mechanism in Organic Chemistry*, 5th ed., Longman, London, UK and New York, USA.
- Tsai, S.Y., Davis, M.J. and Benioff, P.A. (1985). *Cornhusker Army Ammunition Plant - A Aquifer Restoration Alternatives Study*, Technical Report No. AMXTH-AS-CR-850132, US-Army Aberdeen Proving Ground, Aberdeen, Maryland.
- Urban, H. and Danz, M. (1976). "Tumorinduzierende Wirkung von Trinitroso-trimethylen-triamin in Verbindung mit Dimethylsulfoxid," *Archiv Geschwulstforschung*, Vol. 46, No. 8, pp. 657-662.
- US EPA (1994). *Code of Federal Regulations, 40 CFR 261 - Identification and Listing of Hazardous Waste*. Berman Press, Lanham, Maryland.
- Walsh, J.T., Chalk, R.C. and Merritt, C. (1973). "Application of Liquid Chromatography to Pollution Abatement Studies of Munitions Wastes," *Analytical Chemistry*, Vol. 45, No. 7, pp. 1215-1220.
- Wujcik, W.J., Lowe, W.L. and Marks, P.J. (1992). "Granular Activated Carbon Pilot Treatment Studies for Explosives Removal from Contaminated Groundwater," *Environmental Progress*, Vol. 11, No. 3, pp. 178-189.
- Yinon, J. (1990). *Toxicity and Metabolism of Explosives*. CRC Press: Boca Raton, Ann Arbor, Boston, USA.

## Appendix A Notation

$A$	Arrhenius-parameter ( $\text{L}\cdot\text{mol}^{-1}\cdot\text{min}^{-1}$ )
$c$	Concentration ( $\text{mg/L}$ )
$c_i$	Influent concentration ( $\text{mg/L}$ )
$c_0$	Concentration at $t = 0$ ( $\text{mg/L}$ )
$c_e$	Equilibrium, end or effluent concentration ( $\text{mg/L}$ )
$\bar{C}$	Dimensionless concentration ( )
$\bar{C}_s$	Dimensionless concentration near the particle surface ( )
$D_g$	Solute distribution parameter ( )
$D_s$	Surface diffusion coefficient ( $\text{cm}^2/\text{s}$ )
$E_a$	Energy of activation ( $\text{kJ}\cdot\text{mol}^{-1}$ )
$k_1$	Pseudo first-order rate constant ( $\text{min}^{-1}$ )
$k_2$	Second-order rate constant ( $\text{L}\cdot\text{mol}\cdot\text{min}^{-1}$ )
$k_f$	Film transfer coefficient ( $\text{cm/s}$ )
$K$	Freundlich-Isotherm capacity constant ( $\text{L/g}$ ) <sup>1/n</sup>
$m_{AC}$	Mass of activated carbon (g)
$m_0$	Dosage of activated carbon ( $\text{g/L}$ )
$1/n$	Freundlich-Isotherm intensity constant ( )
$q_e$	Equilibrium adsorbent phase concentration ( $\text{mg/g}$ )
$\bar{q}$	Dimensionless adsorbent phase concentration ( )
$R$	Particle radius (cm)

$r$	Dimensionless radial coordinate ( )
$R^2$	Linear regression correlation coefficient ( )
$t$	Time (s)
$\bar{t}$	Dimensionless time ( )
$t_{re}$	Empty bed contact time (min)
$V$	Volume (L)
$V_b$	Bed volume (mL)
$\dot{V}$	Flow rate (mL/min)
$\epsilon$	Void fraction ( )
$\phi$	Sphericity ( )
$\tau$	Throughput (bed volumes)

## Appendix B Derivation of the Equations Describing the Homogeneous Surface Diffusion Model (HSDM)

The derivation of the HSDM-model equations was originally published by Hand (1982).

First, the mass of adsorbate in a completely mixed batch reactor (CMBR) at time  $t$  and at  $t = 0$  is equated:

$$\varepsilon \cdot V \cdot c(t) + M \cdot q_{ave}(t) = \varepsilon \cdot V \cdot c_0$$

with

$\varepsilon$ : volume fraction of the reactor occupied by the liquid-phase;

$V$ : reactor volume;

$c(t)$ : adsorbate concentration in the liquid-phase at time  $t$ ;

$M$ : mass of the adsorbent;

$q_{ave}(t)$ : average concentration in the adsorbent at time  $t$ ;

$c_0$ : initial liquid-phase adsorbate concentration at  $t = 0$ ;

The equation for  $q_{ave}(t)$  is obtained by equating the overall mass in a (spherical) particle:

$$q_{ave}(t) \rho_a \frac{4\pi R^3}{3} = \int_0^R q(r,t) \rho_a 4\pi r^2 dr$$

and after dividing

$$q_{ave}(t) = \frac{3}{R^3} \int_0^R q(r,t) r^2 dr$$

with

$q(r,t)$ : adsorbent phase concentration;

$\rho_a$ : particle density (including the pore volume)

LIBRARY SEARCH

03/06/95 7:28:00 + 18:05

SAMPLE: 3-3-95 RDX - HPLC WATER - HYDROLYSATE

CONDS.: 4 MIN @ 30, 6/MIN TO 300 HOLD 60 DB-5MS 30MX.25MM COLUMN

ENHANCED (S 15B 2N 0T)

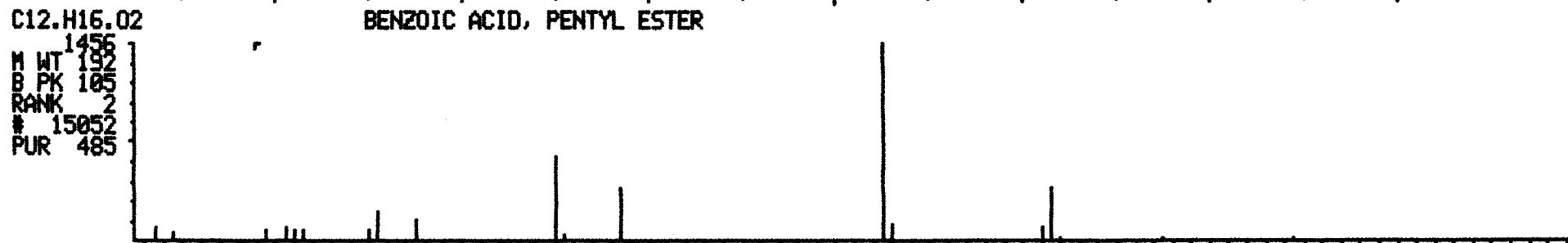
DATA: F9316 #1086

CALI: F9316 # 2

2/500 UL INJ.

BASE M/Z: 70

RIC: 23679.



M/Z 40 60 80 100 120 140 160

LIBRARY SEARCH

03/06/95 7:28:00 + 21:44

SAMPLE: 3-3-95 RDX - HPLC WATER - HYDROLYSATE

CONDS.: 4 MIN @ 30, 6/MIN TO 300 HOLD 60 DB-5MS 30MX.25MM COLUMN

ENHANCED (S 15B 2N 0T)

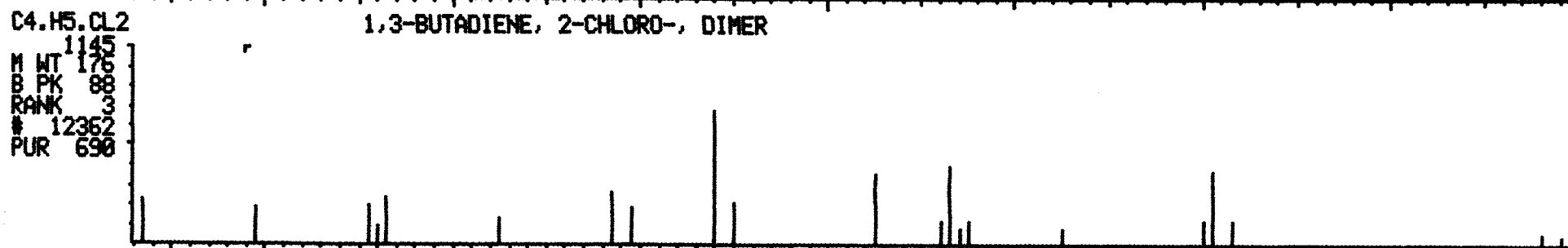
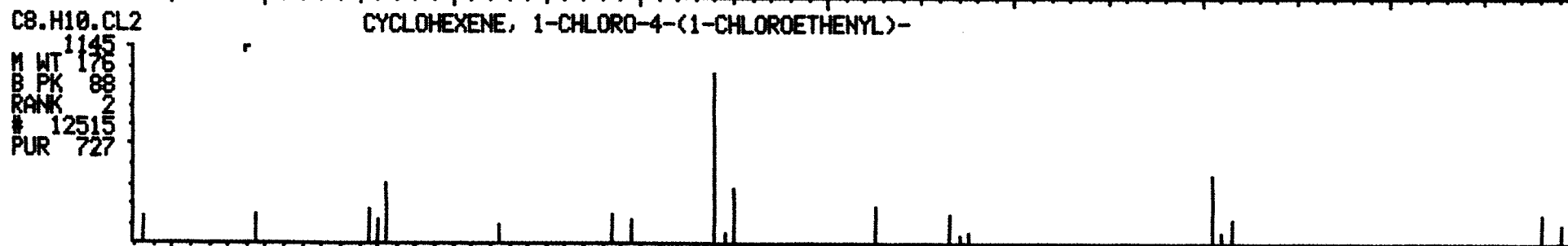
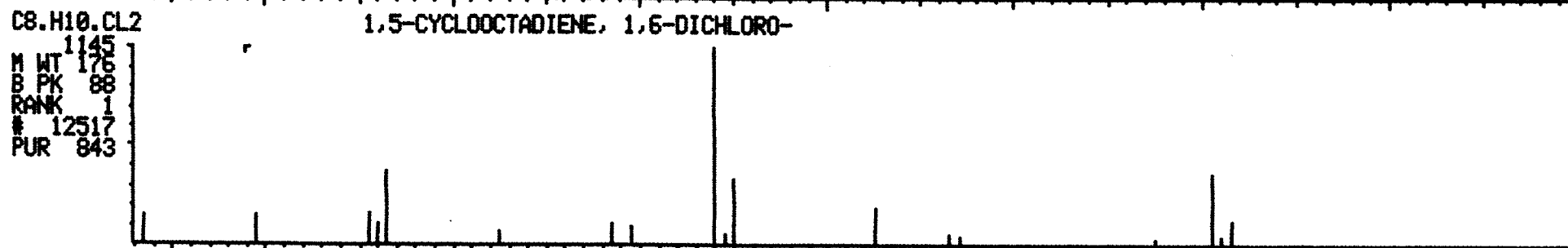
DATA: F9316 #1304

CALI: F9316 # 2

2/500 UL INJ.

BASE M/Z: 88

RIC: 23071.



M/Z 40 60 80 100 120 140 160

LIBRARY SEARCH

03/06/95 7:28:00 + 33:28

SAMPLE: 3-3-95 RDX - HPLC WATER - HYDROLYSATE

CONDS.: 4 MIN @ 30, 6/MIN TO 300 HOLD 60 DB-5MS 30MX.25MM COLUMN

ENHANCED (S 158 2N 0T)

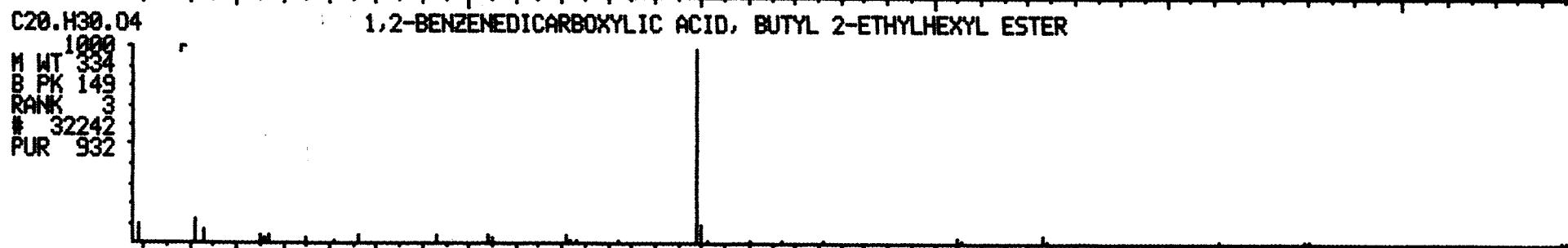
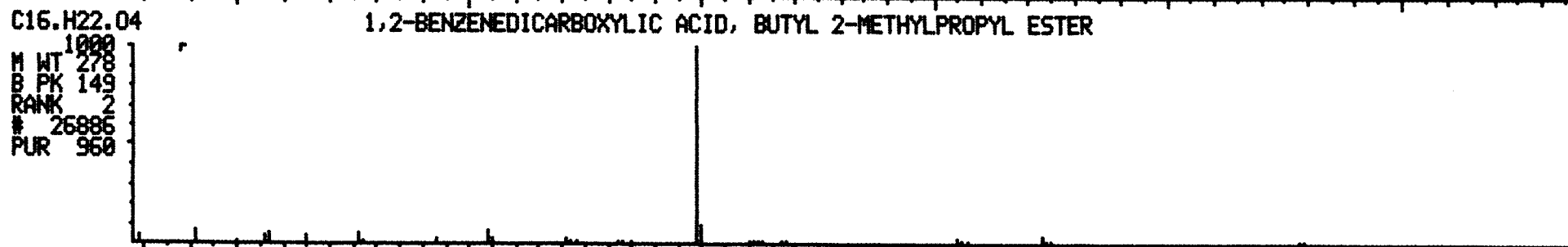
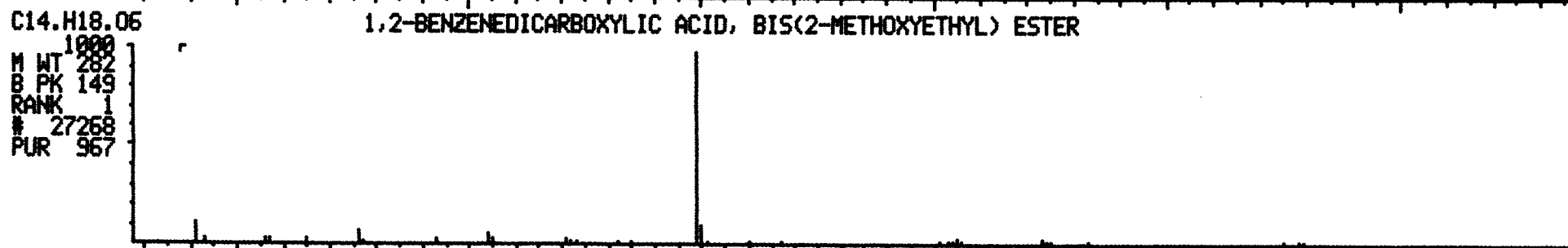
DATA: F9316 #2008

CALI: F9316 # 2

2/500 UL INJ.

BASE M/Z: 149

RIC: 30559.



M/Z 50 100 150 200 250 300

LIBRARY SEARCH

03/06/95 7:28:00 + 42:02

SAMPLE: 3-3-95 RDX - HPLC WATER - HYDROLYSATE

CONDS.: 4 MIN @ 30, 6/MIN TO 300 HOLD 60 DB-5MS 30MX.25MM COLUMN

ENHANCED (S 158 2N 0T)

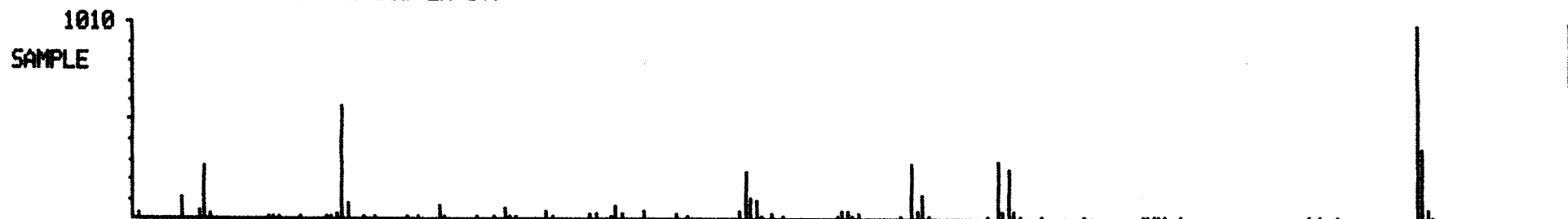
DATA: F9316 #2522

CALI: F9316 # 2

2/500 UL INJ.

BASE M/Z: 277

RIC: 130687.



C21.H19.02.P

ACETIC ACID, (TRIPHENYLPHOSPHORANYLIDENE)-, METHYL ESTER

M WT 1010  
B PK 334  
RANK 1  
# 32259  
PUR 908



C18.H15.0.P

PHOSPHINE OXIDE, TRIPHENYL-

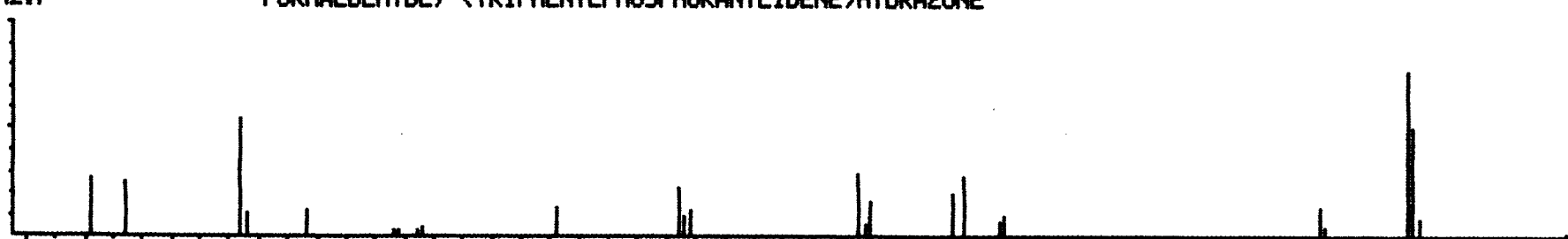
M WT 1010  
B PK 278  
RANK 2  
# 26924  
PUR 891



C19.H17.N2.P

FORMALDEHYDE, (TRIPHENYLPHOSPHORANYLIDENE)HYDRAZONE

M WT 1010  
B PK 304  
RANK 3  
# 29623  
PUR 713



M/Z 50 100 150 200 250 300

LIBRARY SEARCH

03/06/95 8:41:00 + 6:59

SAMPLE: 3-4-95 HMX - HPLC WATER - HYDROLYSATE

CONDS.: 4 MIN @ 30, 6/MIN TO 300 HOLD 60 DB-5MS 30MX.25MM COLUMN

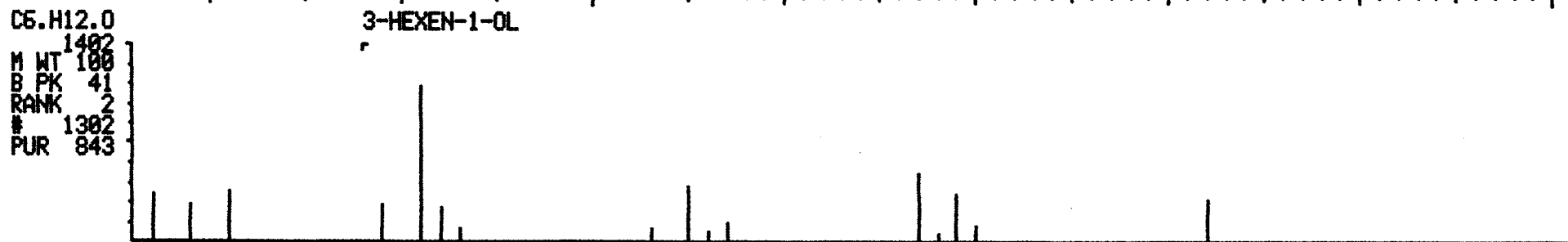
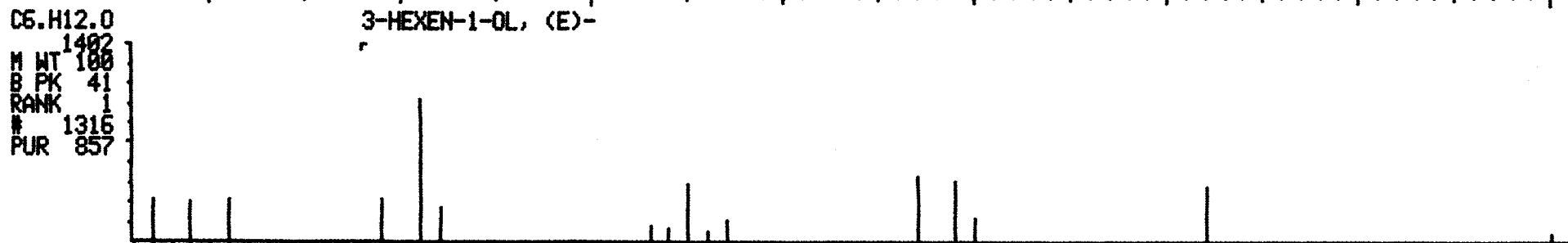
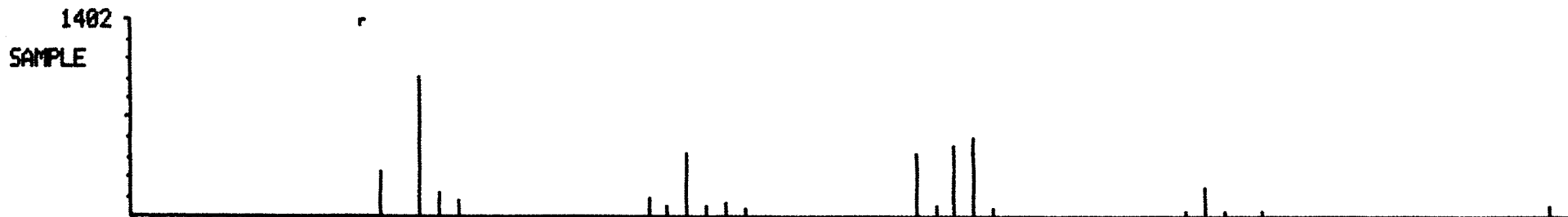
ENHANCED (S 158 2N 0T)

DATA: F9317 # 419

CALI: F9317 # 2

BASE M/Z: 41

RIC: 11743.



M/Z 30 40 50 60 70 80 90 100

LIBRARY SEARCH

03/06/95 8:41:00 + 18:07

SAMPLE: 3-4-95 HMX - HPLC WATER - HYDROLYSATE

CONDS.: 4 MIN @ 30, 6/MIN TO 300 HOLD 60 DB-5MS 30MX.25MM COLUMN

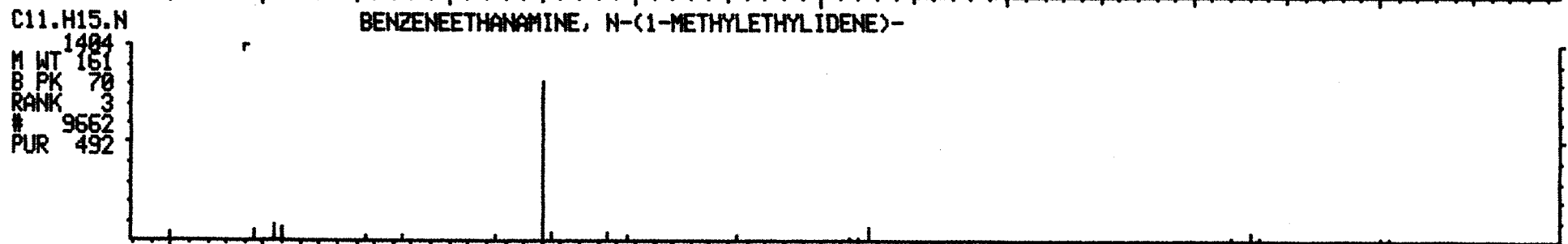
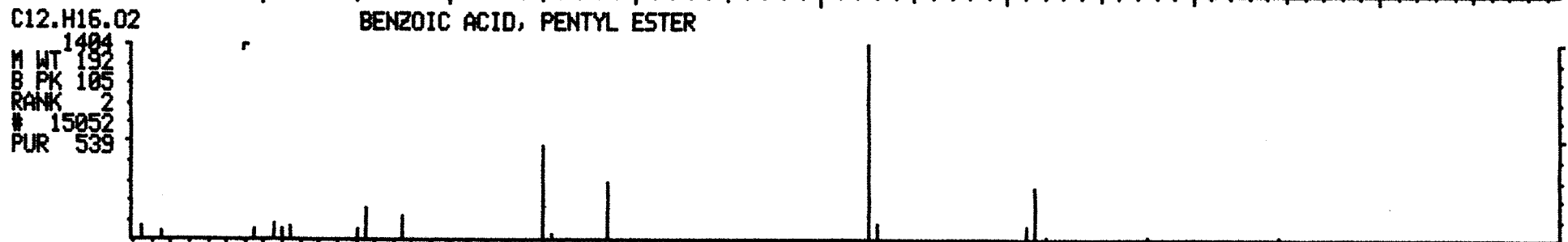
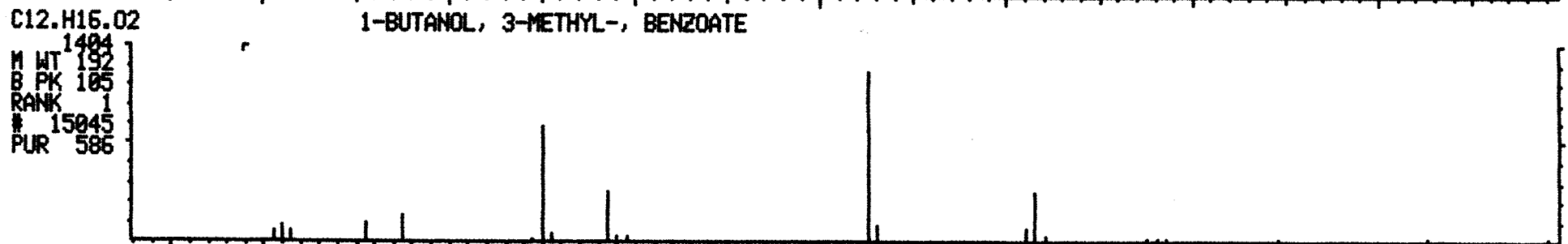
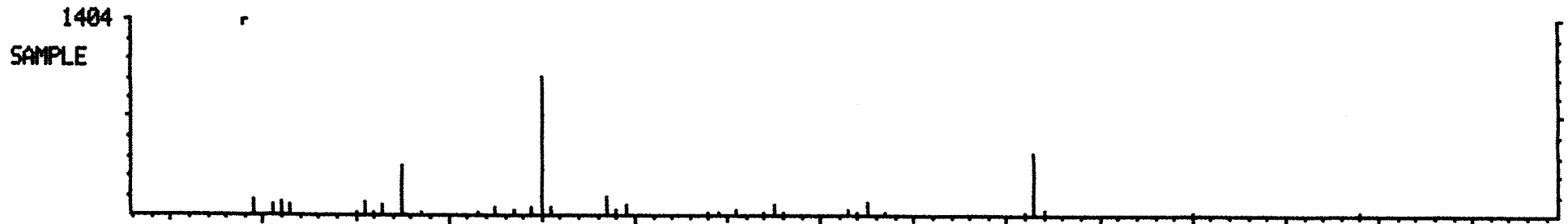
ENHANCED (S 158 2N 0T)

DATA: F9317 #1087

CALI: F9317 # 2

BASE M/Z: 70

RIC: 5631.



M/Z 40 60 80 100 120 140 160

LIBRARY SEARCH

03/06/95 8:41:00 + 21:44

SAMPLE: 3-4-95 HMX - HPLC WATER - HYDROLYSATE

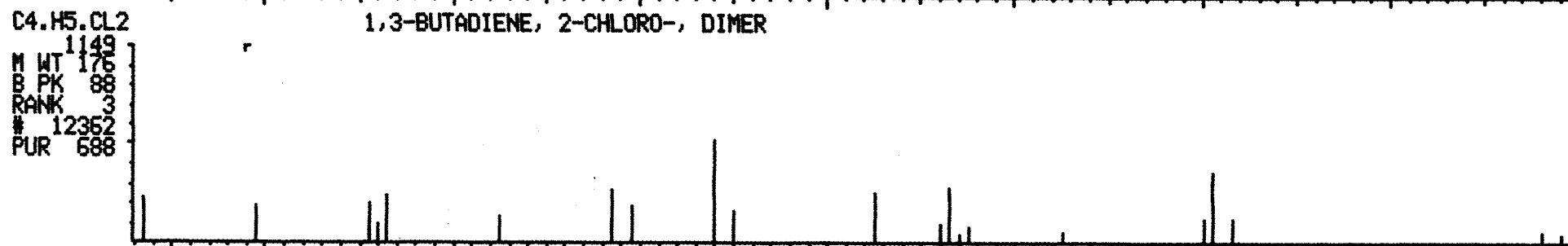
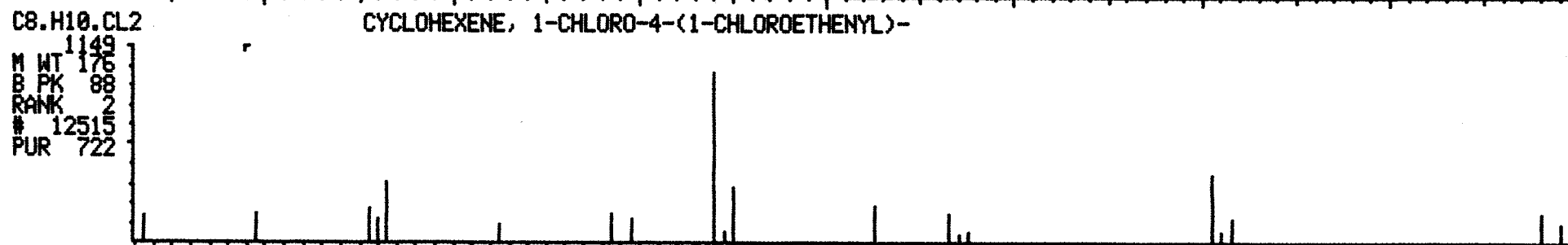
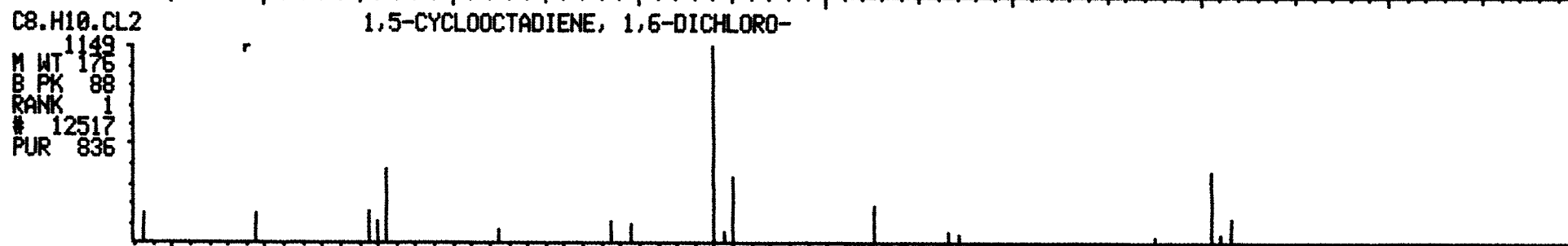
CONDS.: 4 MIN @ 30, 6/MIN TO 300 HOLD 60 DB-5MS 30MX.25MM COLUMN  
ENHANCED (S 15B 2N 0T)

DATA: F9317 #1304

CALI: F9317 # 2

BASE M/Z: 88

RIC: 12527.



M/Z 40 60 80 100 120 140 160

LIBRARY SEARCH

03/06/95 8:41:00 + 33:28

SAMPLE: 3-4-95 HMX - HPLC WATER - HYDROLYSATE 2/500 UL INJ.

CONDS.: 4 MIN @ 30, 6/MIN TO 300 HOLD 60 DB-5MS 30MX.25MM COLUMN

ENHANCED (S 158 2N 0T)

DATA: F9317 #2008

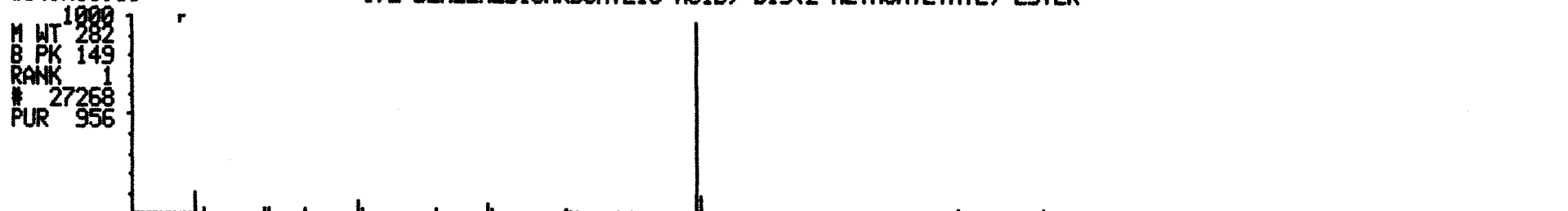
CALI: F9317 # 2

BASE M/Z: 149

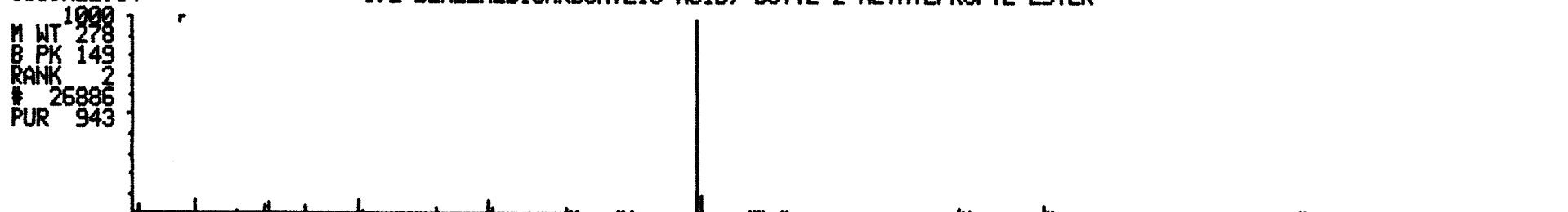
RIC: 10383.



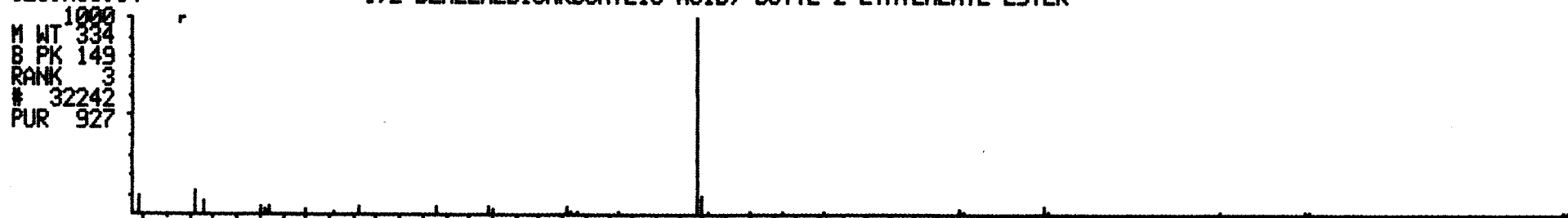
C14.H18.06 1,2-BENZENEDICARBOXYLIC ACID, BIS(2-METHOXYETHYL) ESTER



C16.H22.04 1,2-BENZENEDICARBOXYLIC ACID, BUTYL 2-METHYLPROPYL ESTER



C20.H30.04 1,2-BENZENEDICARBOXYLIC ACID, BUTYL 2-ETHYLHEXYL ESTER



M/Z 50 100 150 200 250 300

LIBRARY SEARCH

03/06/95 8:41:00 + 41:59

SAMPLE: 3-4-95 HMX - HPLC WATER - HYDROLYSATE 2/500 UL INJ.

CONDS.: 4 MIN @ 30, 6/MIN TO 300 HOLD 60 DB-5MS 30MX.25MM COLUMN

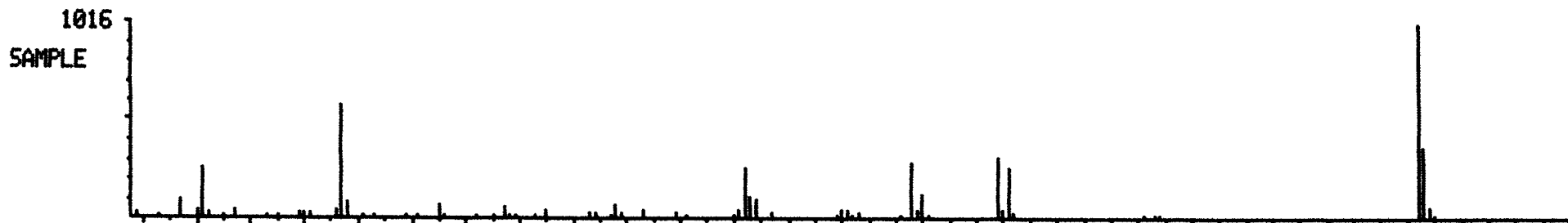
ENHANCED (S 15B 2N 0T)

DATA: F9317 #2519

CALI: F9317 # 2

BASE M/Z: 277

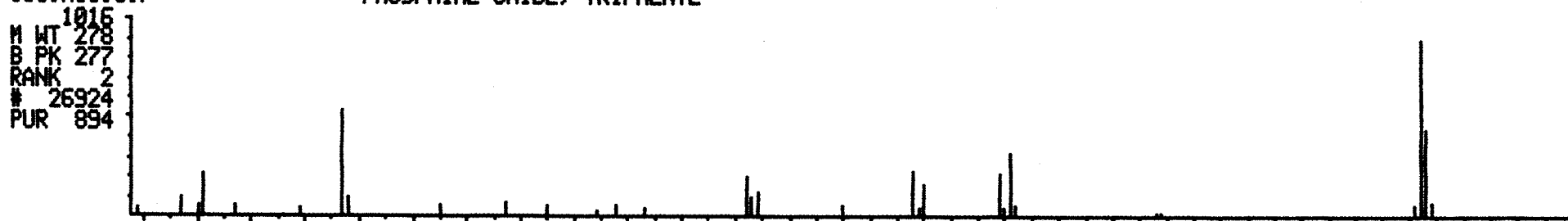
RIC: 49653.



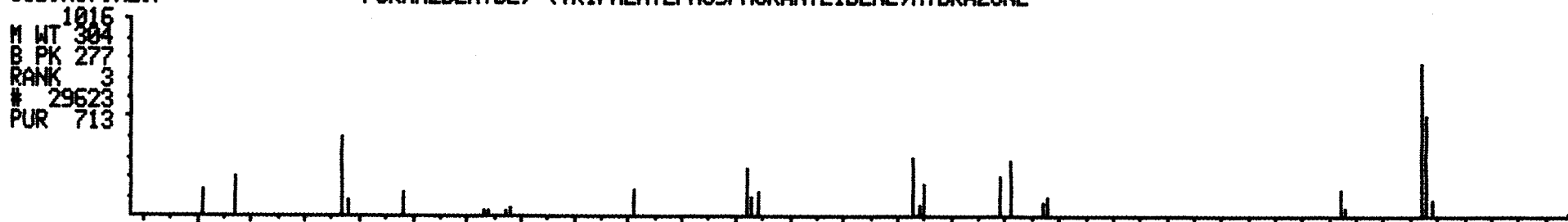
C21.H19.02.P ACETIC ACID, (TRIPHENYLPHOSPHORANYLIDENE)-, METHYL ESTER



C18.H15.0.P PHOSPHINE OXIDE, TRIPHENYL-



C19.H17.N2.P FORMALDEHYDE, (TRIPHENYLPHOSPHORANYLIDENE)HYDRAZONE



M/Z 50 100 150 200 250 300